

1976

Glacial Dispersal Of Rocks And Minerals In The Lac Mistassini - Lac Waconichi Area, Quebec, With Special Reference To The Icon Dispersal Train

Ronald Norman Dilabio

Follow this and additional works at: <https://ir.lib.uwo.ca/digitizedtheses>

Recommended Citation

Dilabio, Ronald Norman, "Glacial Dispersal Of Rocks And Minerals In The Lac Mistassini - Lac Waconichi Area, Quebec, With Special Reference To The Icon Dispersal Train" (1976). *Digitized Theses*. 903.
<https://ir.lib.uwo.ca/digitizedtheses/903>

This Dissertation is brought to you for free and open access by the Digitized Special Collections at Scholarship@Western. It has been accepted for inclusion in Digitized Theses by an authorized administrator of Scholarship@Western. For more information, please contact tadam@uwo.ca, wlsadmin@uwo.ca.

INFORMATION TO USERS

THIS DISSERTATION HAS BEEN
MICROFILMED EXACTLY AS RECEIVED

This copy was produced from a microfiche copy of the original document. The quality of the copy is heavily dependent upon the quality of the original thesis submitted for microfilming. Every effort has been made to ensure the highest quality of reproduction possible.

PLEASE NOTE: Some pages may have indistinct print. Filmed as received.

Canadian Theses Division
Cataloguing Branch
National Library of Canada
Ottawa, Canada K1A 0N4

AVIS AUX USAGERS

LA THESE A ETE MICROFILMEE
TELLE QUE NOUS L'AVONS RECUE.

Cette copie a été faite à partir d'une microfiche du document original. La qualité de la copie dépend grandement de la qualité de la thèse soumise pour le microfilmage. Nous avons tout fait pour assurer une qualité supérieure de reproduction.

NOTA BENE: La qualité d'impression de certaines pages peut laisser à désirer. Microfilmée telle que nous l'avons reçue.

Division des thèses canadiennes
Direction du catalogage
Bibliothèque nationale du Canada
Ottawa, Canada K1A 0N4

GLACIAL DISPERSAL OF ROCKS AND MINERALS
IN THE LAC MISTASSINI - LAC WACONICHI AREA, QUEBEC
WITH SPECIAL REFERENCE TO THE ICON DISPERSAL TRAIN

by

Ronald Norman Wells DiLabio

Department of Geology

Submitted in partial fulfillment
of the requirements for the degree of
Doctor of Philosophy

Faculty of Graduate Studies
The University of Western Ontario
London, Ontario

May, 1976

© Ronald Norman Wells DiLabio 1976

ABSTRACT .

This project was undertaken to study the patterns and processes of glacial dispersal on local and regional scales in the Lac Mistassini - Lac Waconichi area. The Quaternary units in the area were mapped and regional dispersal trends of indicator rocks and minerals were determined. Chalcopyrite-bearing dispersal trains related to copper mineralization at the Icon Sullivan Joint Venture mine were investigated at a detailed scale.

Samples of glacial drift were collected from natural and man-made exposures. Till pebble and striae orientations were measured. Laboratory analyses, mainly on till samples, were: (1) textural analysis of the minus 4 mm. fraction; (2) lithologic analysis of the 4 to 64 mm. fraction; (3) carbonate analysis of the minus 0.063 mm. fraction; and (4) heavy mineral analysis.

The following Quaternary units were determined in the area: unit A, basal till of regional extent; unit B, ice-contact stratified drift and ablation till; unit C, basal till restricted to the Waconichi River valley; unit D, outwash gravel; unit E, varved clayey silt; and unit F, alluvium and peat. They were deposited during the Wisconsinan and Holocene as the products of a simple glacial cycle of: major southward advance - recession - minor southward readvance - completed recession - glaciofluvial sedimentation - glaciolacustrine sedimentation -

postglacial organic sedimentation. Basal tills (units A and C) were found to reflect the local bedrock lithology better than ablation till, ice-contact stratified drift, outwash gravel, and postglacial lake or stream sediments.

The dispersal trains at the Icon mine are three-dimensional bodies in unit C. The North Train is 1650 m. long by 75 m. wide and the Icon Train is 570 m. long and 250 m. wide. The Icon Train has a longitudinal shape of an elongated tear-drop in vertical section. The trains have high geochemical and lithological contrast with the surrounding till. They were formed by glacial erosion (mainly quarrying), transport, and deposition during the readvance that deposited unit C. These processes were orderly, not chaotic. It is possible and useful to map dispersal trains at a detailed scale.

In unoxidized unit C, chalcopyrite has a clast mode between 8 and 1 mm. and a matrix mode from 0.063 to 0.016 mm. The clast mode developed after short glacial transport, but the matrix mode required at least 100 m. of transport to develop. When samples are collected from unoxidized till during mineral exploration, the size range to be analyzed for copper should include the matrix mode. Chalcopyrite is most abundant in the range 32 to 8 mm., and malachite is most abundant in the range 0.5 to 0.037 mm. in strongly oxidized unit C. Sampling of oxidized carbonate-bearing till for geochemical analysis for copper should include the malachite-rich size range.

Mapping the abundance of chalcopvrite-bearing pebbles in the Icon Train is a more efficient guide to the location of the ore in place than analysis for copper in the soil on the train. Therefore, when clasts containing economically interesting minerals are found in a till, the abundance of those clasts should be mapped.

ACKNOWLEDGEMENTS

I thank Dr. A. Dreimanis for his guidance, constructive criticisms and discussions. Dr. R. W. Hutchinson and Dr. G. M. Young made many helpful suggestions for improvement of the thesis.

Several people associated with Icon Sullivan Joint Venture aided my work. I thank Mr. J. N. Botsford, general manager, and Mr. E. W. Watt, mine manager, for permission to work on the Icon mine property. Mr. G. Darcy, mine geologist, encouraged the field work and supplied maps and geological information. Mr. A. J. Troop, manager of the Icon Syndicate, suggested the project and sponsored my first visit to the Icon mine.

Geologists who provided discussions in the field include Dr. G. O. Allard, Dr. J.-L. Caty, Dr. E. H. Chown and Mr. B. Warren. Mr. D.G.F. Long provided information on the bedrock geology near Lac Waconichi.

Mr. A. O. Grins, University of Western Ontario, tirelessly and carefully performed carbonate and textural analyses.

I thank my wife, Sharon, for providing able field assistance and for being a constant source of encouragement.

Financial support was provided from National Research Council of Canada grant A4215 to Dr. A. Dreimanis.

TABLE OF CONTENTS

	Page
CERTIFICATE OF EXAMINATION	ii
ABSTRACT	iii
ACKNOWLEDGEMENTS	vi
TABLE OF CONTENTS	vii
LIST OF PHOTOGRAPHIC PLATES	x
LIST OF TABLES	xii
LIST OF FIGURES	xiii
CHAPTER 1. INTRODUCTION	1
Purposes and scope of investigation	1
Location and access	2
Previous work	3
History of exploration	7
Methods of study	12
CHAPTER 2. BEDROCK GEOLOGY	14
PART 2.1. Stratigraphy	14
Archean	14
Proterozoic	17
Chibougamau Formation	17
Mistassini Group	18
Southeastern Gneisses	22
PART 2.2. Structure	22
PART 2.3. Mineral Deposits	24
Copper	24
Lead and zinc	28

CHAPTER 3. QUATERNARY GEOLOGY	30
PART 3.1. Surficial Geology	30
Physiography and drainage	30
Bedrock-controlled landscapes	32
Drumlinoid landforms	32
Eskers and ice-disintegration landforms	34
Lacustrine plains and lake terraces	36
Regional glacial flow patterns	37
PART 3.2. Stratigraphy and Provenance	45
Unit A	47
Unit B	52
Unit C	60
Unit D	69
Unit E	70
Unit F	73
Quaternary history	74
Regional glacial dispersal trends	76
CHAPTER 4. DISPERSAL TRAINS AT ICON MINE	86
PART 4.1. The North Train	88
Size and shape	88
Origin	90
PART 4.2. The Icon Train	92
Size, shape and structure	92
Origin	100
Depth of erosion	108
Comparison of prospecting methods	110

Comparison of units A, B, C and D as sampling media	114
Comparison of the Icon train to other sulphide-bearing dispersal trains	120
CHAPTER 5. GLACIAL COMMINUTION OF CHALCO- PYRITE	123
Unoxidized till	123
Weathering of chalcopyrite-bearing till	129
CHAPTER 6. CONCLUSIONS AND RECOMMENDATIONS	136
Conclusions	136
Recommendations for future research	139
REFERENCES	140
APPENDICES	149
Appendix A. Analysis of till pebble orienta- tions	149
Appendix B. Methods and results of textural, carbonate, and lithological analyses of Quaternary units	154
Appendix C. True distribution of chalcopyrite in unoxidized till	164
Appendix D. Distribution of heavy minerals and chalcopyrite in oxidized till	168
VITA	173

LIST OF PLATES

Plate	Descriptions	Page
1	View to east along strike of number one ore zone at Icon mine	27
2	Quartz crystals in chalcopyrite in the number one ore zone at the Icon mine	27
3	Glacial landforms near Waconichi River	35
4	Vertical exposure of unit A showing its fissile structure and gross texture	49
5	Transverse section through a drumlinoid ridge composed of unit A	49
6	Mound of unit B about 30 m. downglacier from the subcrop of the number one ore zone at Icon mine	54
7	Folded interbedded pebbly sand and till of unit B overlain by thin unit C	54
8	Rain-washed surface of unit C showing its coarse rubbly texture	61
9	Unit C cemented by limonite and malachite ..	63
10	Unit C overlying west end of the subcrop of number one ore zone at Icon mine	63
11	Angular blocks of unit A in unit C overlying <u>in situ</u> unit A	65
12	Oblique section through folded lens of sand in unit C	65
13	Interbedded sand and till of unit B in sharp contact with overlying unit C	66
14	Horizontal exposure of unit C filling oval groove in surface of unit A	66
15	Mining unit C from the Icon Train	68
16	Boulder of quartz-carbonate vein rock in coarse gravel of unit D	71

Plate

Description

Page

17

Varved clayey silt of unit E draped over
chalcopyrite-rich boulder in unoxidized
unit C

72.

LIST OF TABLES

Table	Description	Page
1	Explorers and organizations using the canoe route between Lac Waconichi and Lac Mistassini in the period 1670-1900	9
2	Bedrock units in the Mistassini basin	15
3	Quaternary units in the study area	46
4	Sulphide-bearing glacial dispersal trains ..	121
5	Description of samples referred to in text in determinations of abundance of chalcopyrite in till	125
A-1	Statistics calculated by VECTOR for three-dimensional analysis of till pebble orientations	152
A-2	Statistics calculated by VECTOR for two-dimensional analysis of till pebble orientations	153
B-1	Texture and lithology of unit A	157
B-2	Texture and lithology of unit B	158
B-3	Texture and lithology of unit C	159
B-4	Texture and lithology of units D, E and F ..	163
C-1	Abundance of chalcopyrite with respect to grain size in unoxidized till samples	166
D-1	Abundance of heavy minerals and chalcopyrite in oxidized till samples	169

LIST OF FIGURES

Figure	Description	Page
1	Location map	4
2	Schematic diagram of a failed attempt to discover the source of chalcopyrite-bearing boulders on the west bank of Waconichi River	11
3	Generalized bedrock geology of the Lac Mistassini area	16
4	Bedrock geology of the study area	20
5	Bedrock geology of the Icon mine	26
6	A) Physiographic regions of the Lac Mistassini - Lac Waconichi area; B) drainage basins of the same area	31
7	Surficial geology of the study area	33
8	Mirror-image rose diagrams of till pebble orientations (unit A) in the study area	39
9	Mirror-image rose diagrams of till pebble orientations in a drumlinoid ridge (unit A)	40
10	Mirror-image rose diagrams of till pebble orientations in a transverse section in a drumlinoid ridge (unit A)	41
11	Ternary diagram of the texture of units A, B, C and E	48
12	Vertical variability in lithology and texture of unit A in a section in a drumlinoid ridge 2.3 km. east of the Icon mine	51
13	Ternary diagram of the texture of units A, B and C	56
14	Particle size distributions of the less than -2 ϕ (4 mm.) fraction of unit A and till from unit B	57

Figure	Description	Page
15	Abundance of distal rock types versus abundance of igneous and gneissic rock types in the 4 to 64 mm. fraction of unit B from the Icon mine and unit A from the Icon mine and the surrounding area	59
16	Abundance of Upper Albnel Formation rock types in the 4 to 64 mm. fraction of unit A in the Lac Mistassini - Lac Waconichi area	77
17	Abundance of igneous and metamorphic rock types in the 4 to 64 mm. fraction of unit A in the Lac Mistassini - Lac Waconichi area	79
18	Median diameter (phi units) of the minus 4 mm. (-20) fraction of unit A in the Lac Mistassini - Lac Waconichi area	81
19	Abundance of carbonates in the minus 0.063 mm. fraction of unit A in the Lac Mistassini - Lac Waconichi area	82
20	Abundance of Chibougamau Formation rock types in the 4 to 64 mm. fraction of units A and B near Lac Waconichi	84
21	Perspective plot of the abundance of copper in the B horizon of the soil profile at the Icon mine, viewed from the southeast	87
22	Abundance of copper in the B horizon of the soil profile over the Icon Train	89
23	Abundance of vein rock types in the 4 to 64 mm. fraction of unit C in the Icon Train	95
24	Perspective plot of the abundance of vein rock types in the 4 to 64 mm. fraction of unit C in the Icon Train, viewed from the west	97
25	Longitudinal section of the Icon Train	98
26	Transverse section of the Icon Train	99

Figure	Description	Page
27	Mirror-image rose diagrams of till pebble orientations in unit C in the northeast part of the Icon Train	102
28	Bedrock topography of the Icon Sullivan Joint Venture property	103
29	Abundance of chalcopyrite-bearing pebbles (4 to 64 mm.) in unit C in the Icon Train ..	111
30	Mirror-image rose diagrams of till pebble orientations in unit A and unit B under the Icon Train	116
31	Abundance of vein rock types in units A, B, C and D in sections on the east side of the Icon Train	117
32	Abundance of vein rock types in units B and C on the west side of the Icon Train ...	118
33	True chalcopyrite distribution in till samples 73-56, 73-57, 73-58 and 73-74	127
34	Apparent heavy mineral and chalcopyrite distributions in till sample 72-12EU56	132
35	True chalcopyrite distribution in till samples 72-12EU56 and 72-12EU46	133

The author of this thesis has granted The University of Western Ontario a non-exclusive license to reproduce and distribute copies of this thesis to users of Western Libraries. Copyright remains with the author.

Electronic theses and dissertations available in The University of Western Ontario's institutional repository (Scholarship@Western) are solely for the purpose of private study and research. They may not be copied or reproduced, except as permitted by copyright laws, without written authority of the copyright owner. Any commercial use or publication is strictly prohibited.

The original copyright license attesting to these terms and signed by the author of this thesis may be found in the original print version of the thesis, held by Western Libraries.

The thesis approval page signed by the examining committee may also be found in the original print version of the thesis held in Western Libraries.

Please contact Western Libraries for further information:

E-mail: libadmin@uwo.ca

Telephone: (519) 661-2111 Ext. 84796

Web site: <http://www.lib.uwo.ca/>

CHAPTER 1

INTRODUCTION

Purpose and scope of investigation

This project was undertaken to investigate Quaternary glacial dispersal of rock and mineral particles in the Lac Mistassini - Lac Waconichi area of Quebec. The area was selected on the advice of Mr. A. J. Troop, formerly of Icon Sullivan Joint Venture, because that organization's property at the south end of Lac Mistassini contained a copper ore deposit with which two dispersal trains were associated. One of the trains, called the Icon train, was well exposed on the surface and in mining faces, which facilitated its sampling and measurement.

The primary objectives of this project were (1) to determine the shape and size of the dispersal trains, (2) to determine their mode of origin, and (3) to find the downglacier abundance trends of their components in order to arrive at a general model of the style of glacial dispersal that might be encountered while prospecting in other areas. Related objectives were (a) to compare traditional soil geochemical analytical surveys with surveys involving the tracing of mineralized pebbles

both as to the quality of results and costs, (b) to compare basal till to ablation till and ice-contact stratified drift as sampling media in prospecting, and (c) to determine the grain size distribution produced by the glacial comminution of chalcopyrite in order to suggest size ranges for sampling unoxidized till by overburden drilling in other areas. Secondary objectives were (i) to compare oxidized to unoxidized copper- and carbonate-bearing till as sampling media in geochemical prospecting, (ii) to estimate the depth of erosion caused by the last glacier to override the copper ore deposit, and (iii) to show the regional glacial dispersal trends of selected indicator rocks using samples of basal till, ablation till, and ice-contact stratified drift.

This thesis is not intended as a replacement for previous mapping reports on bedrock or surficial geology; it will however suggest possible useful additions to existing maps where pertinent. Its main concerns will be to provide a detailed study of the stratigraphy, structure and origin of the drift units at and near the Icon mine, and suggest guidelines for exploration projects in other glaciated areas.

Location and access

The study area comprises parts of Bignell, O'Sullivan, Gauvin, McQuat and Duquet Townships. Detailed work centred around the Icon Sullivan Joint

3

Venture property, which is located at the south end of Lac Mistassini, at Latitude $50^{\circ} 14' 15''$ North, Longitude $73^{\circ} 48' 20''$ West (Fig. 1). Access to the mine is via the Albanel Road from Chibougamau, 64 km. to the southwest. The Albanel Road is an all-weather gravel road traversing the region, and its branches and road cuts provide good access to the Quaternary sediments and bedrocks of the study area.

Previous work

The most comprehensive early geological observations in the Chibougamau - Lac Mistassini region are those of Richardson (1872), Low (1885, 1896, 1906), and Faribault et al. (1911). Norman (1940) described the Mistassini fault, a major feature now believed to be a sector of the boundary between the Superior and Grenville Structural Provinces of the Canadian Shield. Bergeron (1957) studied the stratigraphy of the Mistassini Group, which he divided into five formations. The upper unit of the Mistassini Group, the Temiscamie Formation, was studied by Quirké et al. (1960) and Neilson (1953, 1963) as a possible source of iron ore. Gilbert (1958); Deland and Sater (1969), Guilloux (1969), Duquette (1970), Chown and Caty (1973), Caty and Chown (1973) and Gros (1975) described the lower units of the Mistassini Group as well as the adjacent crystalline rocks. The most detailed study of the Chibougamau Formation is that of Long (1973).

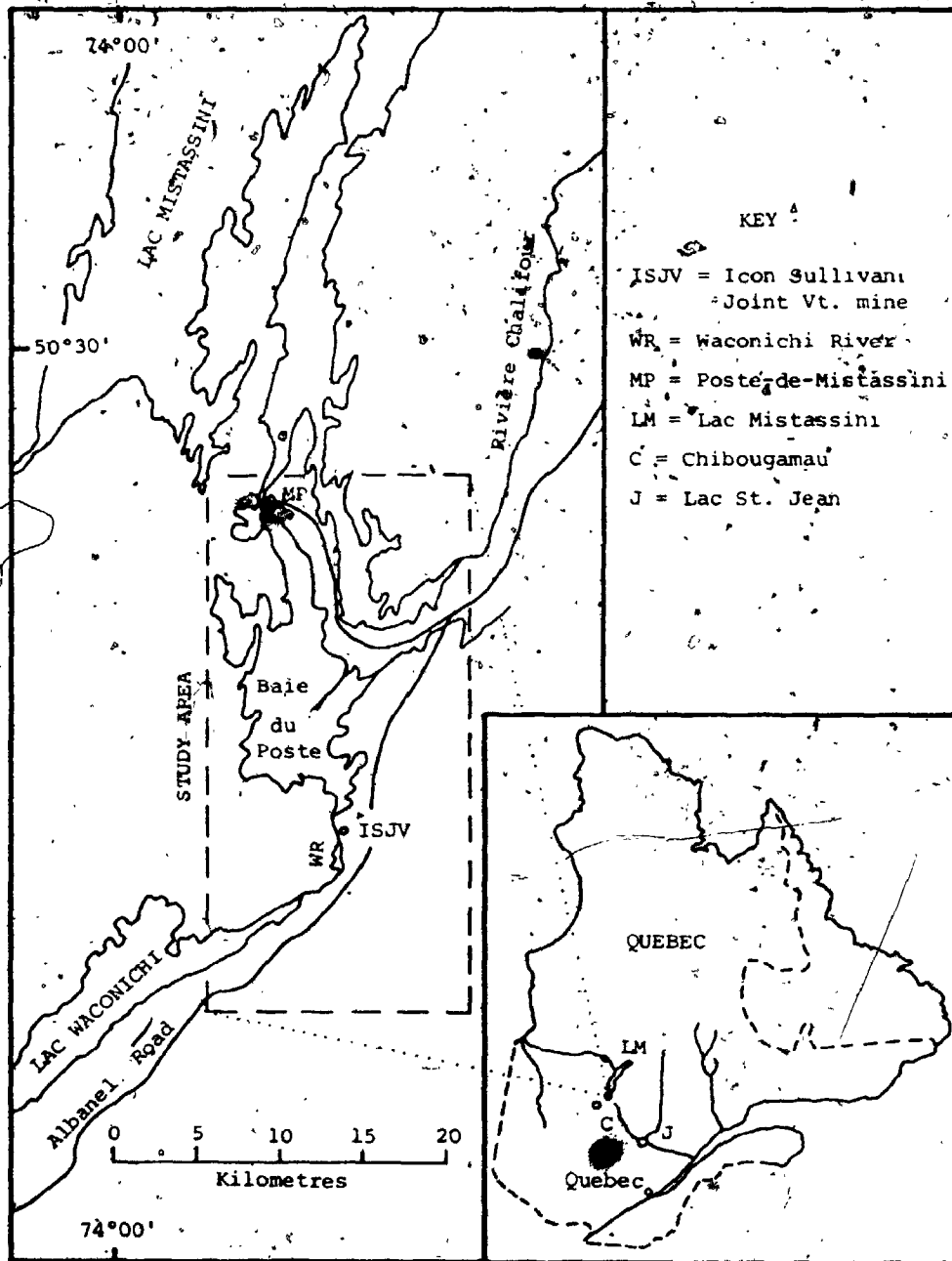


Figure 1. Location map

Base metal mineral deposits of the area have been described by Guilloux (1972), Troop and Darcy (1973), Catv and Chown (1973), Collins et al. (1974) and Gros (1975). Radiometric ages for the Temiscamie Formation have been determined by Quirke et al. (1960) and Frver (1972). Radiometric ages of greenstones and gneisses of the Superior Province in areas south and west of the Mistassini basin were determined by Jones et al. (1974) and Dallmeyer (1974).

Concerning the Quaternary geology of the region, Low (1885, p. 32) made an early observation of glacial dispersal: "In the vicinity of Lake Mistassini, no rounded boulders of limestone were met with in directions to the east and north-west of the lake, and the probability is that the drift there was from north-east to south-west." Later, Low postulated that the central névé for the Laurentide ice sheet was between Latitudes 53° and 55°, midway between the coasts of the Quebec - Labrador peninsula, because of the lack of glacial features in this area and the radiating pattern of striae around it. He stated that the depth of glacial erosion was not greater than 60 metres, and described the drumlins, eskers, and terraces of the region (Low, 1896). Faribault et al. (1911) added a description of the crag and tail hills near Lac Waconichi and commented on the coarse texture of the tills outside the Mistassini basin.

Norman (1938) surveyed the Lake Barlow-Ojibway

beaches near Lac Opemisca, 45 km. west of Lac Waconichi. He also postulated a mode of origin for the De Geer moraines found below the elevations of the beaches.

Norman's (1939) contention that a remnant ice cap advanced from the southeast to form an endmoraine in the north end of the Mistassini basin was disputed by Ignatius (1958), who showed Norman's endmoraine to be part of an outwash complex. Both authors agreed on a general deglaciation pattern of ice recession toward the northeast. Prest (1970, p. 737) gave an age of 6,960±90 radiocarbon years for basal organic sediments in the Chibougamau area.

Allard and Cimon (1974) suggested that only a small amount of glacial erosion may have taken place in the Chibougamau mining camp because of the presence of caps of deeply lateritized rocks on some of the ore deposits. They suggested that this may have been due to ice stagnation at the high elevations of the camp and/or deflection of the most actively advancing parts of the ice sheet by high hills of resistant rock upglacier from the camp.

Warren (1974) produced a report and five surficial geological maps at a scale of 1:50,000 covering 1250 sq. km., including the area of the present study. He mapped the surficial sediments as hummocky moraine-bedrock complex, flutings, drumlins, glaciofluvial sand and gravel, and esker sand and gravel. The project was specifically designed to provide background information for prospecting parties working in this glaciated area of

rare outcrop. Gros (1975) collected stream sediment samples within the same area to test the usefulness of stream sediment geochemistry as a prospecting tool.

Studies of glacial dispersal trains for prospecting purposes have mostly taken place in Fennoscandia, and many papers on such studies are found in the volume of Kvalheim (1967), in the proceedings of the Trondheim and Edinburgh conferences on prospecting in areas of glacial terrain (Jones, 1973, 1975), and in Bradshaw (1975). Canadian dispersal trains that have been mapped include the Steep Rock iron ore train (Dreimanis, 1956); the train of sphalerite-bearing boulders at George Lake, Saskatchewan (Kårup-Møller and Brummer, 1970), the trains derived from the ultramafic rocks at Thetford Mines, Quebec (Shilts, 1973), the Kidd Creek, Ontario train (Skinner, 1972), the train related to the Gullbridge ore deposit in Newfoundland (O'Donnell, 1973), and the Mount Pleasant train in New Brunswick (Szabo et al., 1975). O'Donnell (1973, pp. 51-67) provided an excellent literature review on the types of dispersal trains and the sediments found in them, and how such trains may be used in exploration.

History of exploration

The history of exploration of the Chibougamau - Lac Mistassini region prior to discovery of the Icon Sullivan Joint Venture copper deposit provides an example

of how circumstances and inadequate understanding of local geology may combine to inhibit the discovery of an important ore deposit.

Two ore zones were present at the bedrock surface under the bed of the Waconichi River at the second and third rapids downstream from Lac Waconichi on the canoe route to Lac Mistassini. A glacial dispersal train containing chalcopyrite-bearing boulders was associated with the subcrop of each ore zone on the west bank of the river. Since 1671, when Father Charles Albanel passed through the area on his mission to Hudson Bay, the Waconichi River has been the main canoe route for traders and explorers (Table 1) between southern points such as Chibougamau and Lac St. Jean and the Lac Mistassini area, but portages around the rapids were made on the east bank. Low (1906) reported that disseminated chalcopyrite had been seen in 1905 in arkose of the Chibougamau Formation 2 km. upstream from the then-undiscovered ore zones, and in 1911 Faribault et al. reported galena and sphalerite in dolostone of the Mistassini Group at the Hudson Bay Co. post, 24 km. downstream, both showings being on the canoe route. These discoveries undoubtedly spurred interest in the area, but because the portages remained on the east bank of the river, the dispersal trains went unnoticed.

In 1956, Stratmat Ltd. discovered the copper-bearing dispersal trains, but was unable to locate the bedrock

Table 1. Explorers and organizations using the canoe route between Lac Waconichi and Lac Mistassini in the period 1670-1900.

Explorer or Organization	Year	Reference
Charles Albanel, S.J.	1671-72	Low (1885, p. 12)
Andre Michaux, Botanist	1792	Low (1885, p. 13)
Hudson Bay Company	c. 1810-present	Low (1885, p. 13)
North-West Company	c. 1810-1821	Low (1896, p. 14)
James Richardson	1870	Richardson (1872)
Prof. John Galbraith	1881	Faribault <i>et al</i> (1911, p. 38)
A. P. Low	1885	Low (1885)
Prof. W. J. Loudon	1889	Faribault <i>et al</i> (1911, p. 40)
A. P. Low	1892-93	Low (1896)
R. W. Brock	1896	Bell (1897)
C. E. Lemoine	1899	Faribault <i>et al</i> (1911, p. 43)

source of the mineralized boulders because of misunderstandings concerning the local geology. Apparently believing that the dispersal trains directly overlay steeply dipping mineralized zones like those present in greenstone belts of the Superior Province, Stratmat drilled 6 diamond drill holes at 45 degrees through the trains (Fig. 2). The drilling results were negative partly because the trains were formed by glacial action, not by in situ weathering, and therefore were displaced from their bedrock sources, and partly because the mineralization was conformable with gently dipping rocks of the Mistassini Group. All the drill holes were collared in the footwall rocks (G. Darcy, pers. comm.).

On June 4, 1965, the Icon Syndicate began ground checking of electromagnetic conductors found in its airborne survey in order to distinguish mineralized zones in the area from barren graphitic argillite beds. Only two days later, after the discovery of chalcopyrite-bearing boulders in till on the west bank of the Waconichi River at the second rapid, by inspector Paul Bedard, the entire field party was involved in a systematic search for additional boulders in an attempt to define the source of the dispersal train. Seven trenches were excavated exposing the copper-rich till. Drilling upglacier from the train confirmed the presence of an ore deposit, and production began May 24, 1967 (Troop and Darcy, 1973).

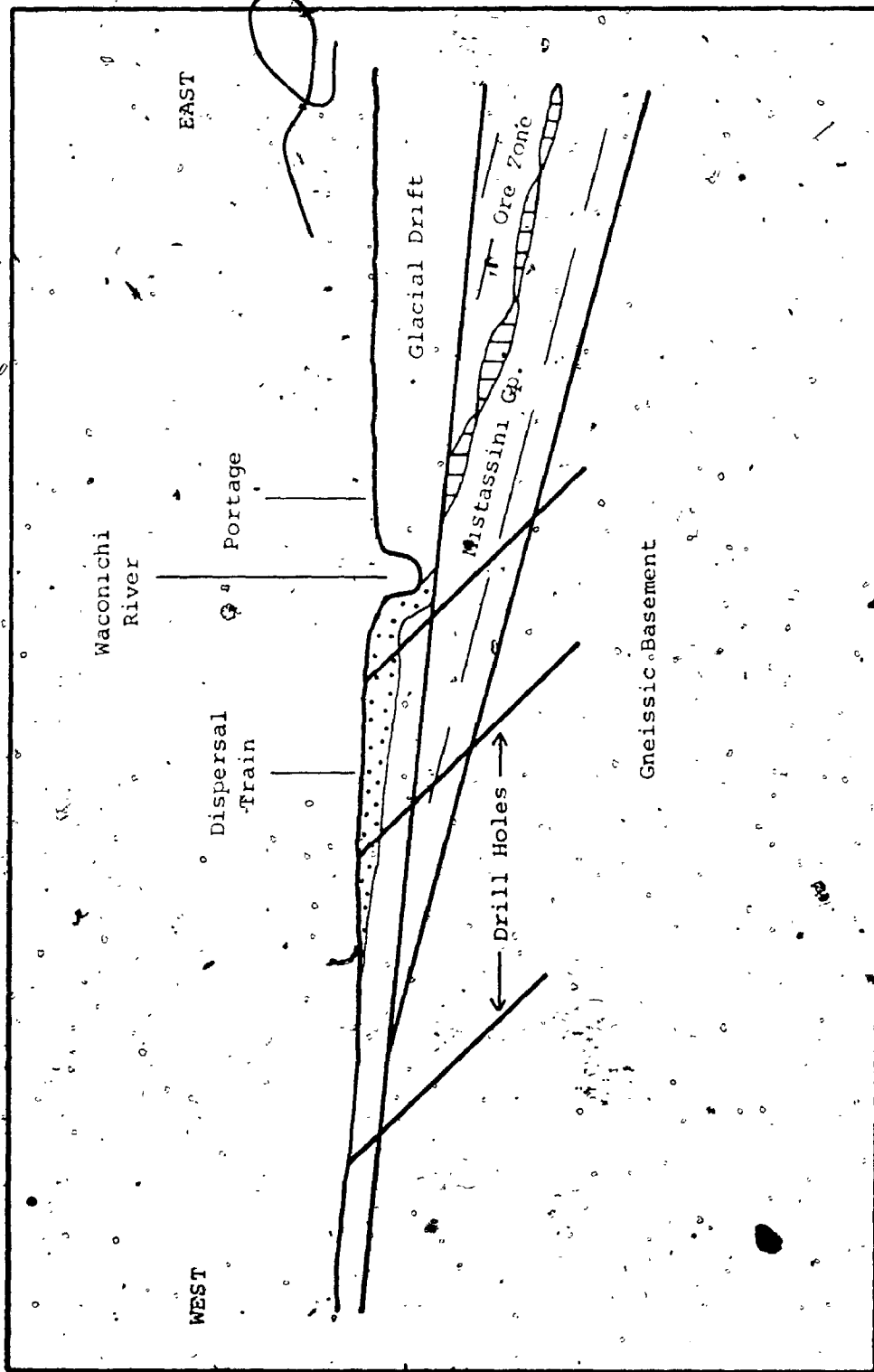


Figure 2. Schematic diagram of a failed attempt to discover the source of chalcopyrite-bearing boulders on the west bank of Waconichi River. Diagram is not to scale.

Methods of study

Samples of glacial drift were collected from natural and man-made exposures near the Albabel Road covering a distance of 25 km. parallel with the glacial trend. Sections were measured where strata were well exposed. Till pebble orientations were measured at sites where till was found in an undisturbed state.

At the Icon mine, a baseline oriented subparallel to the local striae was cut through the forest west of the Icon dispersal train and eleven crosslines were cut to cross the train at 61 m. (200 ft.) intervals. Samples were collected from test pits at 30.5 m. (100 ft.) spacings along the crosslines (Fig. 23). Sequential samples were collected from sections exposed in mining faces. Till pebble orientations and striae were measured at several localities at the mine. Four bulk samples of approximately 50 to 60 litres in size were collected from unoxidized chalcopyrite-bearing till to determine the grain size distribution of glacially comminuted chalcopyrite.

The types of laboratory analyses that were routinely performed were: (1) textural analysis of the minus 4 mm. fraction; (2) lithologic analysis of the 4 to 64 mm. fraction; and (3) carbonate analysis of the minus 0.063 mm. fraction. Most of the samples analysed routinely were till. Textural analysis was by hydrometer and sieve methods using a modified form of the American Society for Testing and Materials (ASTM, 1964) procedure.

A modified form of the gasometric method of Dreimanis (1962) was used in the carbonate analyses to determine the amount of calcite and dolomite in the samples. The till pebble orientations were plotted as mirror-image and plunge-sensitive rose diagrams and as contoured stereographic projections using a modified version of Starkey's (1970) computer plotting programme. The four bulk samples of till were split at 1 phi intervals from -7 phi to 10 phi, and for each fraction the abundance of chalcopyrite was determined volumetrically or by point counting. More detailed descriptions of the laboratory methods are found with the appropriate appendices.

Because only limited access was available to the west and north parts of the area, the mapping and sampling of the Quaternary units on a regional scale must be considered as reconnaissance. This applies in particular to the regional distribution of lithologic components in unit A as shown on Figures 16 to 20. The distribution of units C and D (Fig. 7) was not fully mapped for the same reason. The lack of deep exposures prevented the detection of older Quaternary sediments which may be present in the area. In addition, till pebble orientations were measured only on one side of the drumlinoid ridge shown on Fig. 9 because only that side was accessible.

CHAPTER 2

BEDROCK GEOLOGY

PART 2.1 Stratigraphy

A study of the provenance of glacial drift units in any area must include descriptions of the rock types present in the bedrocks of that area and in the region upglacier from it. In the Lac Mistassini - Lac Waconichi area distinctive rock types which occur as bedrock in and upglacier from the study area were selected as indicator rock types. The major bedrock units in this region are described below and listed in Table 2. All of these units occur within the study area except for the Papaskwasati, Cheno, Upper Albanel, and Temiscamie Formations, which are found upglacier from it in the Mistassini basin.

Archean

The oldest rock in the area is the Waconichi Formation, the lowest unit in the Roy Group (Duquette, 1970) which underlies the wedge-shaped area between the Waconichi and Mistassini faults (Fig. 3). The rocks are dark green amphibolites derived from pillowed basalts,

Table 2. Bedrock units in the Mistassini basin, after Duquette (1970), Long (1973), and Caty and Chown (1973).

PROTEROZOIC	Southeastern Gneisses	Biotite, hornblende gneisses and granitic gneisses. May include remobilized older units.
	TECTONISM	
	Mistassini Group Temiscamie Fm.	Sideritic iron-formation, ferruginous slate
	DISCONFORMITY	
	Upper Albanel Fm. Lower Albanel Fm. Member F Member E Member D Member C Member B Member A Cheno Fm. Papaskwasati Fm.	Pink and buff massive dolostone Pale grey to white dolostone Brown laminated dolostone Grey dolostone, intraformational breccias Laminated dolostone Grey argillaceous dolostone, graphitic argillite Stromatolitic and arenaceous dolostone Black to grey quartz sandstone and subarkose, arenaceous dolostone Green, grey, yellow quartz sandstone and subarkose
UNCONFORMITY		
Chibougamau Fm.	Granitoid conglomerate, arkose, graded laminites, mixtites	
UNCONFORMITY		
ARCHEAN	Granitic intrusions	Hornblende syenite to hornblende biotite diorite, granite
	Gneissic complex	Hornblende and biotite gneisses
	Roy Group Waconichi Fm.	Pillowed basalt, basaltic flows, felsic pyroclastic rocks

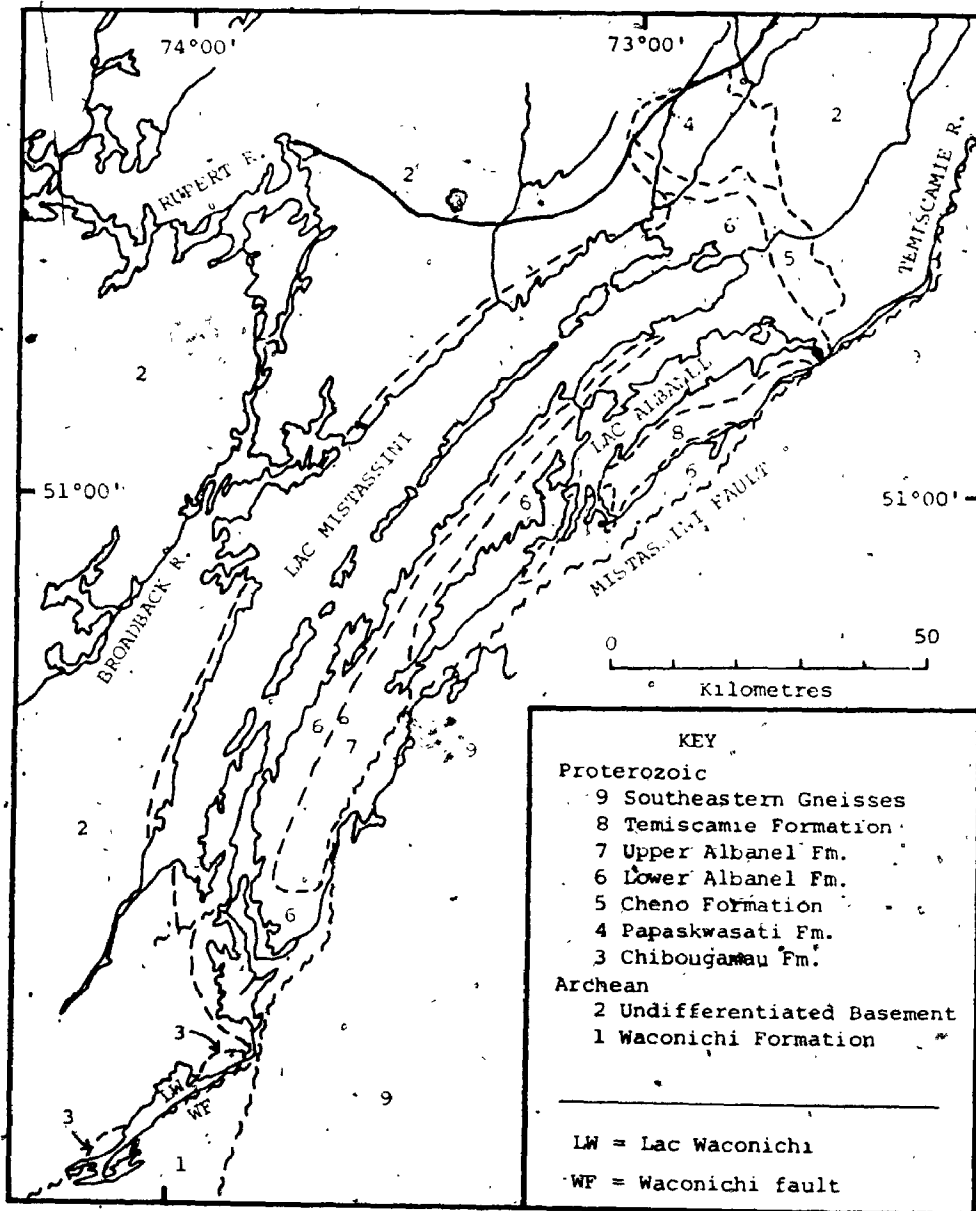


Figure 3. Generalized bedrock geology of the Lac Mistassini area. Compilation from Wahl (1953), Gilbert (1958), Neilson (1963, 1966), Deland and Sater (1967), Duquette (1970), Long (1973), Chown and Caty (1973), and Caty and Chown (1973).

basaltic flows and felsic pyroclastic rocks. Metamorphic rank of the amphibolite increases toward the Mistassini fault. Jones et al. (1974) gave a rubidium-strontium whole-rock age for the Roy Group of 2206 ± 85 m.y. which is post-Archean, but may be too young because of the proximity of some of their sample sites to the Grenville Front. A few small bodies of metaabbro are found within the Waconichi Formation.

A large area north of Lac Waconichi and west of Lac Mistassini is underlain by gneissic rocks. These rocks are quartzo-feldspathic granitic gneisses with biotite, hornblende, and garnet as the dominant accessory minerals. Dallmeyer (1974) determined the $40\text{Ar}/39\text{Ar}$ incremental release ages for two samples of hornblende from these gneisses as 2517 ± 40 m.y. and 2610 ± 40 m.y. The corresponding potassium-argon ages are 2504 ± 56 m.y. and 2607 ± 62 m.y. These rocks are therefore thought to have been last metamorphosed during the Kenoran orogeny.

A late intrusive body of plagioclase-rich hornblende syenite extends westward from the northwest shore of Lac Waconichi.

Proterozoic

Chibougamau Formation

The clastic rocks of the Chibougamau Formation (Long, 1973, 1974) overlie the Archean rocks with great unconformity around the eastern shores of Lac Waconichi

(Fig. 3). In terms of thickness and subcrop areas, the formation is dominated by varicoloured arkoses. Thick granitoid conglomerates cap the Lac Waconichi sections. Mixtites and laminated slaty argillites with dropstones are intercalated with the arkoses in the lower portion of the succession. The metamorphic rank of these rocks is lower greenschist, and they are thought to be early Aphebian in age (McGlynn, 1970, p. 59). An age of approximately 1000 m.y. for argillites from the Chibougamau Formation was determined by the rubidium-strontium whole rock method. The age is interpreted as a resetting of the rubidium and strontium abundances in the rocks by alkali metasomatism during the Grenvillian Orogeny (B.J. Fryer, pers. comm.). Because no dolostone clasts have been found in the Chibougamau Formation around Lac Waconichi, it is believed that this formation is older than the adjacent Mistassini Group (Fig. 3).

Mistassini Group

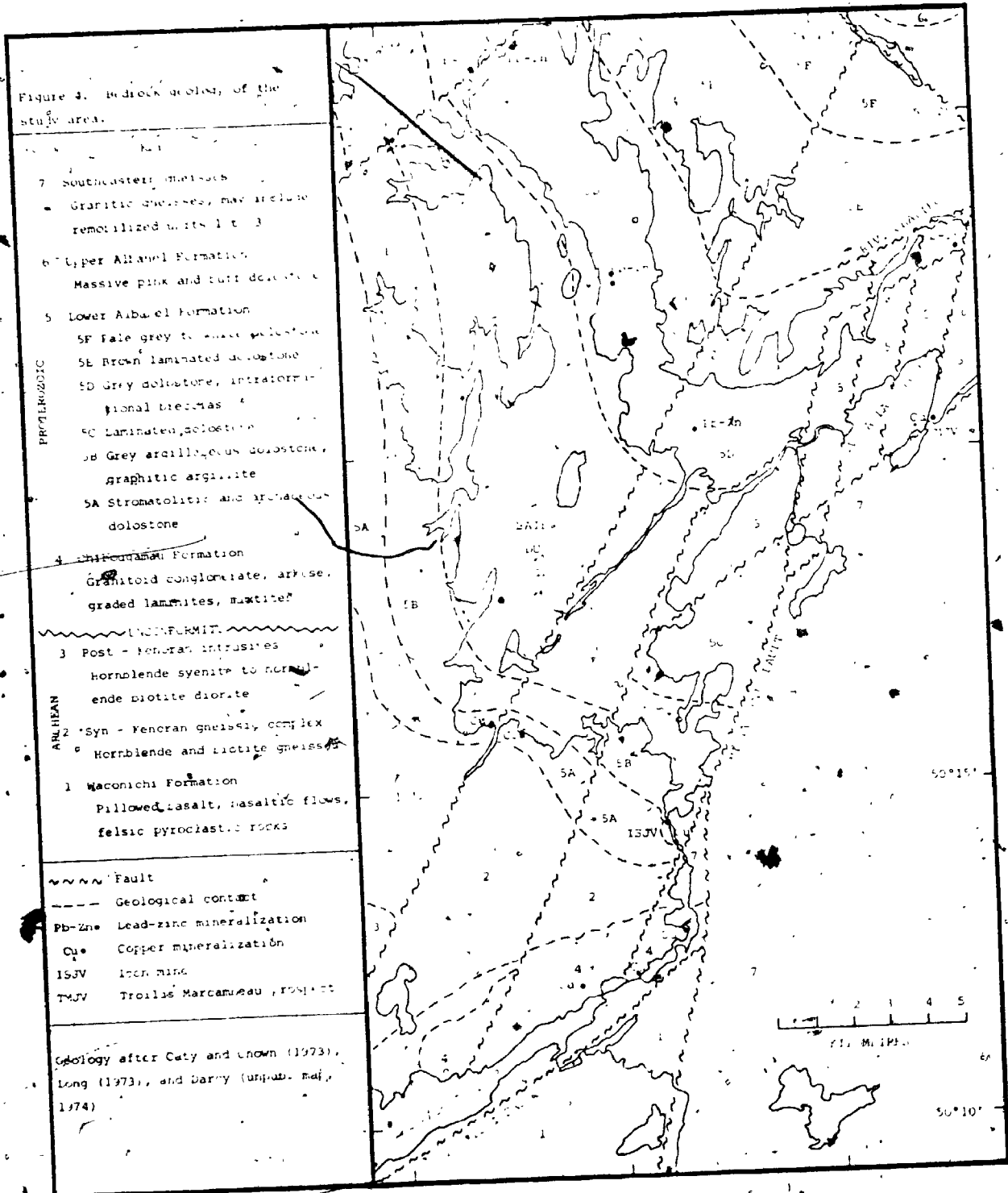
The stratigraphy of the Mistassini Group was first described by Bergeron (1957), but modifications and more detailed descriptions have since been provided by Neilson (1963, 1966), Deland and Sater (1967), Chown and Caty (1973), and Caty and Chown (1973). The group consists of five formations, from base to top: the Papaskwasati, the Cheno, the Lower Albanel, the Upper Albanel, and the Temiscamie (Fig. 3).

As described by Neilson (1966) and Chown and Caty (1973), the Papaskwasati Formation is a basal clastic unit up to 490 m. thick found only around the northeast end of Lac Mistassini. The dominant rock types are pale green to greyish white arkose, subarkose, and conglomeratic arkose. Because of similarity of rock types, thicknesses, and internal stratigraphy, the Papaskwasati Formation is said by Chown and Caty (1973) to be correlative with the Indicator Formation of the Otish Group, which is exposed 40 km. northeast of the Papaskwasati.

The Cheno Formation (Chown and Caty, 1973) is also restricted in distribution to the northeast end of Lac Mistassini and is a clastic rock, laterally transitional between the Papaskwasati and Lower Albanel Formations. Its lower member consists of sandstone similar to that of the Papaskwasati Formation, but with a dark grey to black matrix caused by fine sericite, chlorite, iron oxides, and graphite. Black sandy dolostone and black sandstone are present in the upper member.

Caty and Chown (1973) have subdivided the Lower Albanel Formation into six members (Fig. 4) which can be traced along the length of the Mistassini basin. A discontinuous regolith separates this formation from the underlying Archean rocks on the west and south sides of the basin. Two samples of the regolith from its southern limit at the Icon Sullivan Joint Venture operation consist of pebble-sized fragments of angular, exfoliated

Figure 4. Bedrock geology of the study area.



weathered gneiss cemented by dolomite and silica. The lowest member of the Lower Albanel Formation, member A, is a thin grey arenaceous dolostone containing small stromatolites. Member B is made up of laminated argillaceous grey dolostone intercalated with five graphitic argillite beds, the lowest of which is the host for the Icon Sullivan Joint Venture ore deposit (q.v., Fig. 5). Member C is a thick, grey flaggy-bedded argillaceous laminated dolostone. Member D is characterized by many intraformational breccias and black chert lenses in grey dolostone. Rusty-weathering laminated grey dolostones make up member E. Member F is transitional between the Lower and Upper Albanel Formations, changing from grey argillaceous laminated dolostone at the base to pink-weathering white massive dolostone at the top. Because the Lower Albanel Formation has a large subcrop area which is parallel to the glacial trend (Fig. 3), none of its rock types is distinctive of local or distant provenance when found in glacial sediments in the study area and none may be traced to a restricted source.

In contrast to the underlying argillaceous grey dolostones, the rocks of the Upper Albanel Formation are mainly pink and buff massive dolostones (Deland and Sater, 1967). These hard and dense rocks cap a prominent cuesta between Lac Albanel and Lac Mistassini.

The work of Wahl (1953), Neilson (1953, 1963), and Quirke et al. (1960) shows that the Temiscamie Formation is

made up mostly of sideritic iron-formation and ferruginous slate. Its subcrop is between Lac Albanel and the Mistassini fault; and it disconformably overlies the Lower Albanel Formation. Quirke et al. (1960) determined a potassium-argon age for argillite from the Temiscamie Formation of 1290 m.y., but they stated this age could only approximate the time of lithification of the rock because the sample was of uncertain origin and composition. Fryer (1972) found a rubidium-strontium whole-rock age of 1787 ± 55 m.y. for the Temiscamie Formation.

Southeastern gneisses

Most of the metamorphic rocks of the Grenville Province in this region are lithologically indistinguishable from the gneissic rocks of the Superior Province. The rock types are dominantly plagioclase-quartz gneisses with hornblende, biotite, and garnet as accessory minerals. Using the potassium-argon method, Quirke et al. (1960) determined the age of biotite from Grenville Province gneiss at the northeast end of the Mistassini basin to be 1000 m.y.

PART 2.2 Structure

The gneisses and metavolcanic rocks of the Superior Province generally strike east-northeast with moderate to steep dips, whereas the metamorphic rocks of the Grenville Province have a strong north-northeasterly strike.

The rocks of the Chibougamau Formation are found in an asymmetric, canoe-shaped synform on the downthrown (northwest) side of the Waconichi fault. Beds in the northwestern limb dip at between five and twenty-five degrees, while the southeastern limb has dips of seventy-five to ninety degrees. Shearing extends up to four hundred metres from the fault (Long, 1973).

Deland and Sater (1967) stated that the rocks of the Mistassini Group form a gently north-plunging syncline, the axis of which strikes north-northeast. The folding of the group was de-emphasized by Caty and Chown (1973), who thought faults were the most important structures affecting the Mistassini Group. Stockwell (1970, p. 52) placed the rocks of the Mistassini Group, Otish Group, and Chibougamau Formation in the Mistassini Homocline, a subprovince of the Superior Province.

In general, the rocks of the Mistassini Group strike northeast and dip at low angles toward the southeast. Near the Mistassini fault, the beds change their attitude abruptly to have northeast strike and steep northwestward dips. The Mistassini fault is an east-dipping thrust (Norman, 1940) which has been interpreted as the position of the Grenville Front in this region (Laurin, 1969). Many faults in the Mistassini basin are parallel or en echelon to it. The Waconichi fault is the northeastward extension of the Gwillim Lake fault, which has a minimum strike length of 100 km. (Duquette, 1972).

PART 2.3 Mineral Deposits

Copper

Occurrences of copper mineralization in the Chibougamau Formation (Fig. 4) have been known for many years (Low, 1905; Faribault et al., 1911, p. 212). The Portage showing (Guilloux, 1969) is found at the foot of the falls at the outlet of Lac Waconichi. Chalcopyrite occurs there in a narrow northeasterly-trending quartz-carbonate lens and disseminated in the enclosing arkose. The Bouzan showing (Guilloux, 1969) is found near the northern limit of Chibougamau Formation outcrop on the west bank of the Waconichi River. This occurrence is similar to, and probably an extension of, the Portage showing (Gilbert, 1958, p. 34). The Blondeau showing (Guilloux, 1969) is located 1200 m west of the outlet of Lac Waconichi, where large chalcopyrite grains occur with quartz and calcite in small fractures. Although repeatedly drilled, none of these showings has proved to be economic.

Caty and Chown (1973) and Gros (1975) reported two showings of chalcopyrite with quartz-carbonate in brecciated dolostone of member A of the Lower Albanel Formation on the south shore of Lac Mistassini west of the Icon Sullivan Joint Venture property (Fig. 4). Drilling of these showings encountered low copper abundances over narrow widths.

The geology of the Icon Sullivan Joint Venture copper

deposit (Fig. 5) has been described by Troop and Darcy (1973), Guilloux (1972), and Gros (1975). The ore is a coarse-grained quartz-carbonate vein ranging in vertical thickness from 0.3 m. to 13 m. which occurs with the lowest of the five graphitic argillite beds in member B of the Lower Albanel Formation. This concordant vein dips at about 6 degrees to the northeast, except where it has been upturned along the Mistassini fault. The richest ore is found on the north limbs of wallrock monoclines, the axial planes of which strike east-west and dip south (Plate 1). These monoclines reflect undulations in the bedding of member A of the Lower Albanel Formation caused by the presence of stromatolitic mounds (Troop and Darcy, 1973; Collins et al., 1974).

The mineralogy of the vein is simple. Quartz and ferroan dolomite are the most common minerals. The quartz is white and very coarse-grained. Terminated quartz crystals up to 3 m. long and 0.6 m. in basal diameter have been found (Plate 2). The ferroan dolomite is ankeritic, rusty-weathering, and medium to coarse-grained. A few large calcite crystals have been found with the sulphides. Chalcopyrite, pyrite, marcasite, pyrrhotite, sphalerite, bornite, and millerite are the sulphide minerals. Chalcopyrite is by far the most abundant, and it is usually very coarse-grained.

Most workers agree that this vein is of low-temperature hydrothermal origin, emplaced in dilatent

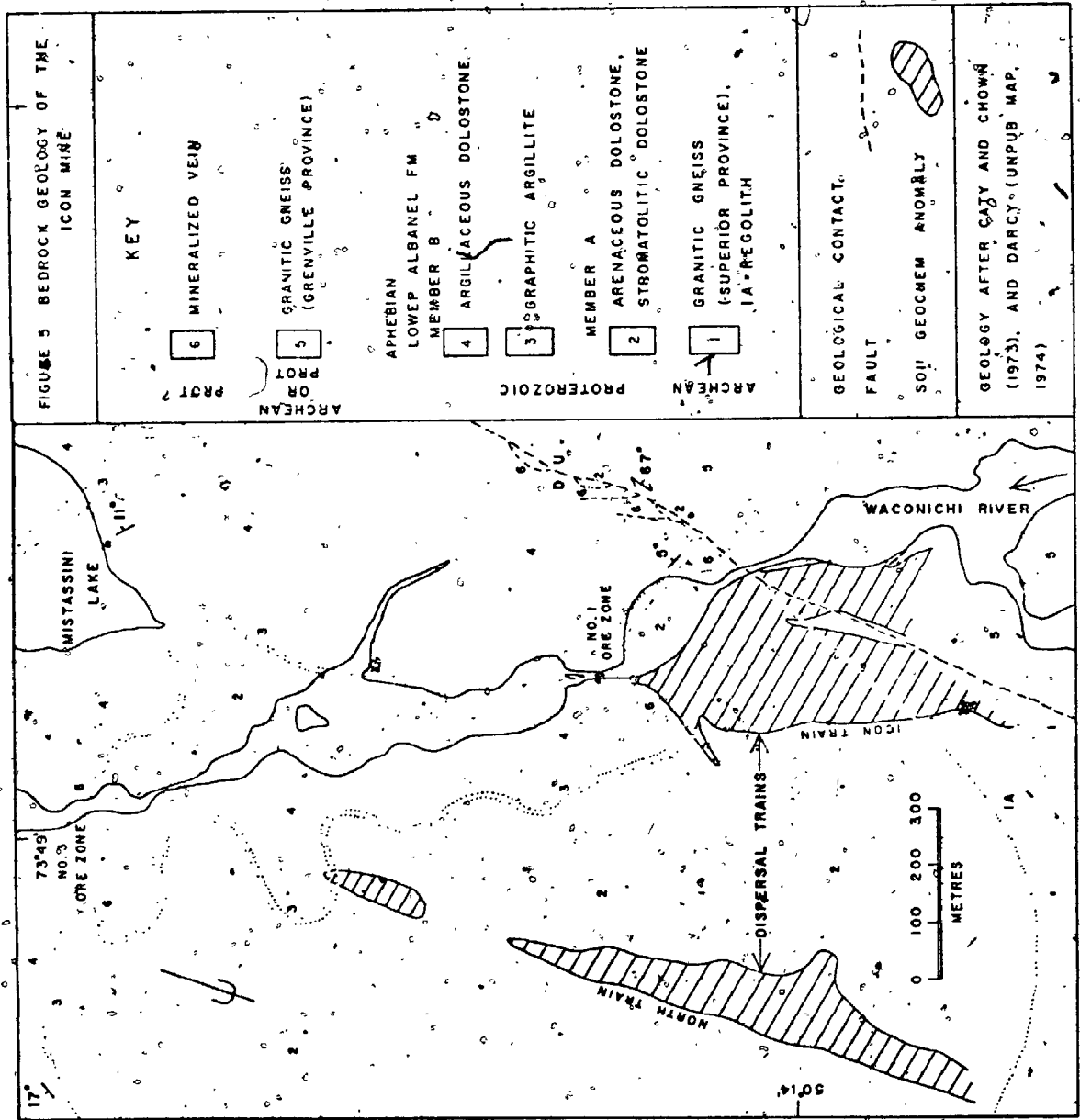




Plate 1. View to east along strike of number one ore zone at Icon mine. Vein is light-toned unit at base of section. North-dipping lens of sulphides (dark) is in white quartz-carbonate gangue on right side of vein exposure.



Plate 2: Quartz crystals in chalcopyrite in the number one ore zone at the Icon mine. Scale bar is 30 cm.

openings on a bedding-plane thrust fault associated with the Mistassini fault (Troop and Darcy, 1973; Guilloux, 1972; Collins et al., 1974; and Gros, 1975).

Between May 1967, when production began, and December 1974, the mine produced 43 million kilograms of copper from 1,460,450 tonnes of ore containing an average of 2.94 percent copper. The ore was exhausted and the mine closed in May 1975 (Fielder, 1975, p. 141).

The Troilus Marcarbeau Joint Venture copper prospect is located 13 km. north-northeast of the Icon mine (Fig. 4). The mineralized zone is in the fifth and uppermost graphitic argillite bed of member B of the Lower Alabert Formation. This deposit is mineralogically similar to the Icon deposit, except that quartz and chalcopyrite are less abundant. The mineralized zone has the same stratabound morphology, and its relationship to the Mistassini fault is the same as that of the Icon deposit (Forgeron, 1971; Gros, 1975).

Lead and zinc

Caty and Chown (1973) described several occurrences of galena - sphalerite mineralization in the area (Fig. 4). All these showings are within concordant, intraformational breccias of member D of the Lower Alabert Formation in the fractured hinges of folds near minor faults. The mineralization consists of coarse-grained galena, sphalerite, and carbonates between intraclasts and in fractures

in the breccias. Anthraxolite is commonly found as globules with the sulphides.

CHAPTER 3

QUATERNARY GEOLOGY

PART 3.1: Surficial Geology

Physiography and drainage

The study area includes the junction of four physiographic divisions of the Canadian Shield as defined by Bostock (1970) (Fig. 6a). The Abitibi Upland and Eastmain Lowland are underlain by Archean rocks of the Superior Structural Province. They are areas of low relief and poor drainage. The Mistassini Hills are subparallel hills and valleys partly inundated by Lac Mistassini. Most of the hills are subdued, north-facing cuestas formed of the rocks of the Mistassini Group. The Laurentian Highlands are underlain by the southeastern gneisses of the Grenville Province. This division has a peneplained upland surface and moderate relief.

The divide separating drainage into James Bay from that into the St. Lawrence River follows the Grenville Front over much of its length (Fig. 6b). The drainage basin that feeds Lac Mistassini corresponds roughly with the area of the Mistassini Homocline. The lake drains into James Bay via the Rupert River system. Westward

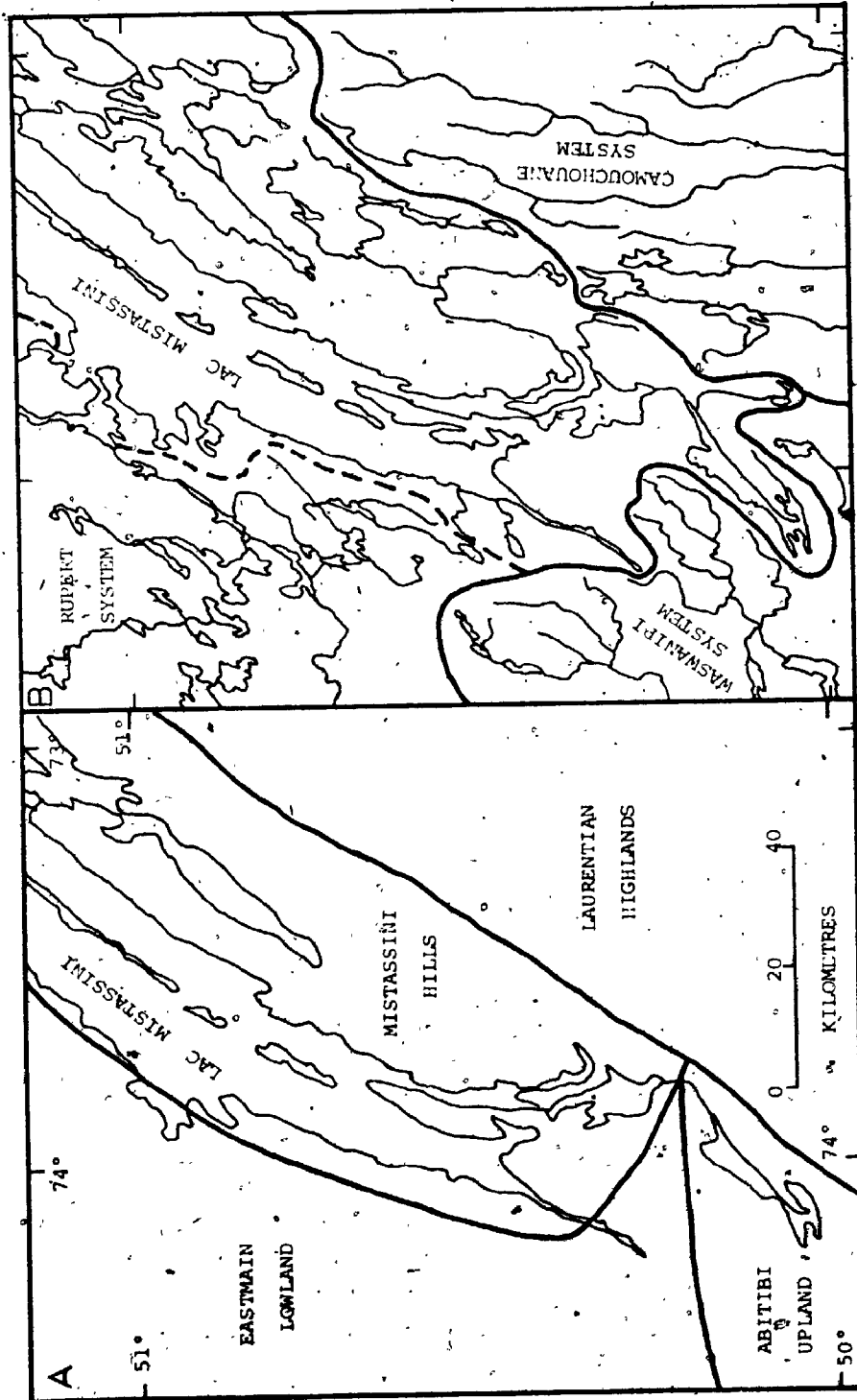


Figure 6. A) Physiographic regions of the Lac Mistassini - Lac Waconichi area, after Bostock (1970) and Geol. Surv. Can. Map 1254A. B) Drainage basins of the same area. Divide between Rupert System and Lac Mistassini is shown by the dashed line.

drainage of the Lac Mistassini - Lac Waconichi area is blocked by a divide having an elevation of about 440 m.

Bedrock-controlled landscapes

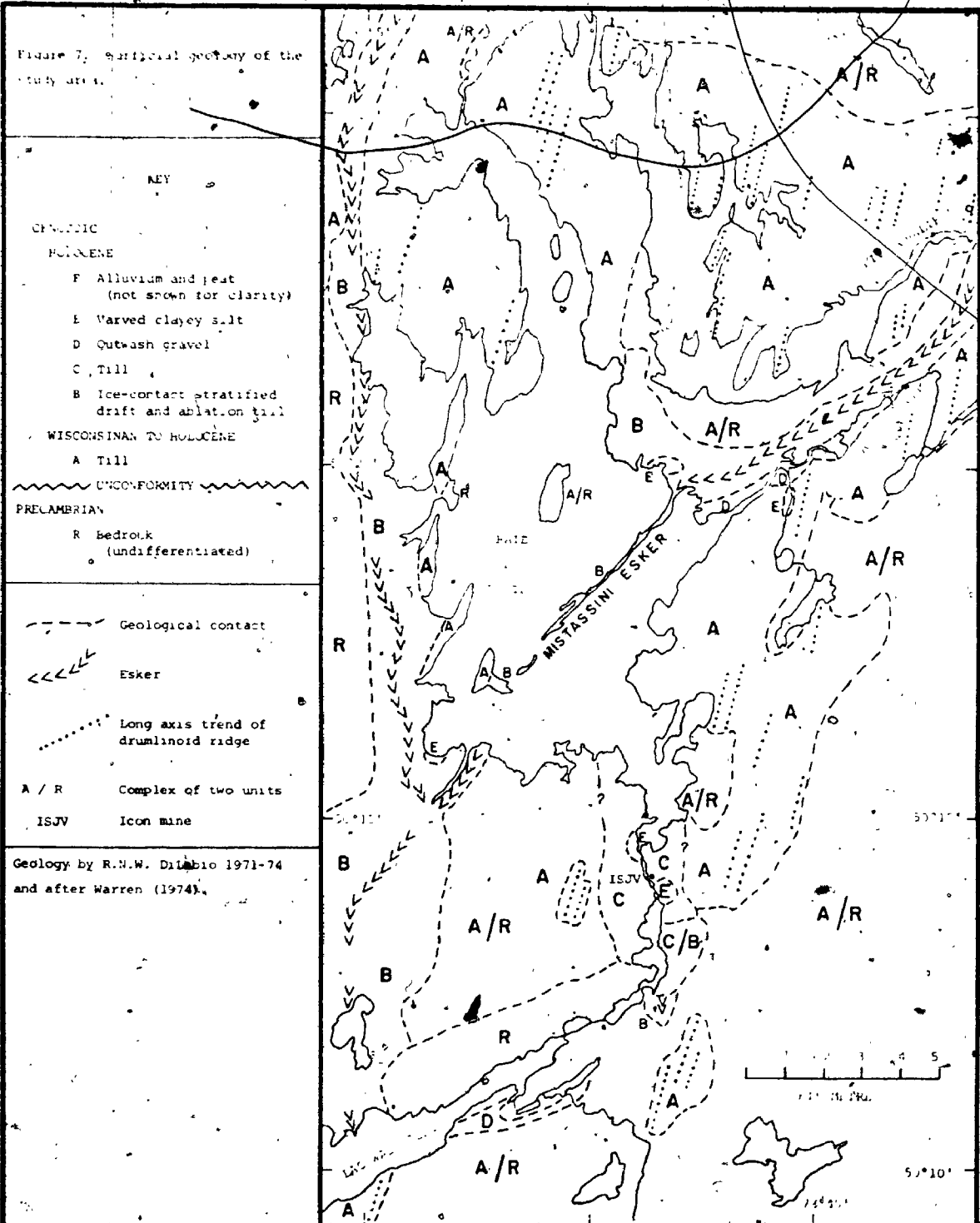
Although the bedrock of the region is almost completely covered by drift, there are a few areas of abundant outcrops (Fig. 7). Chibougamau Formation conglomerates are well exposed on top of the hills north of Lac Waconichi, and the more resistant units of the Mistassini Group are exposed in the Mistassini basin.

Within the study area, there are no large exposures of bedrock except those of the Chibougamau Formation. Drift cover is generally thick (5 to 35 m.), except near the drainage divides, where the bedrock surface rises to higher elevations; there the drift cover gradually becomes thin (less than 5 m.) but continuous.

In addition to the influence of the elevation of the bedrock surface on drift thickness, the structure of the bedrock has apparently affected the glacial flow path. Glacial flow features (flutings, drumlinoid ridges, and striae) tend to be parallel to the strike of the bedrock. This is best developed over Mistassini Group rocks where drumlinoid ridges are parallel to the arcuate structure of the bedrock units.

Drumlinoid landforms

Most of the area is a drumlinized till plain (Fig. 7



and Plate 3). Flutings and drumlinoid ridges (Prést, 1968) are the most common landforms; "ideal" drumlins (Flint, 1971, p. 101) having a shape like the inverted bowl of a spoon are rare. The drumlinoid ridges are up to 3 km. long, 500 m. wide, and 50 m. high, with straight sides and level crests. On the average, they are 1.8 km. long and 200 m. wide (Warren, 1974); and their long axes trend north-northeast. These features are common in areas of thick drift over relatively soft bedrock such as the Lower Albanel and Waconichi Formations. Most of the drumlinoid ridges are composed entirely of compact silty sand till, although some of those overlying the Waconichi Formation have bedrock bosses under their stoss ends.

Eskers and ice-disintegration landforms

Three eskers cross the area (Fig. 7). The south end of the generally northeast-southwest trending Mistassini esker (Ignatius, 1958) forms a long narrow peninsula in Baie du Poste of Lac Mistassini and terminates in Lac Waconichi. This esker is of the "giant" type, and was first described by Norman (1939), who mapped it to the northeastern end of Lac Mistassini, a total distance of about 115 km. The esker and its associated flanking sand deposits are up to 3 km. wide. Many steep-sided kettles adjoin the sharp-crested central ridge which is up to 40 m. higher than the surrounding terrain. The southward dip of bedding and crossbedding of the esker sediments in gravel

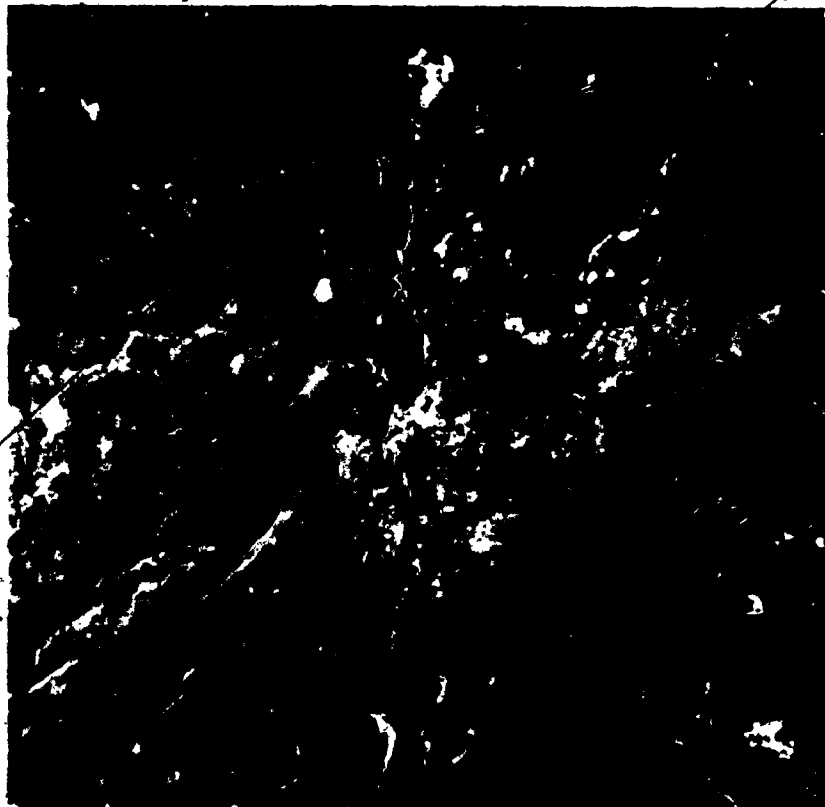


Plate 3. Glacial landforms near Waconichi River. Drumlinized ridges (1) are dominant; eskker segment (2) and ice-disintegration complex (3) also present. Compare to Fig. 7. From Canada Dept. of Energy, Mines and Resources air photograph A 15266-41. Scale bar is 2 km.

pits indicates that those sediments were deposited by southward-flowing currents. A smaller esker on the west side of Fig. 7, trends southward from Mistassini Post to join the Mistassini esker at the southwest end of Baie du Poste.

A small esker segment was found 3.5 km. south of the Icon mine and 2.4 km. east of the outlet of Lac Waconichi (Fig. 7). The esker is a sharp-crested ridge with a north-south trend. It is about 300 m. long, 25 m. wide, and 15 m. high. Its southern end onlaps the drumlinized till plain and its northern end disappears in an area of knob-and-kettle topography (Plate 3). The kames and kettles in this hummocky area are interpreted as ice-disintegration deposits. No other large areas of hummocky drift were found in the study area.

Lacustrine plains and lake terraces

Several authors (Norman, 1938, 1939; Shaw, 1944; Ignatius, 1958; Gillett, 1962; and Prest, 1970) have described and attempted to explain the glacial lake phases in central Quebec. The simplistic view of Norman (1939) that only one lake, Lake Barlow-Ojibway, formed there in front of the wasting Laurentide ice sheet is basically correct. Prest (1970) disputed Norman's (1939) claim that this lake extended into the Mistassini basin as a single body of water. Prest (1970, pp. 723-725) offered an alternative explanation by postulating that there were several separate

lake phases between 8,400 B.P. and 7,500 B.P. in central Quebec, having different outlets depending on the position of the ice margin during the Cochrane advance southwest of James Bay and a later stillstand east of the bay.

Wave-cut terraces were noted by Low (1896) around Lac Waconichi at an elevation of 393 m. and by Neilson (1953) and Wahl (1953) around Lac Albanel at an elevation of 404 m. No high level beaches have been found around the Mistassini basin, and perhaps these terraces mark the highest stand of a glacial lake there. It is not known whether Glacial Lake Opemiska (Prest, 1970, p. 724), with its highest eastern shoreline at 438 m. (Norman, 1938), was connected to the lake in the Mistassini basin, but the author believes they were separate lake phases because of the lower elevations of beaches and glaciolacustrine sediments in the basin.

Lacustrine plains in the study area are small peat-covered areas at low elevations. One of the highest of these surfaces is at the Icon mine, at an elevation of 381 m. Several occurrences of lacustrine silt have been mapped by Warren (1974) near the present elevation of Lac Mistassini (375 m.). Undoubtedly, many other small lacustrine plains will be found under low-level bogs.

Regional glacial flow patterns

The regional glacial flow patterns are best defined by the orientation of the long axes of drumlinoid ridges, by the orientation of striae and by the orientation of elongate

pebbles in till (Fig. 8). The drumlinoid ridges have little variation in their orientation within the map area, apparently being controlled by the general flow path of the glacier. On the other hand, striae on the bedrock surface range through forty degrees, glacial flow being locally re-directed by irregularities of the bedrock surface. There is no evidence in the orientations of the drumlinoid ridges or striae to indicate that glacial advance took place in more than one direction.

The orientations of the long axes of till pebbles were measured at 23 sites in the drumlinized till plain to determine the relationship between any preferred orientation of the till pebbles and the orientation of the long axes of the drumlinoid ridges (Fig. 8). Thirteen of these sites were chosen in a single drumlinoid ridge to search for variation in the preferred orientation of till pebbles in one of these landforms (Figs. 9, 10).

The data for each site were processed with a modified version called FABRIC8 of Starkey's (1970) computer plotting programme which produces scatter diagrams, contoured diagrams, mirror-image rose diagrams, and plunge-sensitive rose diagrams. A modified version called VECTOR of the computer programme of Andrews and Shimizu (1966) was used to calculate statistics applicable to the data. The statistics are tabulated in Appendix A.

Mirror-image rose diagrams plotted by FABRIC8 have been selected to represent the pebble orientation data

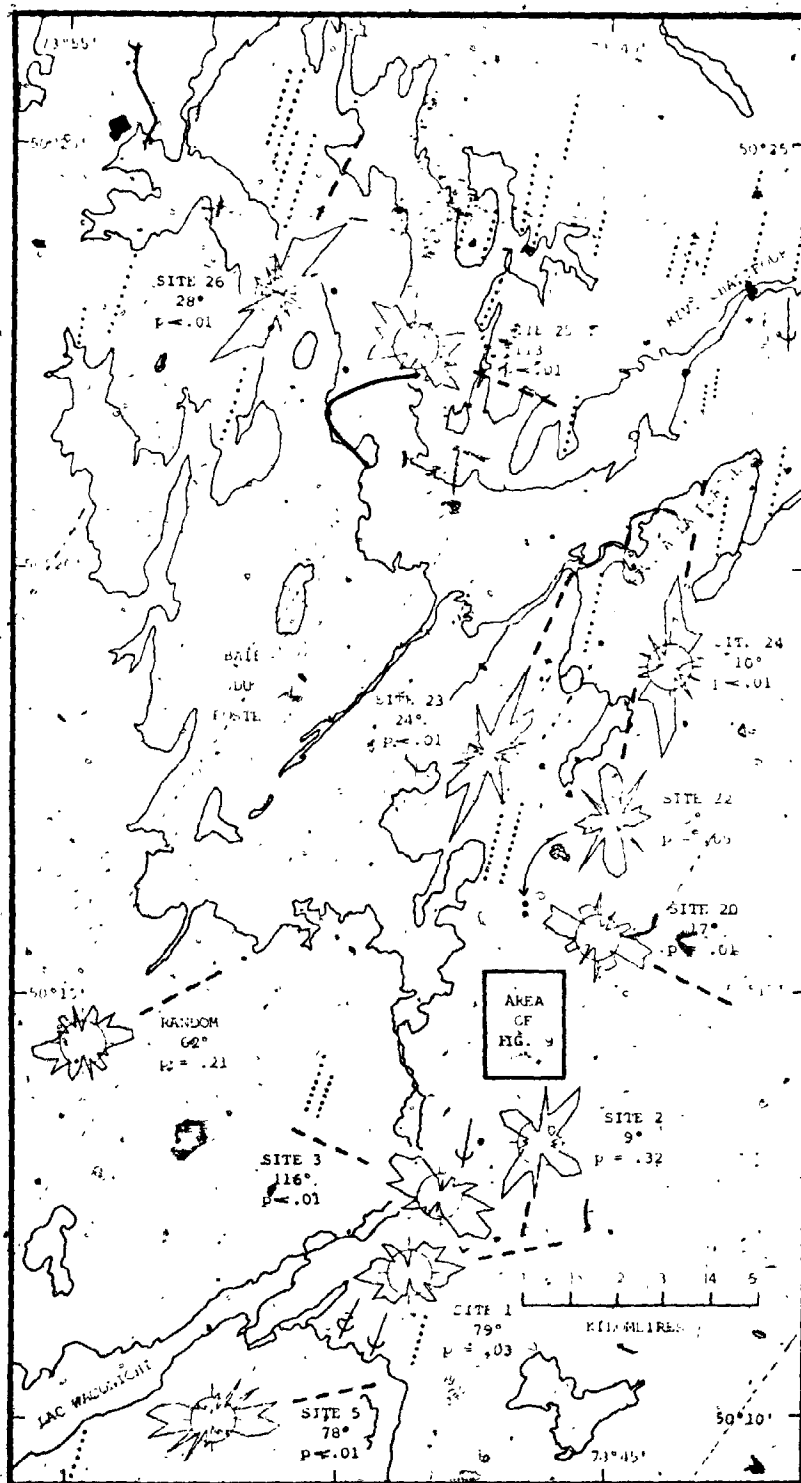


Figure 8. Mirfor-image rose diagrams of till-pebble orientations (unit A) in the study area. Each diagram has a scale circle at 5 percent and is accompanied by its site number, the calculated resultant trend (also shown by a dashed line), and p , the probability of randomness. Long axis trends of drumlinoid ridges are shown by dotted lines.

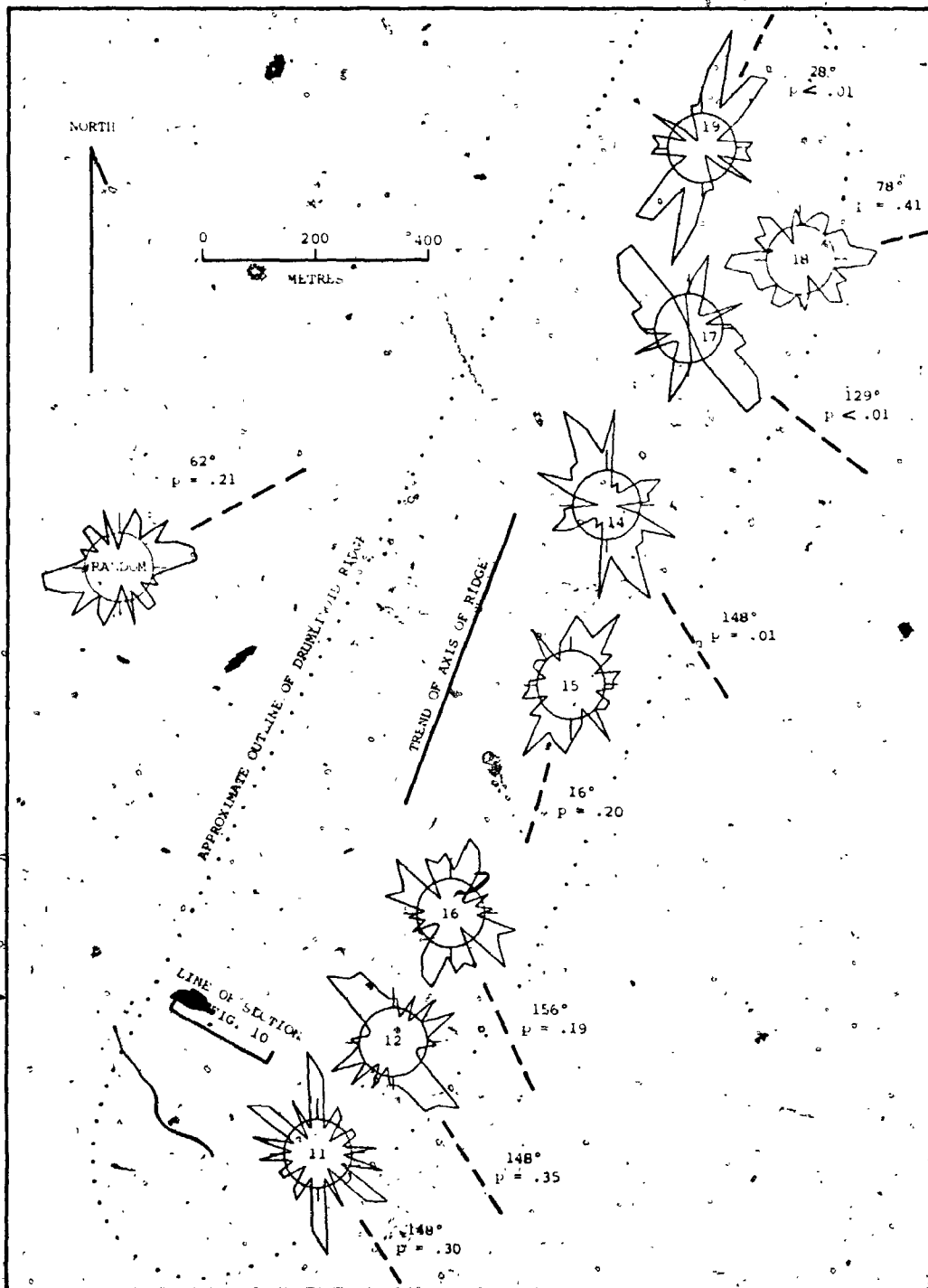


Figure 9. Mirror-image rose diagrams of till pebble orientations in a drumlinoid ridge (unit A). See Fig. 8 for locations. Site number as inside 8 percent scale circle. Calculated resultant trend is shown by labelled dashed line. p = probability of randomness.

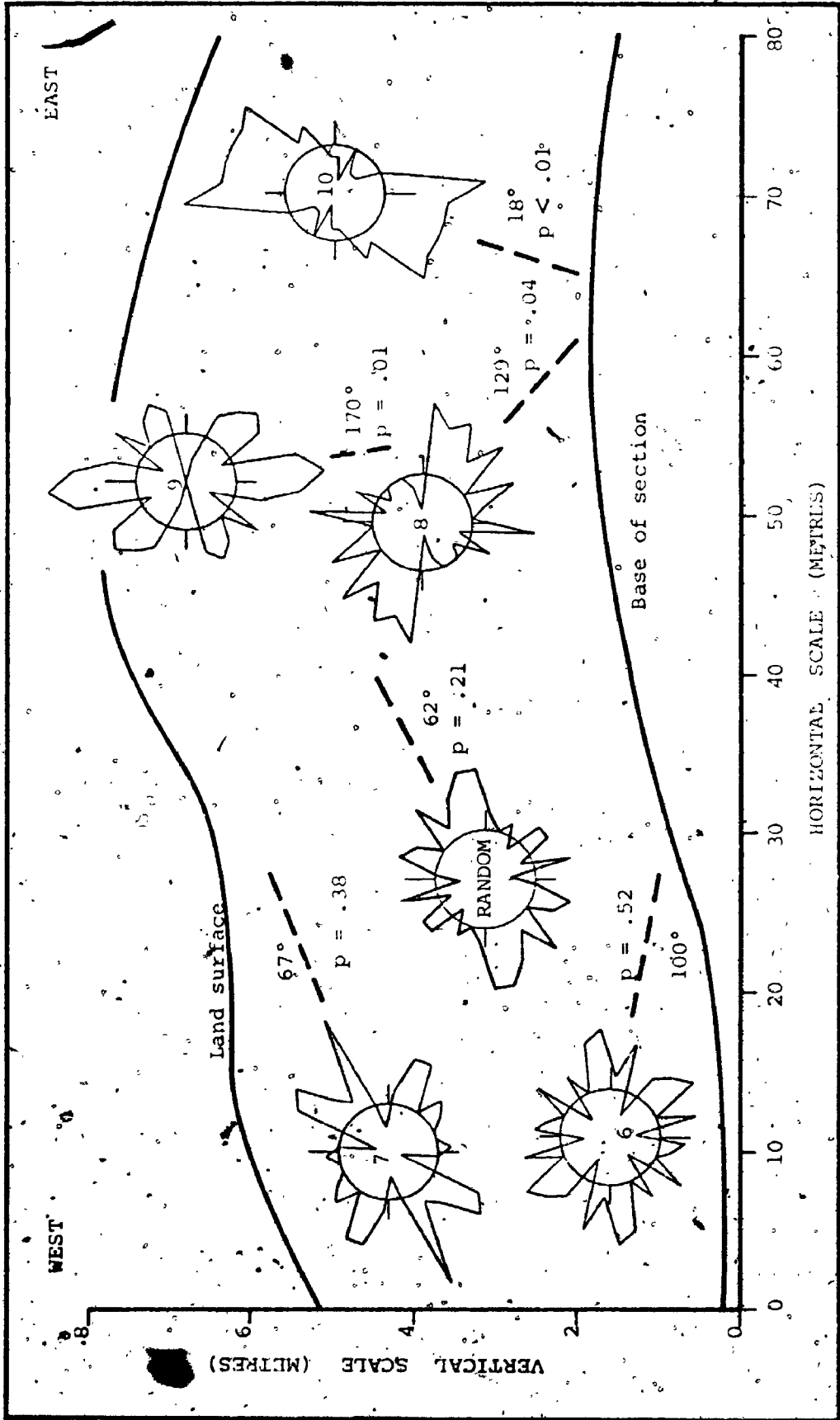


Figure 10. Mirror-image rose diagrams of till pebble orientations in a drumlin-oid ridge (unit-A). See Fig. 9 for location of section. Site number is inside 8 percent scale circle. Calculated resultant trend is shown by labelled dashed line. p = probability of randomness.

42

(Figs. 8, 9, 10, etc.). These diagrams show the orientations of the long axes of the pebbles, with observations grouped in classes of ten degrees. Direction of plunge is not considered. Accompanying each rose diagram are the statistics calculated by VECTOR based on the two-dimensional vectorial techniques of Curray (1956). Because Curray's (1956) equations do not consider the plunge of the pebbles, and the orientation angles are doubled before being resolved into vector components, cancellation of vectors does not occur. However, many distributions of till pebble orientations are bimodal or multimodal, implying the presence of more than a single population. A vector solution performed on such data often produces a resultant that lies between the modes and which may only be an artifact of the method of calculation.

VECTOR calculates the direction in degrees and the magnitude in percent of the resultant. It also uses the Rayleigh formula to test for randomness in the two-dimensional orientation distributions. The Rayleigh formula is expressed as follows:

$$p = e^{(-L^2/n)} (10^{-4})$$

where L = vector magnitude in percent

n = number of observations

p = probability of obtaining a greater vector magnitude by a pure chance combination of random orientations = prob. of randomness

No resultant is considered acceptable unless the value for p is less than 0.05, except for cases in which the data distribution is multimodal, and a subjective interpretation of the major mode may be made.

A set of random numbers from Dixon and Massey (1969) was treated in the same manner as a set of real observations and is included on all figures showing rose diagrams. This synthetic set was found to be less random than several of the real ones.

Of the rose diagrams on Figure 8, only diagrams number 2 and 22 have values of p equal to or greater than 0.05, and that is caused by their multimodal nature. The till at site number 5 was found to be interbedded with sand, and that at site 25 has been interpreted as colluvium, so they will not be considered further. The resultants at sites 23, 24, and 26, and the major modes at sites 2 and 22 have an en echelon or "herring-bone" pattern relative to the long axis orientation of the drumlinoid ridges, which is 15 degrees. The resultants found for sites 1, 3, 20 may be "transverse" to glacial flow (Holmes, 1941), or they may have been caused by creep of the till in the exposure. The latter is thought to have happened at site 1.

Within the drumlinoid ridge that was sampled in detail (Figs. 9, 10), only the diagrams at sites 14, 17, 19, 8, 9, and 10 have p values below 0.05, and of the unacceptable diagrams, numbers 12, 16, and 15 are of the simple multimodal type. The scatter at sites 6, 7, 8, 11, and 18 is

believed to have been caused by creep of the till. The resultants at sites 14, 19, and 9 and the major modes at sites 15 and 16 show a "herring-bone" pattern relative to the long-axis orientation of the drumlinoid ridge, 15 degrees. This pattern is similar to, but the reverse of that found by Shaw and Freschauf (1973) in flutings near Athabasca, Alberta. They noted that till pebble orientations on the flanks of a fluting converged downglacier toward the axis of the fluting, differing from the orientation of the ridge by about twenty degrees. In the present study, many of the pebble orientations diverge downglacier from the axis of the ridge (Figs. 9, 10). Only the diagram at site 10 has a resultant near 15 degrees.

An attempt could be made to explain the resultants at sites 1, 3, 20, 8, and 14, and the major modes at sites 12 and 18 by suggesting that the till was originally deposited by a glacial advance from the west or east, and later eroded and remolded into the drumlinoid ridges by an advance from the north-northeast. However, there is no stratigraphic evidence for such a phenomenon in the drumlinoid ridge studied in detail (Figs. 9, 10), and the striae at site 3 (Fig. 8), where the east-west trend is strongest in the till pebbles, are oriented at 10 degrees. No striae in the area have an east-west orientation. The simplest explanation is that the till in the drumlinized till plain was deposited by one glacial advance from the north-northeast, and the till pebbles are preferentially

45

aligned subparallel to that glacial flow direction (sites 2, 9, 10, 14, 15, 16, 19, 22, 23, 24 and 26) or are "transverse" to it (sites 3, 12, 17 and 20). The original orientations of the pebbles at sites 1, 6, 7, 8, 11, 18 and 25 have been changed by post-depositional creep of the till in the exposures.

PART 3.2. Stratigraphy and Provenance

Many authors have stressed the importance of understanding the stratigraphy and history of Quaternary sediments when exploration projects are undertaken in glaciated terrain. Studies by Dreimanis (1960), Skinner (1972), Shilts (1971, 1973, 1976), Kokkola (1975) and others have shown conclusively that differences in provenance and transport direction, mode of transport, and depositional style will produce basic differences in the properties of the glacial drift units at a single site, hence the units must be identified and their history deciphered so that they may be sensibly used as guides to ore.

This section contains descriptions and interpretations of the Quaternary lithostratigraphic units (Table 3) in the study area. The interpretations are based on outcrop tracing, stratigraphic position, internal structure, geomorphology, texture of the minus 4 mm. fraction, carbonate content of the minus 0.063 mm. fraction, and lithology of the 4 to 64 mm. fraction of samples of the units. Data from these analyses are tabulated in Appendix B.

Table 3. Quaternary units in the study area.

TIME-STRAT.	LITHO-STRAT.	MATERIALS	DISTRIBUTION	LANDFORMS	PROVENANCE	DEPOSITIONAL PROCESSES
	Unit F	Alluvium and peat	Discontinuous, widespread	Bogs and stream beds	Local	Post-glacial stream and organic sedimentation
	Unit E	Varved clayey silt	Discontinuous, widespread	Lacustrine plains	Regional	Glaciolacustrine sedimentation
	Unit D	Outwash gravel	Discontinuous, widespread	Valley fills	Regional to local	Glaciofluvial sedimentation
	Unit C	Basal till	Waconichi R. valley	Palimpsest on units A and B	Local	Glacial sedimentation
	Unit B	Ice-contact stratified drift and ablation till	Discontinuous, widespread	Eskers and hummocks	Regional to distal	Ice-wastage sedimentation
	Unit A	Basal till	Widespread	Drumliifoid ridges, flutings	Regional	Glacial sedimentation

Holocene

WISCONSIN
NAN 70
HOLOCENE

Unit A

This unit is the oldest and most widespread of the Quaternary units (Fig. 7). It is a massive hard till containing about 10 percent of clasts larger than 4 mm. The clasts are well abraded and striated. The minus 4 mm. fraction (matrix) of the till is a sandy silt (Fig. 11), according to Elson's (1961) classification. The minus 0.063 mm. fraction of this till contains between 15 and 30 percent carbonates, almost all of which is dolomite. The till quickly develops a subhorizontal fissility during freeze-thaw cycles above the frost line (Plate 4). The moist colour of the till matrix ranges from dark grey (5Y 4/1; Munsell, 1971) to dark olive grey (5Y 3/2) when unoxidized, to olive grey (5Y 5/2) when oxidized. Oxidation reaches 5 m. below surface at well-drained sites. Its massive structure, poor sorting, striated clasts, and its occurrence in drumlinoid ridges (Plate 5) and overlying striated bedrock indicate that unit A is a basal till. The orientation of drumlinoid ridges and striae, and stoss-and-lee relationships on the bedrock surface indicate that the till was deposited by a glacier advancing from the north-northeast.

No older Quaternary units were found under unit A. Its maximum exposed thickness is 15 metres, at the Troilus Marcambeau Joint Venture prospect. At the Icon mine, thin lenses of unit A were found between the bedrock and the younger Quaternary units (Fig. 25), and blocks and slabs of

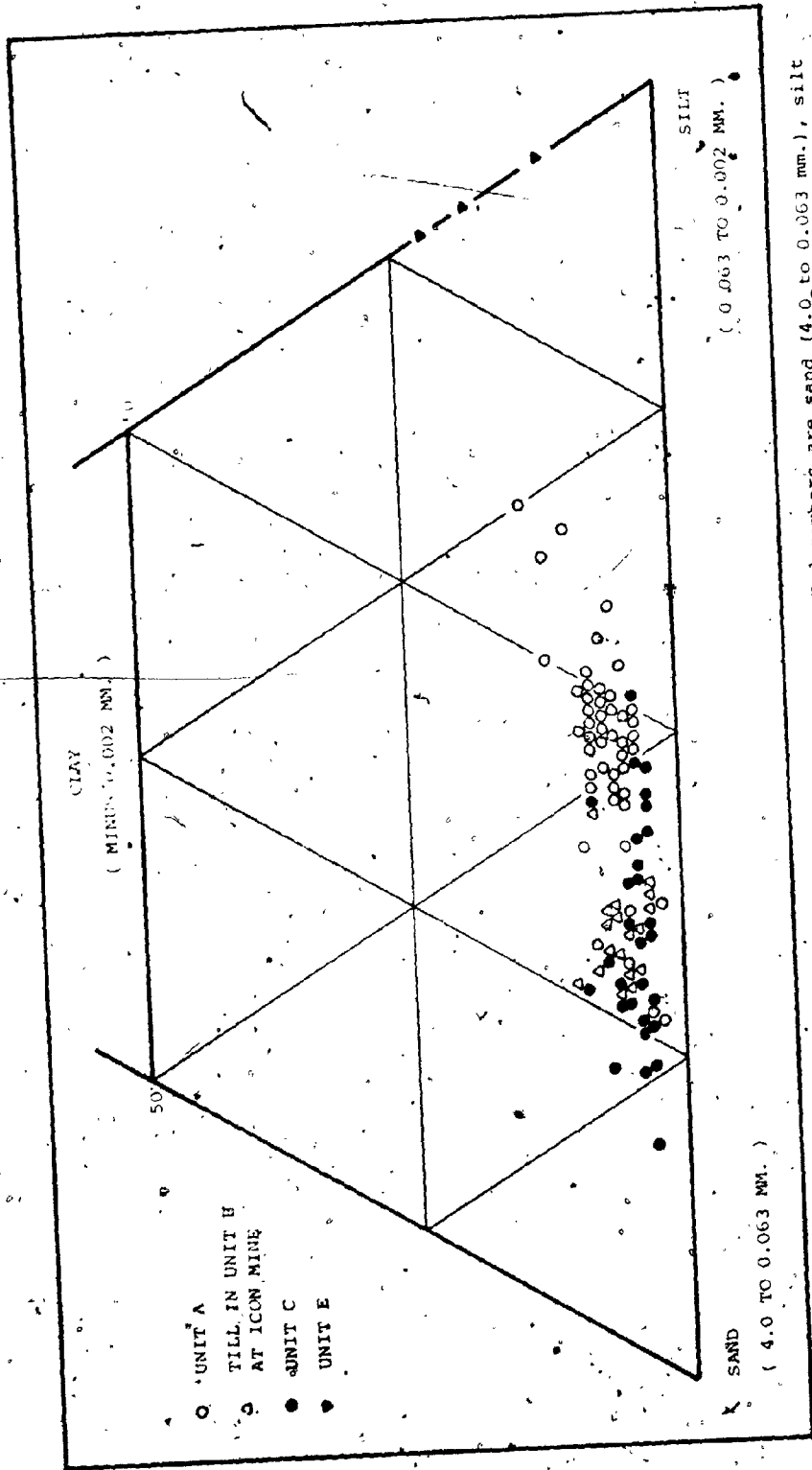


Figure 11. Ternary diagram of the texture of units A, B, C, D, and E. End members are sand (4.0 to 0.063 mm.), silt (0.063 to 0.002 mm.), and clay (minus 0.002 mm.).



Vertical exposure of unit A showing its fissile and gross texture.



Plate 5. Transverse section through a drumlinoid ridge composed of unit A. Till pebble orientations measured in this section are shown in Fig. 10.

unit A were found in unit C. The lithology of unit A in relation to the Icon ore deposit will be discussed in Chapter 4.

An experiment was performed to examine the within-site variability of unit A. A section of visually homogeneous till in a drumlinoid ridge was sampled in a subdivided vertical channel. Five samples consisting of 1 kg. of till matrix and 300 to 600 pebbles were taken from the channel, each being from a separate sequential 0.62 m. (2 ft.) interval of the channel. A sample was taken from the full length of the channel for comparison. The results of the analyses performed on these samples are presented in Figure 12.

The carbonate content, percent sand and silt, and median diameter have low vertical variability, and the results for the full channel sample agree well with the averages of the five interval samples. The abundances of the rock types in the pebble-sized clasts vary over ranges of up to 17 percent, but the averages of the interval samples are close to the values for the channel sample. The lowest sample, which contained 284 pebbles, is farthest from the averages in the pebbles; the others contained 400 to 660 pebbles. On this basis, a sample of at least 400 pebbles is believed to be representative of the lithologic abundances in the till, whereas a 1 kg. sample of the matrix is adequate for carbonate and textural analyses. The disagreement of the results for the full channel sample with

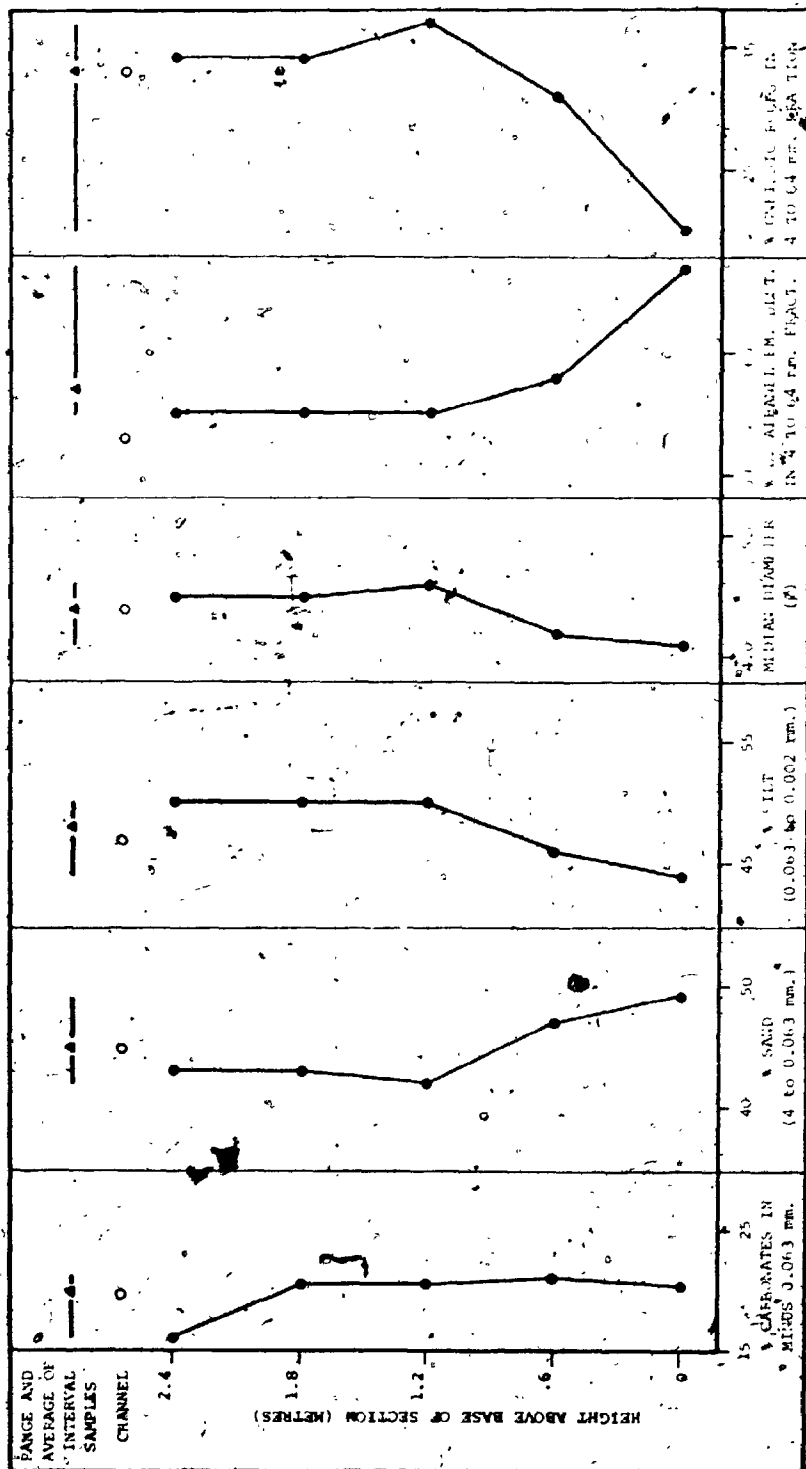


Figure 12. Vertical variability in lithology and texture of unit A in a section in a drumlinoid ridge 2.3 km. east of the Igon mine.

the individual interval samples is interpreted to mean that a grab sample from a small area may not be typical of the till at a given site; it is better to take the sample from the largest possible area or interval when determining the average properties of a till. When local or detailed variations are sought, sequential samples should be taken.

Unit B

Unit B consists of sand, gravel, and till. It forms the eskers in the area; in these, sand and gravel are the dominant sediments. The esker sediments are irregularly bedded, and normal faults are common. The grain size of adjacent beds ranges from fine sand to boulder gravel. The most gravelly parts of the eskers have no obvious bedding. The attitude of bedding and crossbedding is consistent with a southward-flowing depositional current.

The till in unit B occurs in two forms: as irregular bodies interfingering with the esker sediments, and as a discontinuous cover over unit A.

Where the till occurs as surficial material over unit A, its properties are variable. It is usually a loose, weathered bouldery sand till containing 20 to 50 percent of clasts larger than 4 mm. The clasts are poorly striated. Lithologically, the till is similar to unit A. Crude bedding exists in some exposures, and interbeds of sand and gravel are commonly so numerous that the sediment is a poorly sorted gravelly sand. Unit B is found in hummocky

landforms which mask the streamlined landforms of unit A.

Unit B forms a large part of the Quaternary sequence at the Icon mine. Because the interpretation of the sediments at the mine is important in the discussion to follow (Chapter 4), they were examined in detail. At Icon, unit B is a convex-upward lens of sand, gravel, and till beds with a maximum exposed thickness of 7.0 m. (Plate 6). It is overlain by unit C, and its structures are decapitated along the contact, which is sharp. Thin patches of unit A underlie unit B. The matrix of the till beds in unit B is a silty sand with a dark grey (N 4/) unoxidized colour and a light olive grey (5Y 6/2) oxidized colour. The pebble content is about 10 percent, and many of the pebbles are striated. The stratified drift is mainly massive fine sand; a few lenses of poorly sorted pebble to boulder gravel occur in it. Hairpin-shaped folds in the sand and gravel are associated with till lenses; their axial planes dip downslope relative to the surface of the unit (Plate 7). The till beds show gradational contacts with the sand and gravel and they interfinger with the sand as tongues 2 to 5 cm. thick. The bedding of the sand is contorted or absent near the till. These field relations and structures support an interpretation of unit B as ice-contact stratified drift and ablation till deposited during wastage of the glacier that deposited unit A. Tests of this idea are explained below.

The matrix of an ablation till theoretically should be



Plate 6. Mound of unit B (sand with till interbeds) about 30 m. downglacier from the subcrop of the number one ore zone at Icon mine. Less than 0.5 m. of unit C overlies unit B in this section.



Plate 7. Folded interbedded pebbly sand and till of unit B overlain by thin unit C (dark, with rootlets). Glacier that deposited unit C advanced away from the viewer.

coarser than that of its associated basal till (Goldthwait, 1971, p. 17). Comparison of the till from unit B to unit A, its most probable associated basal till (Fig. 11), shows that the till in unit B is coarser than unit A, but the separation of fields is poor. Using different particle size ranges in order to emphasize the coarse sand and granule (4.0 to 0.5 mm.) fraction improves the separation (Fig. 13) of fields. Another approach to this problem is to compare the cumulative curves of the tills (Fig. 14). The envelopes for the units show that the till in unit B is coarser than unit A, and the overall similarity of the particle size distributions suggests that the tills are derived in part from the same glacial debris load with the addition of relatively coarse englacial debris to unit B.

Ablation tills are formed at and near the glacier margin during ice wastage. The debris from ice-melting slides or flows off the glacier and/or gradually subsides onto the substrata. The sediments produced by these processes may contain more of the debris that was held englacially than the associated basal till, which is largely derived from the basal debris load of the glacier. Debris becomes part of the englacial load by compressive flow at obstructions and by erosion of bedrock bosses which protrude above the basal part of the glacier. In this way even soft debris can be transported for long distances with only minor comminution, deposition occurring in the terminal zone of the glacier by wastage. Tills which have been

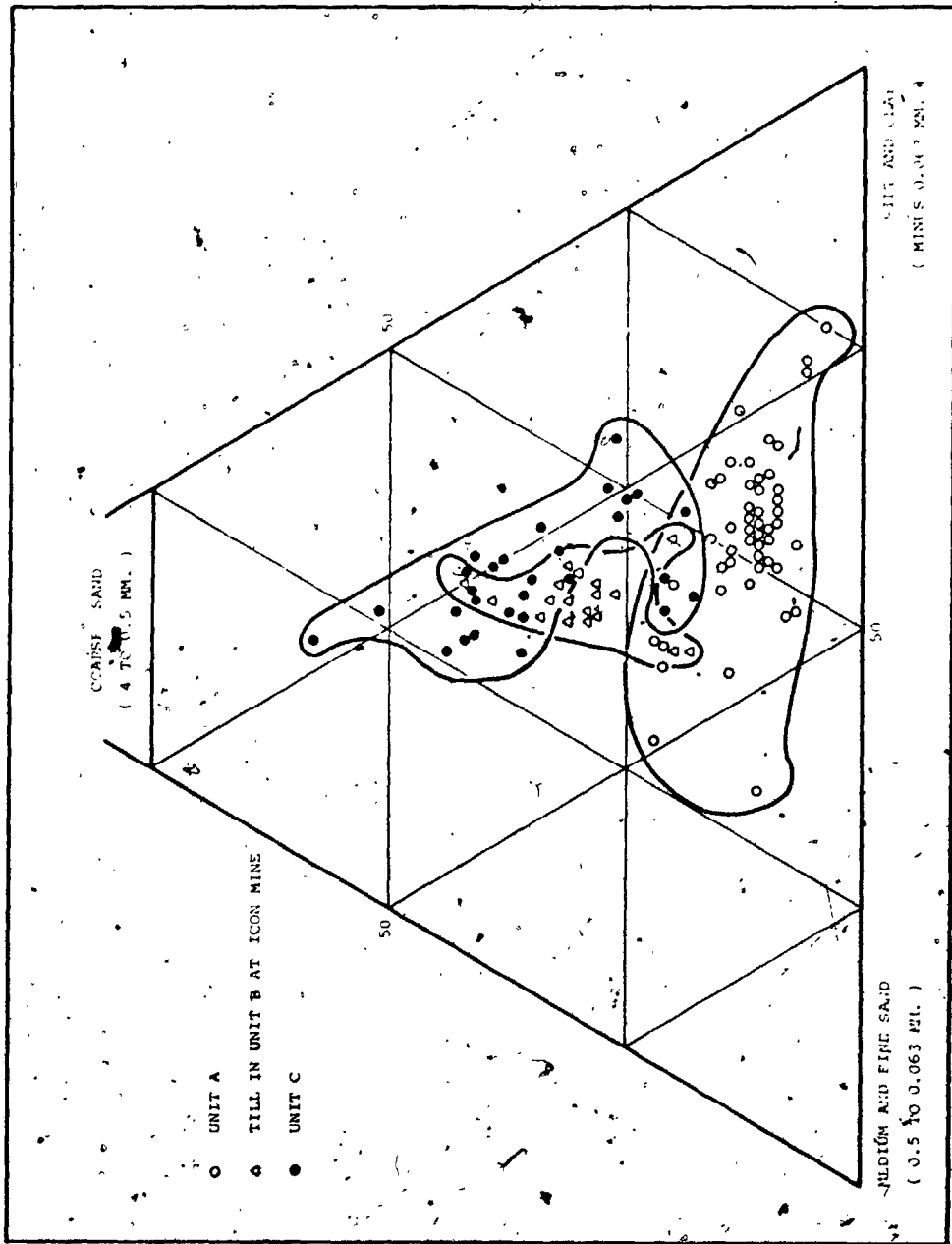


Figure 13. Ternary diagram of the texture of units A, B, and C. End members are coarse sand (4.0 to 0.5 mm.), medium and fine sand (0.5 to 0.063 mm.), and silt and clay (minus 0.063 mm.).

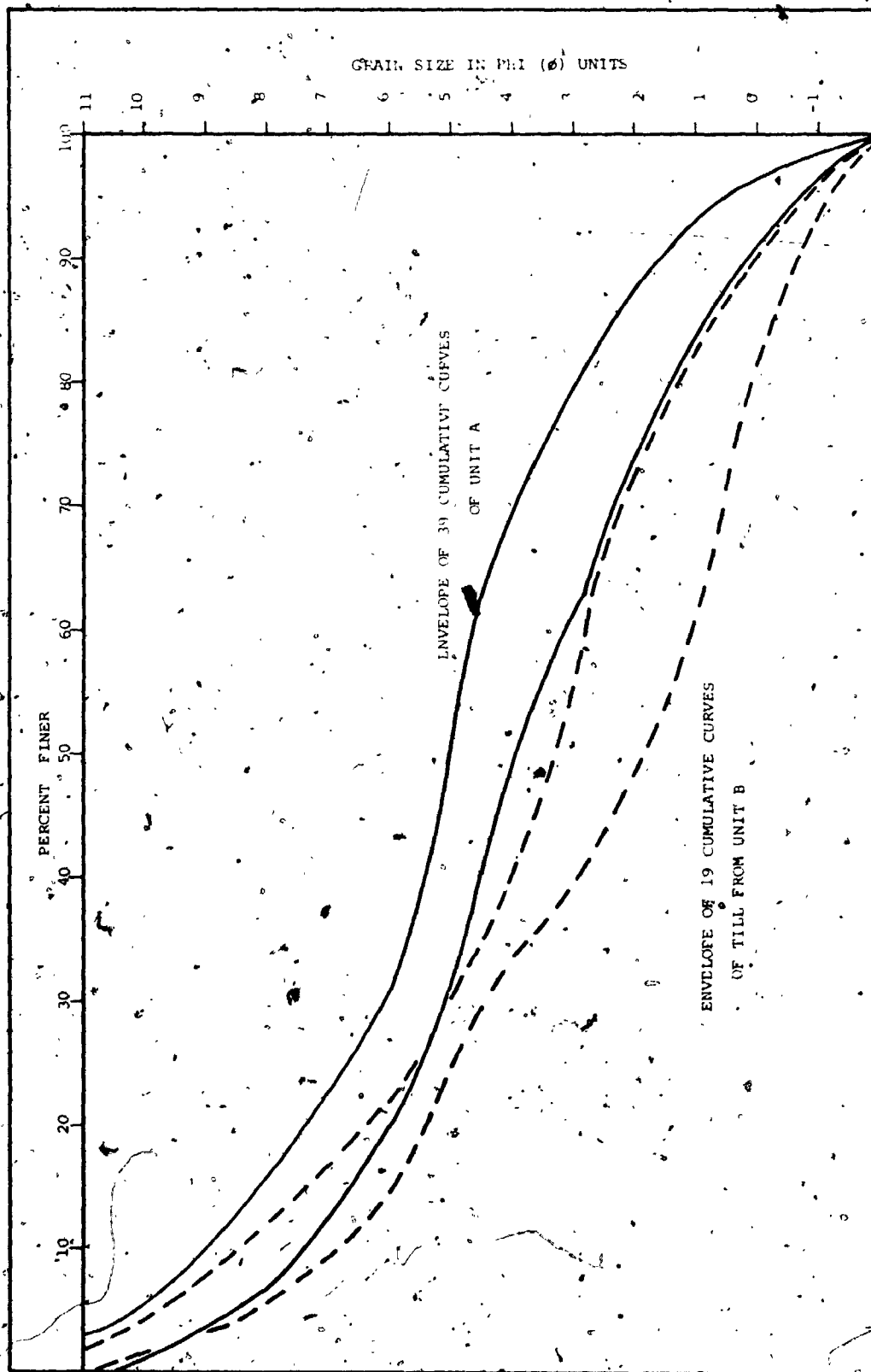


Figure 14. Particle size distributions of the less than -2ϕ (4 mm.) fraction of unit A and till from unit B.

interpreted as ablation tills on other grounds (internal structure, texture, and geomorphology) have been found to contain more far-travelled rock types than the associated basal tills (Dreimanis, 1976; Shilts, 1973). Transportation as englacial debris and deposition by downmelting may be the best way to explain the erratics derived from distant sources which are found near the Wisconsin glacial limit in North America (Flint, 1971, p. 176, p. 183).

If the till beds in unit B at the Icon mine are ablation tills, they may contain more of distal rock types than unit A. The rock types of three formations were selected as indicators of transport over great distances. The iron formation of the Temiscamie Formation and the sandstones of the Papaskwasati and Cheno Formations outcrop 85 km. and 150 km. upglacier from the Icon mine (Fig. 3). The combined abundance of these rock types was plotted against the total abundance of igneous and gneissic rock types (common rock types both locally and distally) in the 4 to 64 mm. fraction of samples from units A and B, (Fig. 15). It is obvious that unit B contains much more of the distal rock types than does unit A. The unit B field overlaps the part of the unit A field which contains the points for samples of unit A from the Icon mine.

This is interpreted to mean that both units were formed from the same glacier, unit A from basal debris, and unit B from basal and englacial debris. Together the two units make up a basal till-ablation till "couple", display-

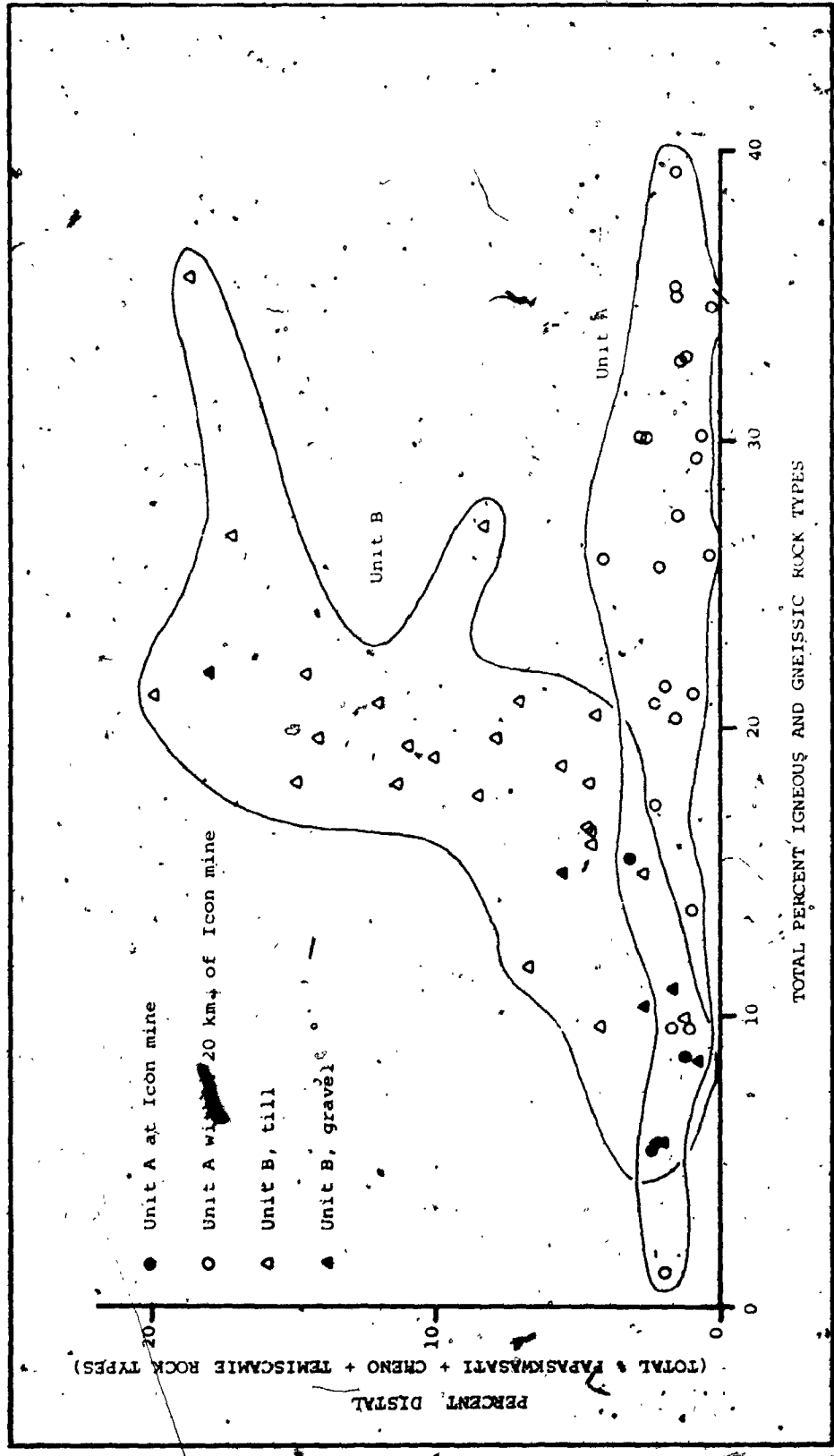


Figure 15. Abundance of distal rock types versus abundance of igneous and gneissic rock types in the 4 to 64 km. fraction of unit B from the Icon mine and unit A from the Icon mine and the surrounding area.

ing structural, textural, and lithologic differences caused by their differing processes of formation from the same glacier.

If unit A is to be elevated to formational rank at a later date, unit B should be included in the formation as a member. (A.C.S.N., 1970, Article 7a).

Unit C

Unit C has a small outcrop area, but because it contains the copper-bearing dispersal trains at the Icon mine, it is the most important of the Quaternary units for this study. Unit C is restricted to the Waconichi River valley.

Unit C is a till, the properties of which are determined by the local upglacier substrata. Where the till was derived from the bedrock, it contains 20 to 35 percent of clasts larger than 4 mm. Boulders up to 2 m. by 3 m. by 4 m. were seen in this till. The clasts are very angular and non-striated. Clast-to-clast contacts are abundant, giving the till a rubbly appearance (Plate 8). Angular, non-striated clasts of soft graphitic argillite are found in the part of the till that was derived from the Icon ore body. These features, together with the dispersal trains that are found in unit C (Chapter 4), are consistent with a short distance of transport for most of this debris and with the domination of crushing over abrasion during transport.

The till matrix is compact and sandy. Coarse sand is more abundant in this till than in units A or B (Fig. 13).



Plate 8. Rain-washed surface of unit C showing its coarse rubble texture. Child for scale is one year old.

On Figure 13, samples of unit C containing detritus incorporated from units A and B plot in the fine end of the unit C field. Samples containing abundant vein detritus plot in the centre of the field if they are unoxidized and in the coarse end of the field if oxidized.

The colour of the till matrix is variable. Where it contains abundant sand derived from unit B it is grey (5Y 5/1) when unoxidized, and light olive grey (5Y 6/2) when unoxidized. If detritus derived from member B of the Lower Albanel Formation, which constitutes the rocks overlying the vein, is dominant, the oxidized colour is olive brown (2.5Y 4/4). In the dispersal trains graphitic argillite from the vein colours the unoxidized till black (N 2.5/); iron-rich vein minerals give the oxidized till a dark brown (7.5YR 3/2) colour. Lenses of till cemented by malachite are pale green (5G 6/2); those cemented by limonite are yellowish brown (10YR 5/8) (Plate 9).

Where unit C overlies bedrock, striae having orientations between 10 and 20 degrees are found on the bedrock surface, although most of the bedrock surface is angular (Plate 10). The contact between unit C and units A and B is commonly deformed. Angular, fractured blocks and slabs of unit A, up to 40 cm. by 20 cm. by 20 cm., are displaced up to 80 cm. vertically from their original position and are found as isolated boulders in unit C (Plate 11). They were probably transported downglacier as well as vertically. Folded, stretched lenses of massive sand from unit B

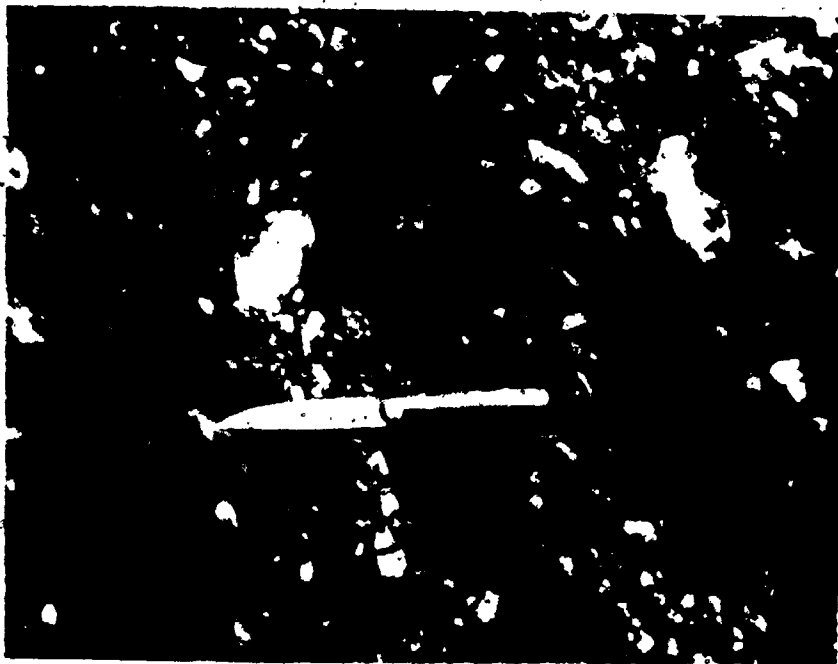


Plate 9. Unit C cemented by limonite and malachite.



Plate 10. Unit C overlying west end of the subcrop of number one ore zone at Icon mine. Note angular bedrock surface and dark lens of cemented unit C (Plate 9) in contact with vein. Glacier advanced away from viewer.

are found in unit C. One 25 cm. thick sand lens is in a tight, asymmetrical overturned antiform whose axial plane dips north at about 10 degrees (Plate 12). Its wavelength is about 1.0 m. and its amplitude 2.0 m. The contacts of the sand with the enclosing till are diffuse. Thrust faults in sand of unit B extend from the contact of unit C to 40 cm. vertically below the contact. These faults dip north at 15 degrees. The bedding of unit B is cleanly truncated everywhere along the contact, which is sharp and clearly defined by the textural and lithologic differences between the two units (Plate 13). Numerous grooves are found in the surface of units A and B where they are overlain by unit C. The grooves have amplitudes of up to 5 cm. and wavelengths of up to 20 cm., and they are oval in plan with major axis orientations trending 10 to 20 degrees (Plate 14). One anomalously large groove was found at the west end of the number 1 open pit (Fig. 26). It is 5.0 m. deep and 8.0 m. wide, and is cut into the vein on its west side and unit B on its east side. The base of this groove rises rapidly to where it is only 1.5 m. below the surface at a distance of 50 m. south of its deepest point.

Unit C is usually less than 1.0 m. thick. At many sites it is so thin that it is entirely above the C horizon of the soil profile, and in some cases it is only found in the upper half of the B horizon. It has a measured thickness of up to 6.0 m. (i.e. in the aforementioned large groove), but these measurements are vertical and not true



Plate 11. Angular blocks of unit A in unit C overlying in situ unit A. Glacier that deposited unit C advanced from right to left.



Plate 12. Oblique section through lens of sand (unit B) in unit C. Direction of glacial advance was away from the viewer.



Plate 13. Interbedded sand and till of unit B in sharp contact with overlying unit C. Glacier that deposited unit C advanced away from the viewer.

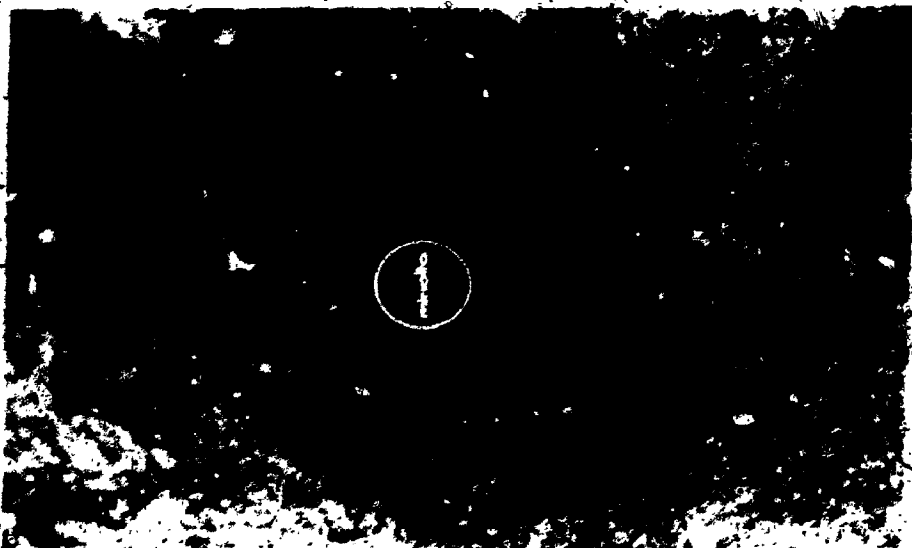


Plate 14. Horizontal exposure of unit C filling oval groove in surface of unit A. Glacier that deposited unit C advanced from right to left.

because unit C was deposited on pre-existing sloping surfaces (Plate 15). Its maximum true thickness is about 3.0 m. (Fig. 25). It is interpreted as a basal till.

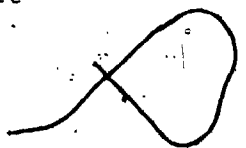
Unit C is at the surface over most of its area of occurrence. It is overlapped by units D, E, and F in small areas near the Waconichi River. The transition from unit C to the younger units marks a change from glacial sedimentation to fluvial and lacustrine sedimentation.

Although unit C can be seen to overlie units A and B in sections at the Icon mine, the genetic relationship between unit C and the older Quaternary units is unclear. It is believed that units A and B are a basal till-ablation till "couple", and that they are glacial deposits of regional extent. Unit C is a volumetrically small unit which is found only in the Waconichi River valley. To determine the relationship between unit C and the older units, exposures were examined near the subcrop of the number 3 ore zone at the Icon mine (Fig. 5). Unit C is present there as a bouldery silt till containing contorted lenses of silt, and as crushed and deformed pebble gravel. Neither of the older two units could be identified. Sections north of Baie du Poste contain only units A and B.

The southern edge of unit C is difficult to determine. Unit C thins rapidly south of the mine, and it is not found in sections outside the Waconichi River valley. The esker segment 3.5 km. south of the mine (Fig. 7) is interpreted as unit B. If the associated ice-disintegration complex is



Plate 15. Mining unit C from the Icon Train. Mound of unit B is light-toned area exposed by stripping in left background. Glacier that deposited unit C advanced from right to left.



interpreted as unit B which the unit C-depositing glacier overrode and upon which it stagnated, the ice-disintegration complex is the terminal position for the glacial advance that deposited unit C.

Unit C is thus interpreted as a basal till deposited during a readvance of a small tongue of ice up the Waconichi River valley. Unit C is most probably part of the drift unit containing units A and B; they are the products of a major advance (unit A), retreat (unit B), and minor readvance (unit C) of the same ice sheet.

Unit D

This unit is bouldery gravel which fills the Waconichi River valley. The sediment has an intact framework and is loose and crudely cross-bedded; the crossbedding is variable in attitude but is consistent with a southward-flowing depositional current. The clasts are generally well rounded and a few are striated; they make up 20 to 50 percent of the sediment volume. The matrix consists of compact coarse sand with a low content of fine sediment. Seven samples of the matrix of unit D have averages of 59 percent sand (4.0 to 0.063 mm.), 38 percent silt (0.063 to 0.002 mm.), and 3 percent clay (less than 0.002 mm.). The minus 0.063 mm. fraction of these samples contains an average of 20.9 percent carbonates. The unit fills a north-south trough in the bedrock surface at the Icon mine under the bed of the Waconichi River. It has a maximum thickness of 6 m.

in the middle of the trough.

Unit D overlies unit C at the north end of the Icon dispersal train (Fig. 25). The contact between the units is sharp and may be erosional. Unit D is the Quaternary unit that overlies most of the subcrop of the number 1 ore zone at the mine. Nevertheless, only two boulders and nine pebbles derived from the vein were found in it. Both boulders were well rounded quartz-carbonate gangue containing traces of chalcopyrite (Plate 16). The transport distance from their sources was probably less than 400 m.

The crudely crossbedded nature of this unit, its geometry, and the lack of vein rock types indicative of local erosion support the conclusion that unit D is a proximal outwash gravel which was deposited in the Waconichi River valley during final deglaciation. It has been recognized as sand and gravelly sand filling other valleys (Fig. 7).

Unit E

Unit E consists of silty varves which fill depressions in the older units up to an elevation of about 381 m. It has been found overlying units C (Plate 17) and D at the Icon mine, and overlies units A and B at lower elevations near Lac Mistassini. Unit E has a flat or lake plain landform, and it is up to 5.0 m. thick.

The varves are usually about 1 cm. thick, dominated by the silty (summer) layer. In a section overlying the east-



Plate 16. Boulder of quartz-carbonate vein rock in coarse gravel of unit D. Boulder is 1 m. above contact between unit D and southern subcrop edge of the number one ore zone.



Plate 17. Varved clayey silt of unit E draped over chalcopyrite-rich boulder in unoxidized unit C.

ern end of the number 1 ore zone of the Icon mine (Fig. 5), 210 varves were counted in an interval 2.0 m. thick. Because of their thinness, and their lack of dropstones, current bedding, and sand, they are interpreted as distal varves. Three channel samples of unit E have averages of 17 percent clay, 83 percent silt, and no sand. The same samples contain an average of 9.7 percent carbonates.

Unit F

Unit F consists of alluvium and peat. The alluvium has a high content of cones, twigs, and pelecypod shells. It is up to 2.0 m. thick on the bed of the Waconichi River, but was also seen as a thin (2 cm.) sand layer supporting large articulated pelecypod shells overlying unoxidized chalcopyrite-bearing unit C on the riverbank. One sample from the thickest section of alluvium contained 91 percent silt and traces of sand and clay. The sample contained 7.3 percent carbonates in the less than 0.063 mm. fraction.

The peat is found in poorly drained sites and often directly overlies unit E. It is well stratified, compressed, woody and fibrous. A maximum thickness of 1.0 m. of peat was seen. Prest (1970, p. 737) gives a radiocarbon date of 6,960±90 years B.P. for gyttja beneath peat near Chibougamau, 65 km. south of the study area. He states that this date indicates the onset of organic growth and not the time of deglaciation, which probably occurred a few hundred years before the development of the peat.

Quaternary history

Stratigraphic evidence presented by McDonald (1971), McDonald and Shilts (1971), Gadd (1971), Skinner (1973), and Grant (1975) for areas on the periphery of the province of Quebec supports a conclusion that the study area was covered by the Laurentide ice sheet from the start of the Wisconsin Stage until deglaciation during the Holocene. The study area is near the presumed starting position of the Laurentide ice sheet, the Labrador-Ungava plateau, and it would have been glaciated early in the history of the ice sheet. There is no evidence in the area to support a concept of glacial retreat north of the area during either the St. Pierre or Port Talbot Interstadial. Therefore, all the Quaternary units are "Wisconsinan to Holocene" in age, moreover, most of them are young, the products of deglaciation. Prest's (1970) postulated deglaciation sequence shows that the Lac Waconichi - Lac Mistassini area became ice-free between 7,800 B.P. and 7,500 years B.P., so all the units deposited during deglaciation (units B to F) are Holocene, i.e., post-10,000 years in age (Hageman, 1971).

The area was glaciated by the Laurentide ice sheet, which advanced from the north-northeast along the elongation of the Mistassini basin. The glaciation began in the early Wisconsinan, and through a series of oscillations, eventually culminated during the Nissouri Stadial (Dreimanis and Karrow, 1972); when the ice margin reached southern Ohio. Unit A was deposited during this glaciation, but it

is not known whether the till was deposited during the advance or recession, or both. Unit A is the material in the drumlinoid ridges of the area, which because of their streamlined morphology, are thought to have formed during active phases of glaciation, but the glacier may have been active discontinuously until deglaciation was complete. Because these landforms were ice-covered until about 7,700 years B.P. (Prest, 1970), the age of unit A can be defined no more narrowly than "Wisconsinan to Holocene".

While deglaciation was progressing and the glacier stagnant, unit B was deposited as eskers and ablation drift, a diachronous unit, i.e. it was deposited later in the north than in the south. Within the mapped area, it is entirely Holocene in age, as are all the younger units.

Starting from a short stillstand which was probably in Baie du Poste, a minor readvance up the Waconichi River valley deposited unit C. The readvance eroded the older Quaternary units and the Icon vein, which produced dispersal trains in unit C. The readvance went no farther than 3.5 km. south of the mine. Based on Prest's (1970) deglaciation sequence, unit C is about 7,700 years old.

Glaciofluvial activity followed, with meltwater streams flowing south from the receding glacier margin. This event produced the coarse proximal gravel of unit D.

With continued recession, a small proglacial lake became ponded in the Mistissini basin. The level of this lake was a few metres above the present level of Lac

Mistassini, with its outlet probably westward via the Broadback River system. During the lake phase, low-level varved sediments of unit E were deposited. The lake is interpreted to have existed about 7,500 years ago (Prest, 1970; Fig. 16w); its duration was at least 210 years because of varve counts. Further glacial recession to the northeast unblocked the Rupert River system, allowing drainage of the lake.

The establishment of organic growth and modern streams in the area produced unit F.

Regional glacial dispersal trends

The lithologic and textural properties of unit A have been mapped to detect dispersal of rock types from known sources and to determine the effect of variation in bedrock texture on the texture of till derived from it. Unit A was selected for this study because it is a basal till of regional extent and because it is the Quaternary unit that is stratigraphically closest to the bedrock.

The abundance of Upper Albanel Formation rock types in the pebble fraction of unit A is shown in Figure 16. This formation was chosen as an indicator because it has an outcrop belt (Fig. 3) which is favourable to the development of an orderly glacial dispersal pattern and because its rock types are distinctive. The abundance of Upper Albanel Formation pebbles in the till declines rapidly from values between 12 and 22 percent to a plateau of values between 7

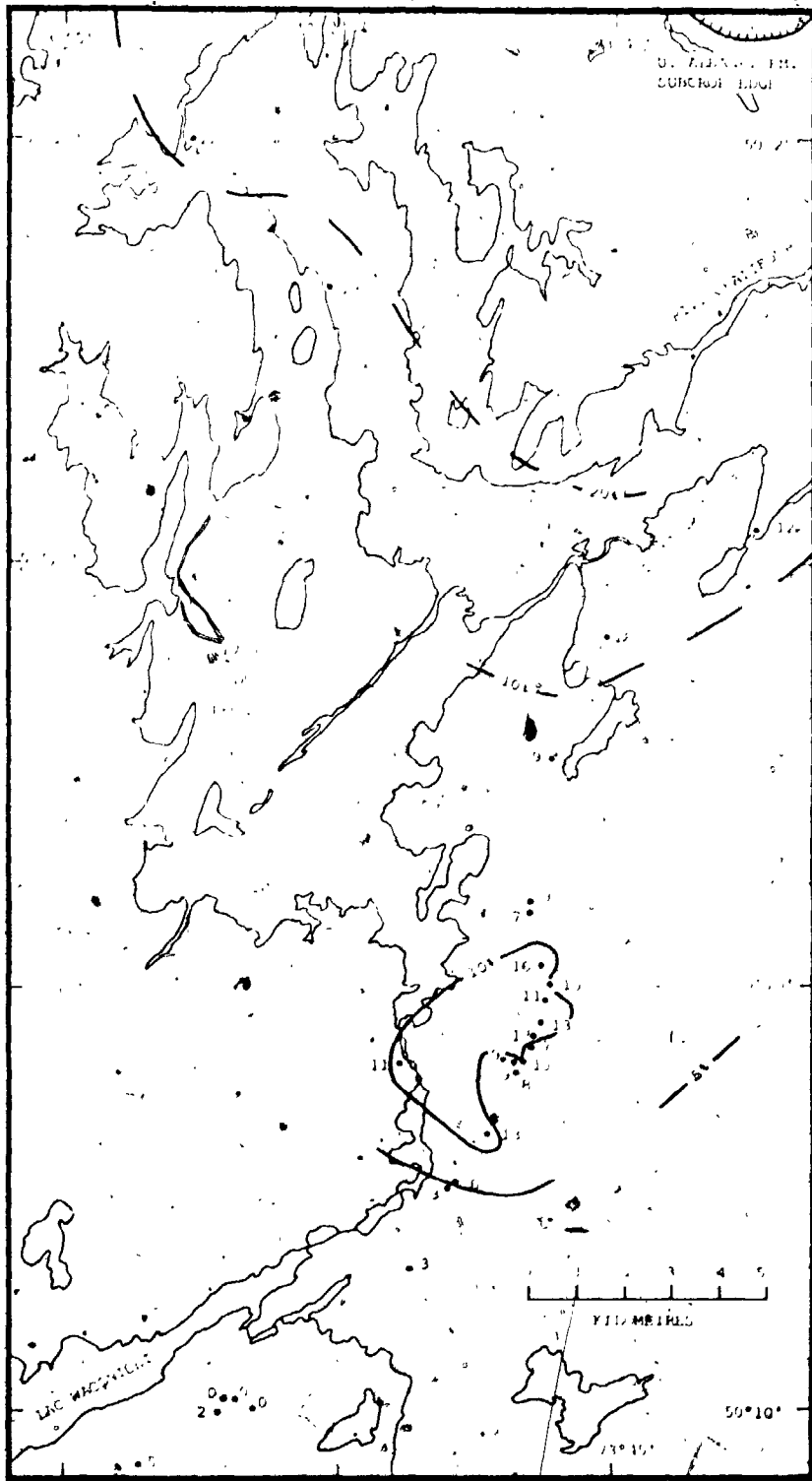


Figure 16. Abundance of Diptera A. and Formation rock types in the 4 to 64 mm fraction of unit A in the Lac Mistouini - Lac Wapichichi area.

and 16 percent. A second rapid decline to abundances of less than 5 percent is mapped on the downglacier side of the plateau. A regression line of abundance versus distance downglacier from the Upper Albnel Formation outcrop shows the abundance of these pebbles decreases at a rate of 0.45 percent per kilometre, but the scatter is high and the mapped pattern appears to be non-linear.

Granitic rocks, gneisses, and amphibolites form a large part of the bedrock in the area. They are grouped as igneous and metamorphic rocks for purposes of discussion, and their abundance as pebbles in unit A is shown on Figure 17. Their abundance is low where the till overlies the Mistassini Group, but it rises rapidly for samples that are only a short distance downglacier from the contact between the Mistassini Group and the igneous and metamorphic rocks. The highest abundances were found for samples taken southeast of Lac Waconichi, where unit A is thin and bosses of amphibolite with rubbly lee sides protrude through the glacial drift.

These analyses (Figs. 16 and 17) show that the pebble lithology of the till responds quickly to changes in the bedrock lithology. This fact, noticed in many other studies, hampers the use of pebble lithology for the mapping of a till, but conversely, it means that the pebble lithology of a till may be used to map bedrock, indirectly determine the glacial flow direction, and trace distinctive rock types to their sources..

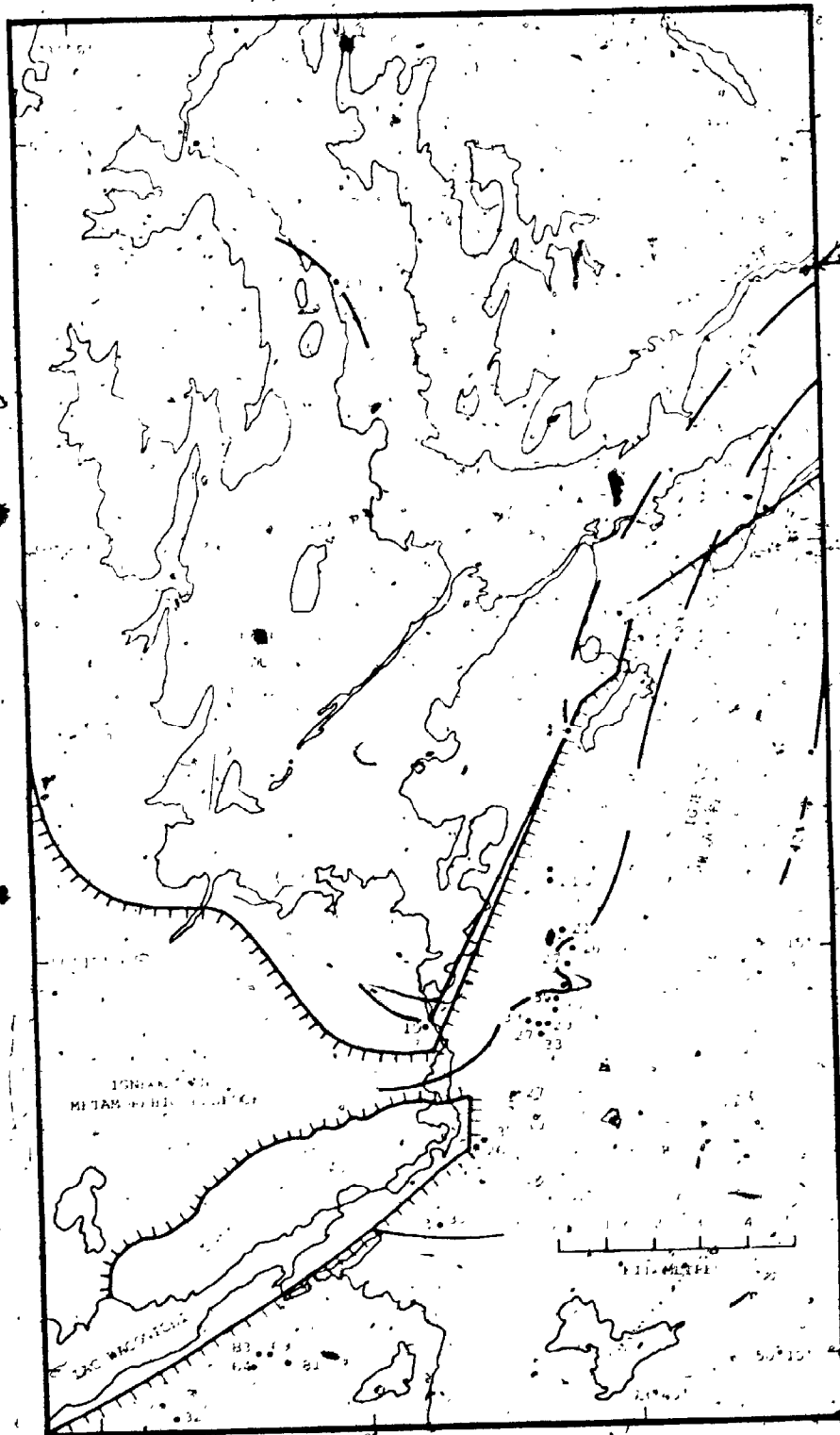
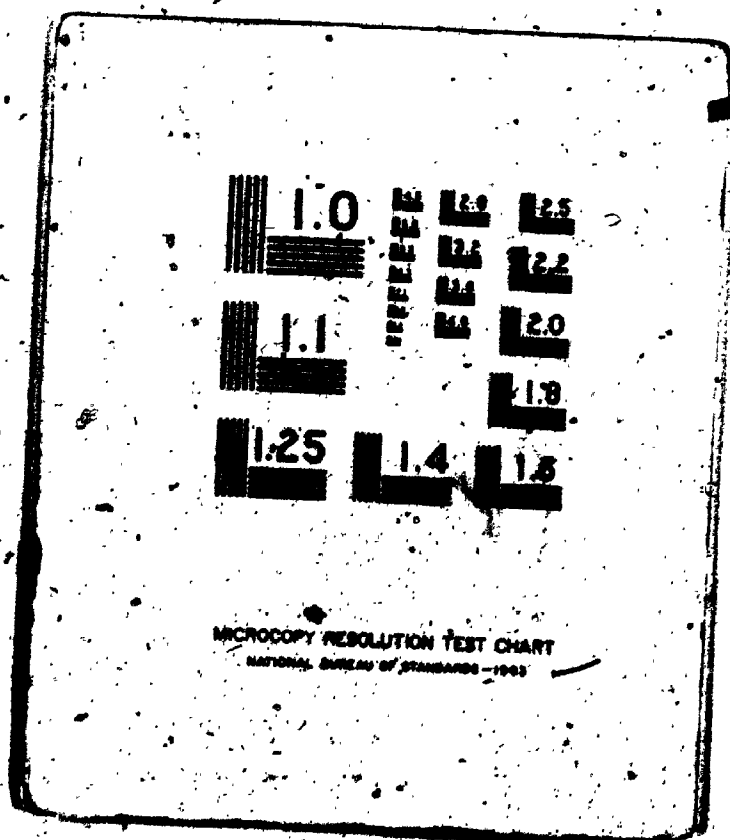


Figure 17. Abundance of igneous and metamorphic rock types in the 4 to 64 mm. fraction of unit A in the Lac Mistassini - Lac Macdonald area. Dashed lines are subcrop edges of igneous and metamorphic bedrock.

2 OF/DE 2



In the same way as the pebble lithology of the till responds to bedrock lithology, it was believed that the texture of unit A would rapidly show the effects of the underlying bedrock. The texture of the till matrix, shown by median diameter (ϕ_{50}) on Figure 18, responds slowly to changes in grain size of the bedrock. The content of igneous and metamorphic (coarse grained) pebbles (Fig. 17) in till overlying the same bedrock is more than double its content where it overlies Mistassini Group rocks (fine-grained). There is no similar trend on Figure 18; in fact, the till is everywhere relatively fine grained, except where it is thin and overlies amphibolites southeast of Lac Waconichi. Where the till is fine grained, the coarse grained bedrock is not masked and protected by thick till because the pebble lithology of the till (Fig. 17) reflects that bedrock. Examination of the abundance of carbonates in the minus 0.063 mm. fraction of the same samples (Fig. 19) showed that the carbonate content behaves in the same manner as the texture of the till. This was expected, because the carbonate content and texture of tills have been shown to be dependent (Dreimanis and Vaqners, 1971) in carbonate bedrock terrains. The carbonate content of the till matrix persists here over the igneous and metamorphic bedrock. Comparison of Figures 17, 18, and 19 shows that abrasion of coarse igneous and metamorphic bedrock cannot be the cause of the persistence of the fine texture of the till because the carbonate content does not decrease over

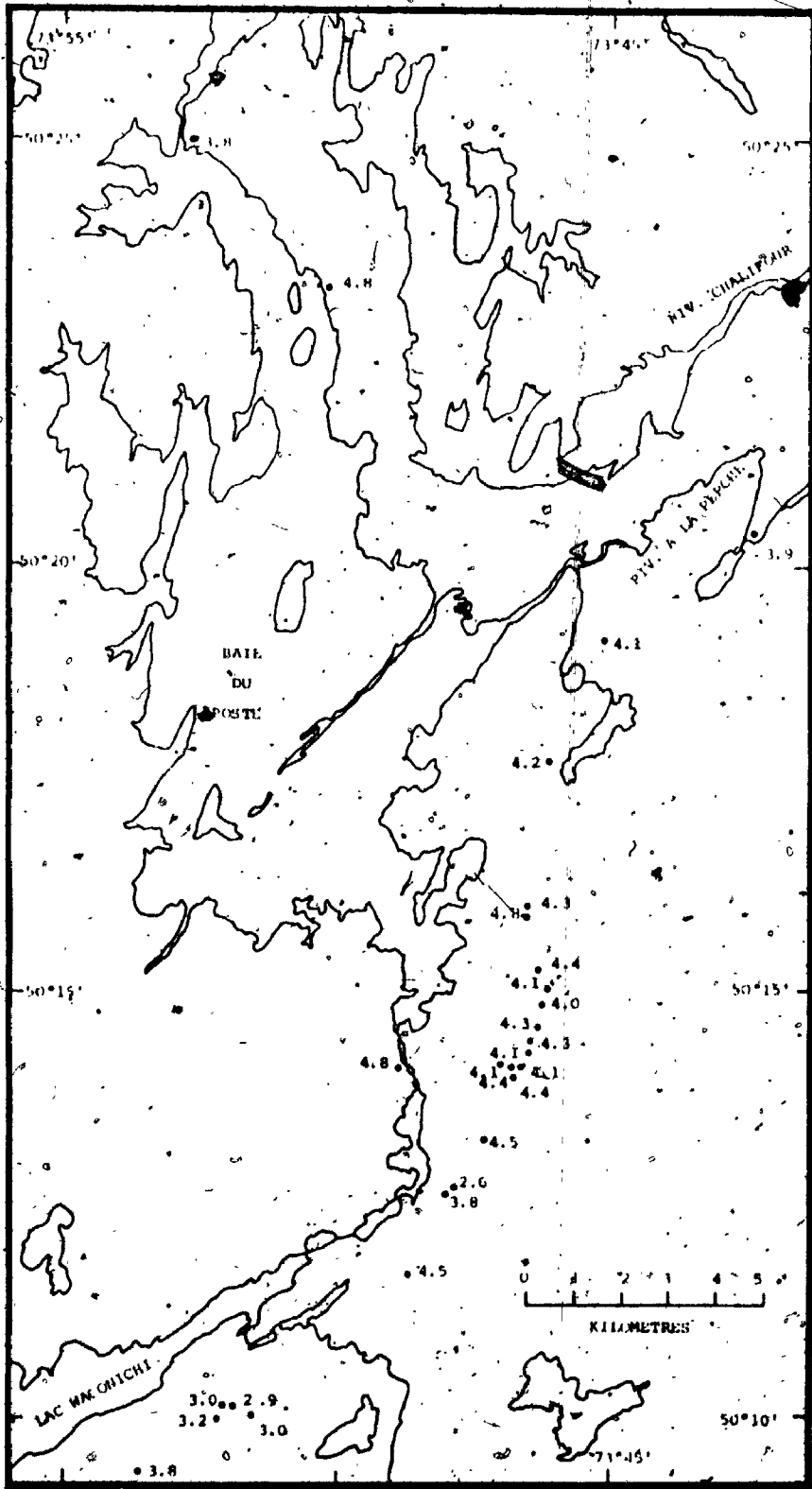


Figure 18. Median diameter (phi units) of the minus 4 mm. (-20) fraction of unit A in the Lac Mistassini-Lac Macopichi area.

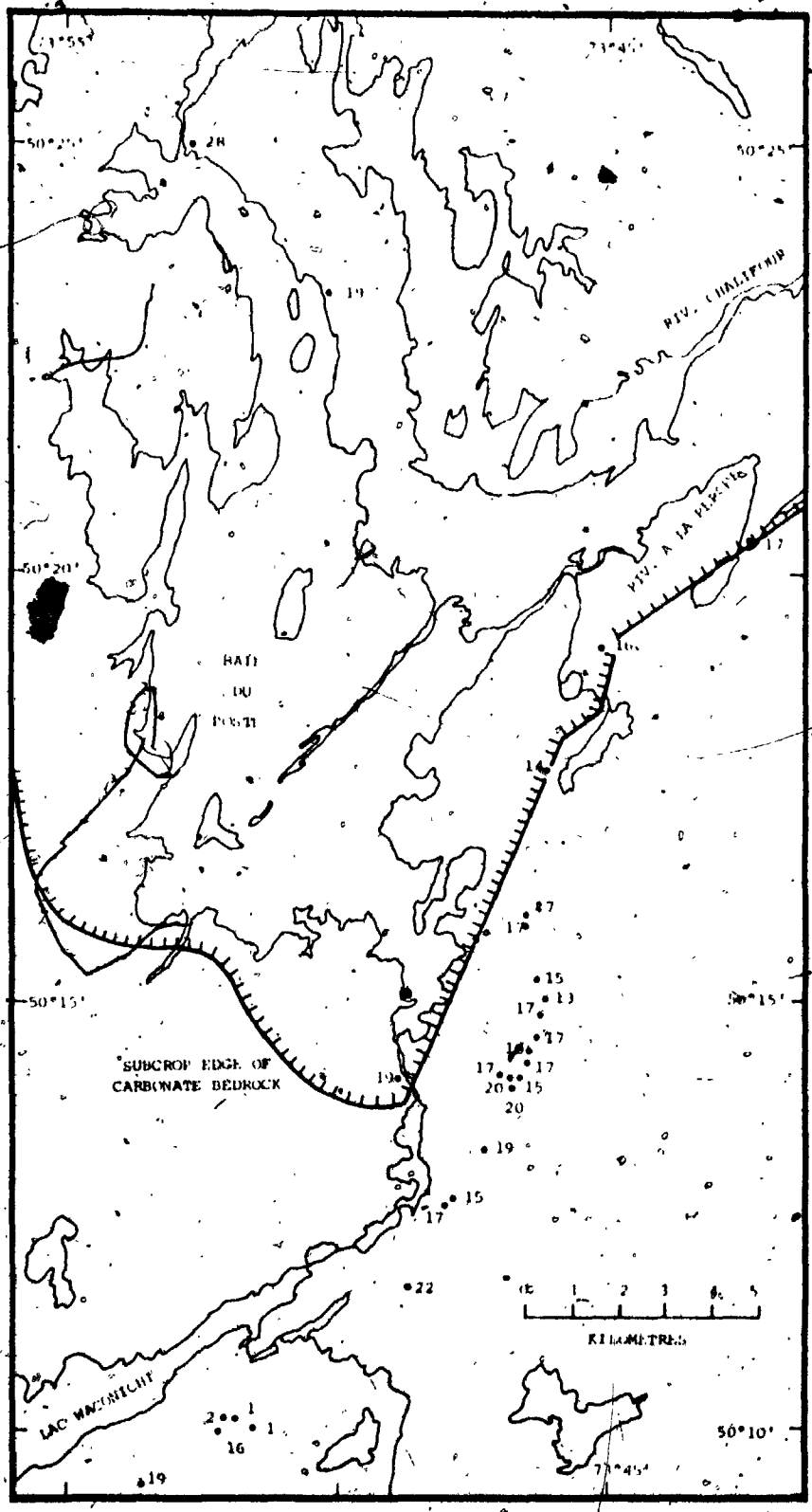


Figure 19. Abundance of carbonates in the minus 0.063 mm fraction of unit A in the Lac Mistassini - Lac Waconicchi area.

that bedrock. Apparently the load of fine detritus of the glacier responded more slowly than the pebble load of the glacier to changes in the subglacial bedrock lithology and grain size. Fine grained carbonate detritus may have been added to the basal debris load of the glacier by continued comminution of Mistassini Group pebbles (see the downglacier decrease in abundance of Upper Albanel Formation pebbles in the till, Fig. 16). The low variability of the texture and carbonate content of the till matrix for long distances downglacier allow their use as till mapping tools.

The eastern limit of the Chibougamau Formation has long been a subject of discussion because the limit should lie at the intersection of the Waconichi and Mistassini faults (Fig. 4). Most authors (Gilbert, 1958; Troop and Darcy, 1973; Long, 1973, 1974) placed the eastern limit about 500 m. east of the Waconichi River, and Long's (1973) pattern is shown on Figures 4 and 20. Guilloux (1969) mapped the formation at least 1000 m. east of the river. The area of interest is thickly drift-covered. The map of abundance of Chibougamau Formation pebbles in units A and B (Fig. 20) shows that several samples contain amounts of this formation that cannot be explained by glacial transport along the local path. The pebbles in question are greenish grey slaty argillites containing isolated granitic granules (laminated argillites with dropstones, Long, 1973). A few of these samples contain rare pebbles of dark grey fine grained limestone, a rock type that has not

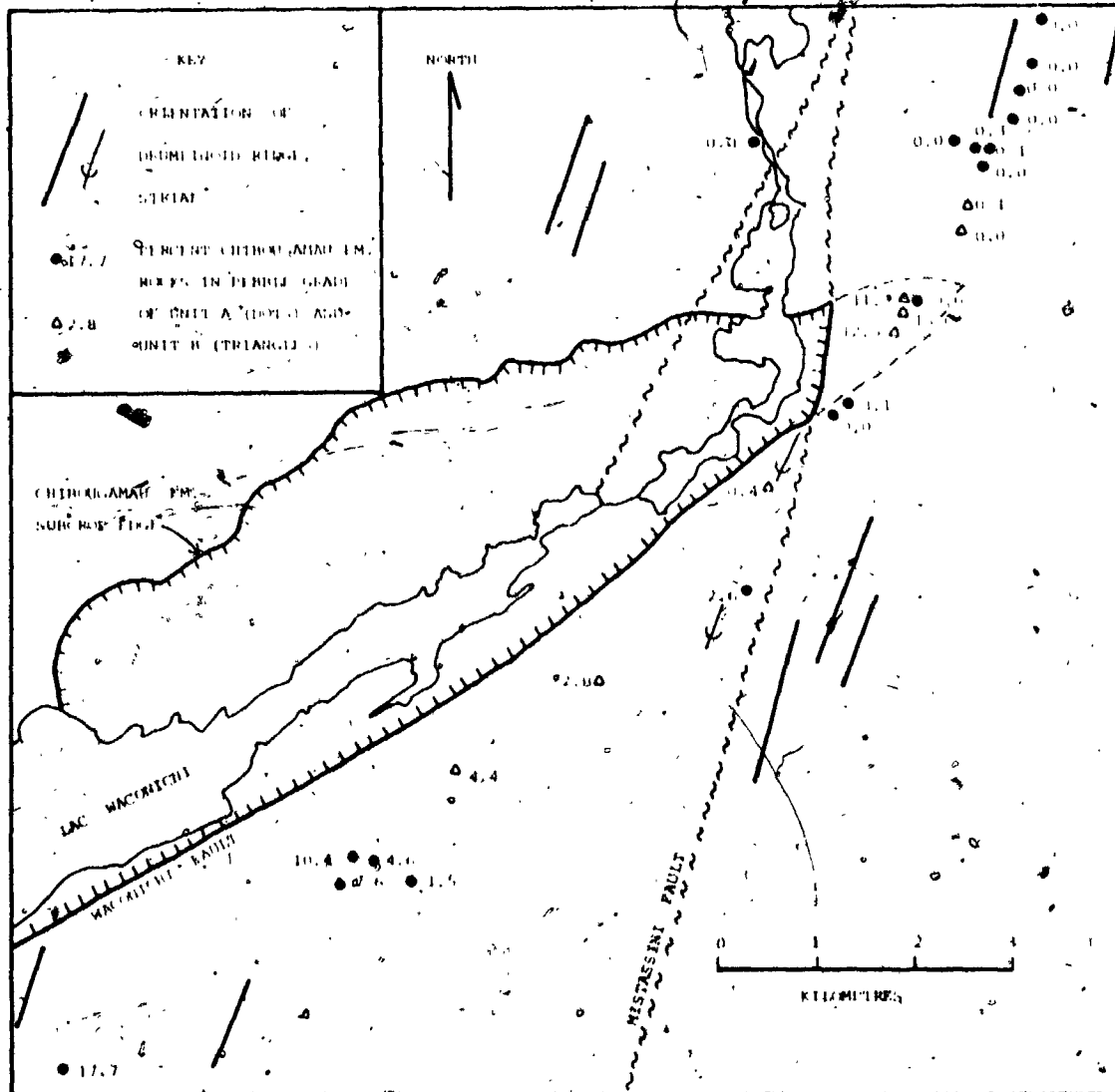


Figure 20. Abundance of Chibougamau Formation rock types in the 4 to 64 μ m. fraction of units A and B near Lac Maconichi. Suggested revision to the eastern limit of the Chibougamau Formation subcrop area is shown by dashed line.

been reported from the Chibougamau Formation or the Mistassini Group. It is possible that there is an unmapped bedrock fault block containing Chibougamau Formation rocks and an unknown limestone bed of the Mistassini Group underlying and upglacier from these sites. Suggested map revisions to the eastern limit of the Chibougamau Formation are shown on Figure 20.

CHAPTER 4

DISPERSAL TRAINS AT ICON MINE

Two dispersal trains were discovered by the Icon Syndicate and Icon Sullivan Joint Venture by boulder and pebble prospecting and by standard soil geochemical analyses for copper (Fig. 21). Soil samples were taken every 31 m. (100 ft.) along lines spaced 62 or 124 m. apart, so that the boundaries of the trains may be accurately defined. Of the 666 samples taken in the soil survey, 96 were judged to contain anomalously high amounts of copper (i.e., their copper contents were above the 85th percentile of the cumulative frequency distribution). The anomalous samples contained at least 60 parts per million copper. Troop and Darcy (1973) stated that background for copper in the soil is about 12 parts per million. The boundaries of the trains (Fig. 5) are placed at the 60 parts per million contour of copper in the soil.

For purposes of discussion, the trains are called the North Train and the Icon Train. The Icon Train was used in the exploration program that discovered the mine, but the North Train was mapped late in the life of the mine.

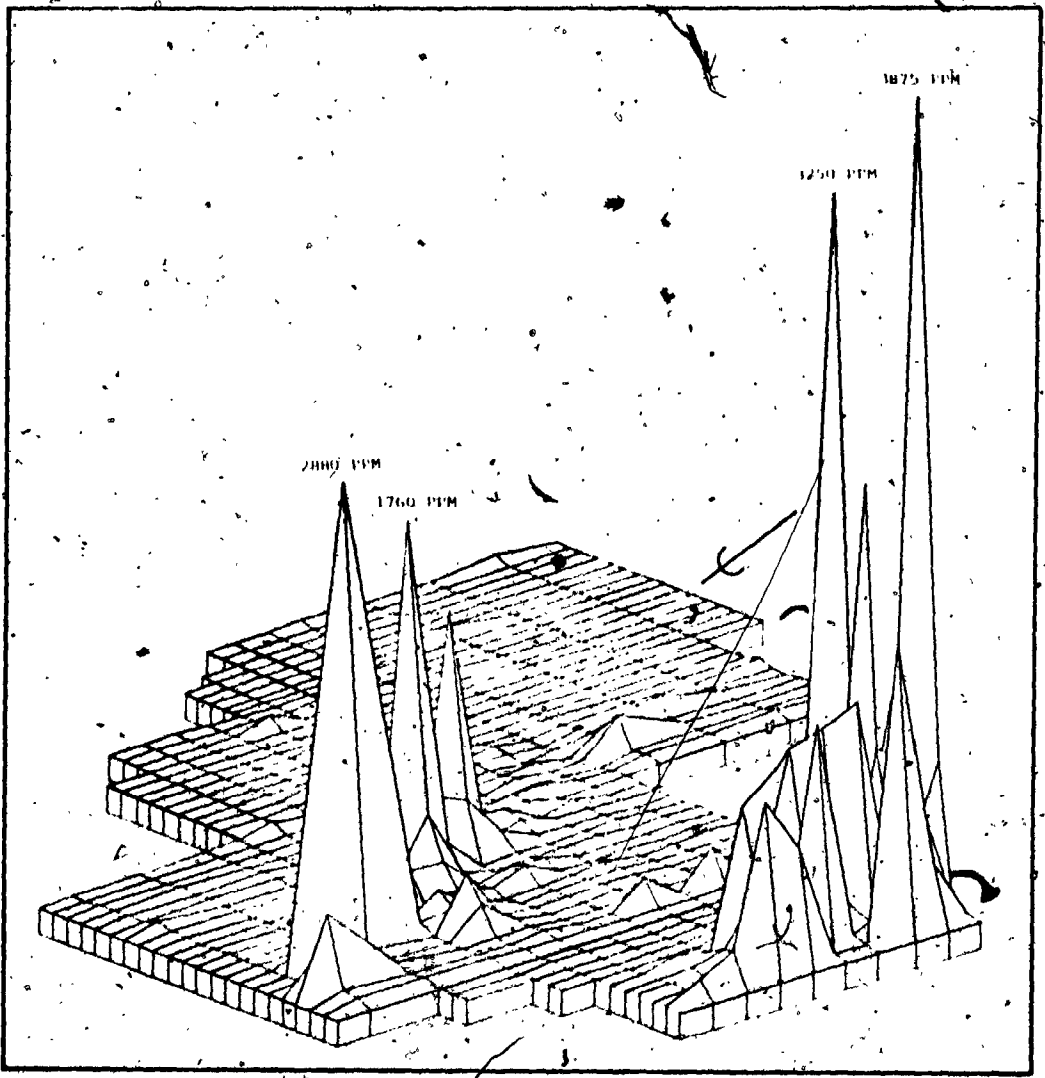


Figure 21. Perspective plot of the abundance of copper in the B horizon of the soil profile at the Iron Mine, viewed from the southeast. Smaller grid rectangles are 10.3 m. (100 ft.) by 0.1 m. (200 ft.). Subcrop of number 1 ore zone is shown behind the Iron Train (right) and subcrop of number 3 ore zone are shown upglacier from the North Train (left).

PART 4.1. The North Train

Size and shape

The North Train first reaches the surface 430 m. downglacier from the eastern subcrop of the number 3 ore zone (Fig. 5). Soil geochemistry indicates that the train is not recognizable upglacier from that point, and unfortunately, no information exists concerning the nature of the till-ore contact because of mining disturbances. If the train exists closer to the ore subcrop in the subsurface, it is masked by the varved silt and clay of unit E, which is the surficial sediment downglacier from the ore subcrop (Fig. 7). The train is exposed discontinuously for a distance of at least 1220 m. The downglacier end of this train is outside the limit of the geochemical survey, but it is at least 1650 m. downglacier from the ore zone. For much of its length, the train is narrow, about 75 m. wide, but it locally reaches a width of 185 m. It is linear or finger-shaped, not fan-shaped as most glacial dispersal trains have been said to be (Hawkes and Webb, 1962, pp. 186-188; Levinson, 1974, pp. 455-458). The train points directly upglacier to the eastern subcrop of the number 3 ore zone (Figs. 5 and 21), and is oriented at 15 degrees.

Pits and trenches excavated in the North Train exposed unit C containing rare quartz-carbonate clasts derived from the vein. The vein clasts were larger and more abundant in the upglacier part of the train than they were in the downglacier part, although their abundance was not

mapped. A few of these pebbles and boulders contained traces of chalcopyrite. Unit C is 1.0 to 2.0 m. thick and directly overlies barren member A of the Lower Albnel Formation.

The soil developed on the till is podzolic, and its B horizon contains up to 2880 parts per million copper. Six of the 35 anomalous samples in the train contained more than 300 parts per million copper, and these high copper abundances were found in the downglacier part of the train (Fig. 21). The contrast is great between the copper abundances outside the train and those within it; that is, the boundaries of the train are sharp and the abundances of copper in the soil often changes from background outside the train to 10 or 100 times background within the 31-metre distance in which the boundary exists. When viewed as a perspective diagram of the soil copper results (Fig. 21), the North Train appears as a sawtoothed ridge standing high above a flat background plain.

Comparison of the elevation of the top of number 3 ore zone to the highest known elevation of the till in the train indicates that detritus derived from the ore zone was transported upslope by the glacier through a vertical distance of 55 m. in a horizontal path length of 1280 m. Therefore, detritus was transported upslope at a gradient of up to 43 m. per kilometre. This gradient is similar to the steepest ones listed by Flint (1971, p. 111) for long transport distances.

Origin

The North Train was formed by erosion of the eastern subcrop of the number 3 ore zone by the glacial readvance which deposited unit C. The subcrop is now small and arcuate (Fig. 5), and assuming its size and shape are similar to what they were before erosion, the glacier traversed a subcrop width of up to 30 m. (mostly about 10 m.) along a strike length of 100 m., measured at right angles to the direction of glacial flow. This part of the ore zone contained abundant copper; a steeply north-dipping lens of massive chalcopyrite up to 3 m. in subcrop width was found in it. The whole number 3 ore zone, including weakly mineralized parts, contained 144,041 tonnes of ore with an average copper content of 7.28 percent (Troop and Darcy, 1973).

The strong linearity and sharp edges of the train are evidence of consistent glacial flow in one direction, along a trend of 15 degrees as indicated by the orientation of striae and the train. There apparently were no major obstacles to glacial flow because the train does not bend nor broaden markedly. The glacier transported the detritus in an orderly manner and it was impeded only by the gradient of the bedrock surface. It is interesting to note that the train is usually narrower than the strike length of its source (100 m.). This may mean that the train, as defined by the copper anomaly in the soil, was derived from the subcrop of the small lens of massive chalcopyrite in the eastern part of the number 3 ore zone, rather than

from the entire mineralized subcrop.

The apparent downglacier decrease in the abundance of vein pebbles may indicate that comminution of the clasts proceeded during transport. Older Quaternary units do not underlie unit C in the train, so dilution from such sources of detritus was impossible. Only the Lower Alban Formation could have supplied detritus (Fig. 5).

The high copper content of a few of the soil samples was caused by malachite, a product of the fixation as a carbonate of copper released during the oxidation of chalcopyrite. No hydromorphic anomaly was produced down-slope from the train. The copper was fixed near its source in the soil because carbonates were abundant and pyrite, which on weathering would produce acidic groundwater to remove copper in solution, was rare in the till.

One unexplained problem is the apparent lack of a dispersal train derived from the western subcrop of the number 3 ore zone (Figs. 5 and 21). No anomalous soil dispersal train which should lie within the limits of the geochemical survey was detected. The western subcrop of the ore zone however is smaller than the eastern one; the glacier traversed a subcrop width of up to 50 m. along a strike length of 40 m. In addition, the ore body here is only about 0.4 m. thick, and is weakly mineralized. The small size and low chalcopyrite content of the western subcrop of the number 3 ore zone may explain the absence of a related soil anomaly. A few boulders of barren quartz-

carbonate vein material are found in unit G where the train should be, but no systematic search for them was conducted. If it exists, this train will probably contain only barren quartz-carbonate clasts.

PART 4.2. The Icon Train

Size, shape and structure

The geochemical soil survey revealed 61 anomalous samples in the Icon Train, downglacier from the subcrop of the number 1 ore zone (Figs. 5 and 22). Twenty-eight of the samples contained more than 300 parts per million copper. When defined by the soil anomaly (Fig. 22), the train is a broad flame-shaped body having two bands of high copper abundance oriented parallel to the glacial transport direction as determined from striae oriented at 15 degrees. The train does not vary greatly in width; it is 260 to 330 m. wide, measured at right angles to the glacial transport direction. It is at least 630 m. long because anomalous sites are found this distance downglacier from the ore subcrop, and the sampled area does not include the downglacier extremity of the train. When viewed as a perspective plot (Fig. 21), the soil anomaly of the Icon Train appears as a cluster of high peaks and ridges rising abruptly out of the flat background plain.

Eight of the soil samples contained more than 1000 parts per million copper; the highest recorded abundance was 3875 parts per million (0.39 percent) copper. These

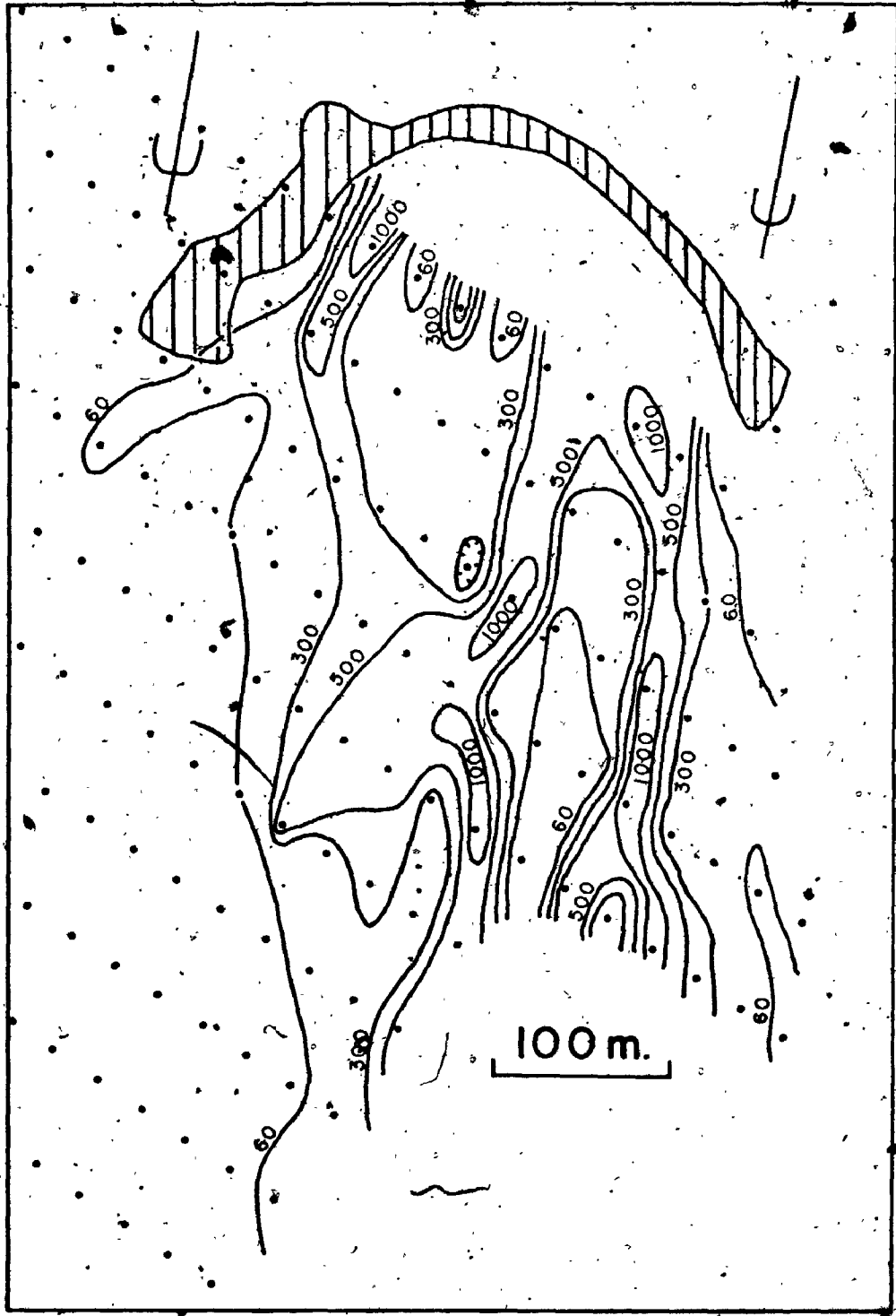


Figure 22. Abundance of copper in the B horizon of the soil profile over the Icon Train. Dots are sample sites. Subcrop of number 1 ore zone is shaded. Contours are at 60, 300, 500 and 1000 parts per million copper.

high copper abundances were caused by chalcopyrite grains, malachite, and azurite. Malachite and azurite occur as discrete sand-sized grains, as coatings on all sizes of other grains, and as cement in the soil. The presence of these minerals as the weathering products of chalcopyrite indicates that hydromorphic dispersion of copper has taken place during soil genesis.

With the a priori knowledge provided by the soil survey of the approximate location, size, and shape of the Icon Train, the author mapped the train by determining the abundance of pebbles of vein rock types in the till in the train (unit C). This procedure was adopted in order to map a variable (percentage of vein pebbles) whose abundance would be primarily controlled by glacial (clastic) dispersal and not by hydromorphic dispersal.

The edge of the train is placed at the 10 percent contour (Fig. 23). The till at sites outside the train usually contains less than 5 percent of vein pebbles, and a 5 percent contour would almost coincide with the 10 percent contour, so the choice of the 10 percent contour as the edge of the train is justified. Defined in this way, the train is 570 m. long and 240 to 270 m. wide. The train is flame-shaped, not fan-shaped, and is oriented parallel to the glacial transport direction, 15 degrees. A belt of high abundances of vein pebbles trends at about 345 degrees within the train and will be considered in the discussion of the origin of the train.

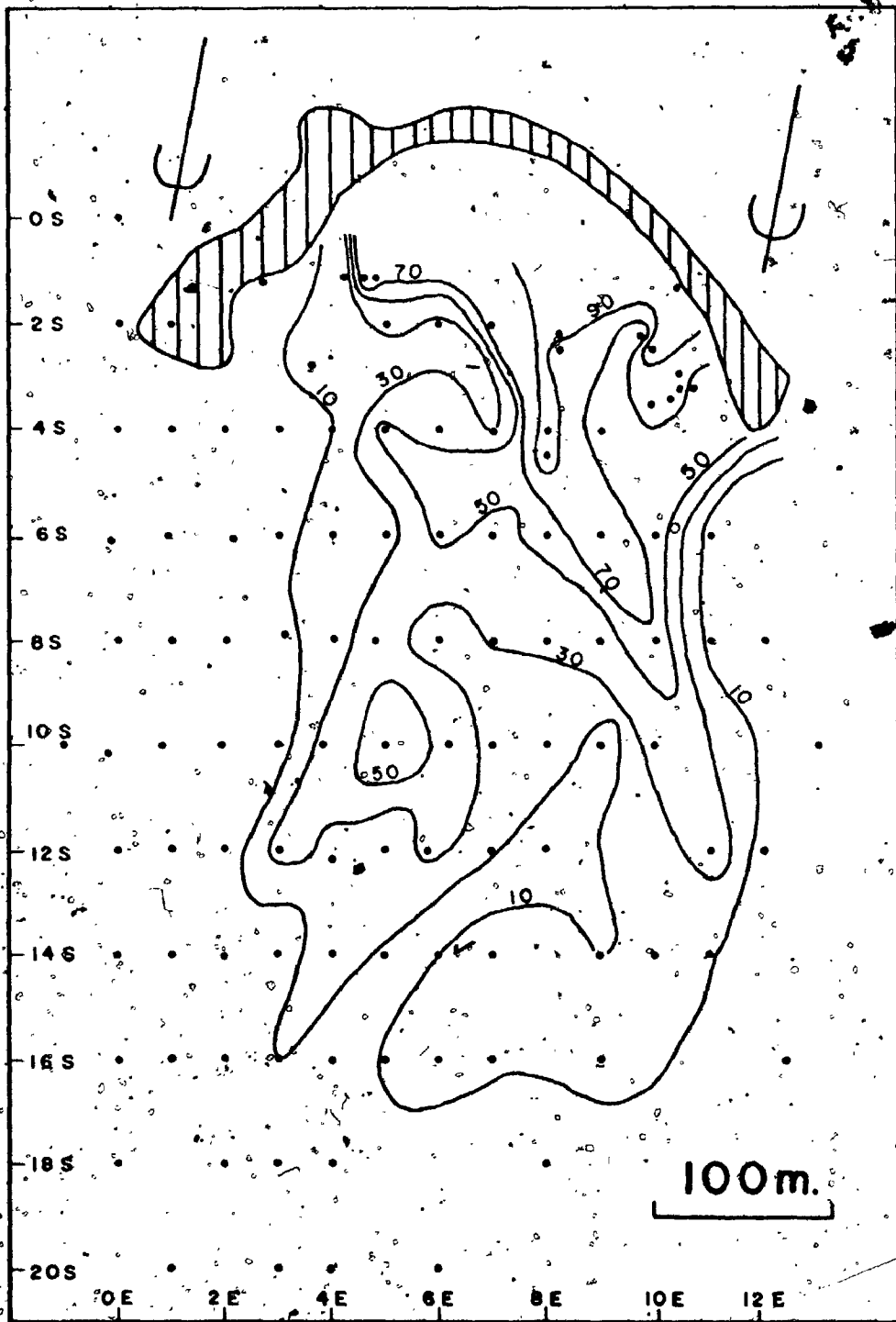


Figure 23. Abundance of vein rock types in the 4 to 64 mm. fraction of unit C in the Icon Train. Dots are sample sites. Subcrop of number 1 ore zone is shaded. Contours are at 10, 30, 50, 70 and 90 percent vein rock types.

A perspective plot of the same data (Fig. 24) shows the contrast between the low abundances outside the train (flat areas) and the high abundances within it. The lateral edges of the train are sharp. The downglacier decay of abundance of vein pebbles is non-linear; it is logarithmic-like. In the upglacier half of the train, the abundances decline steeply from above 90 percent to about 30 percent. The abundances decline more gradually to below 5 percent in the downglacier half of the train (Figs. 23, 24).

The test pits and mining faces which were excavated in the Icon Train allowed examination of its third dimension. It was then possible to describe the train as a three-dimensional body and to suggest ways in which its morphology and lithology have been influenced by the substrata. In longitudinal section (Fig. 25), the train has the shape of an elongated and attenuated tear-drop. Its upglacier end overlies a convex-upward lens of sand and ablation till belonging to unit B (Plates 6 and 15). The till that forms the train, unit C, is up to 6.0 m. thick and dips steeply northward on the upglacier side of the mass of unit B. The attitude of unit C conforms to the attitude of the bedrock surface in the downglacier part of the train; there unit C is less than 1.0 m. thick. In a transverse section across the upglacier end of the train (Fig. 26), unit C appears to be "draped" over unit B and the bedrock. Examination of the contact between these units shows that unit C fills grooves cut in unit B and bedrock. Where unit C

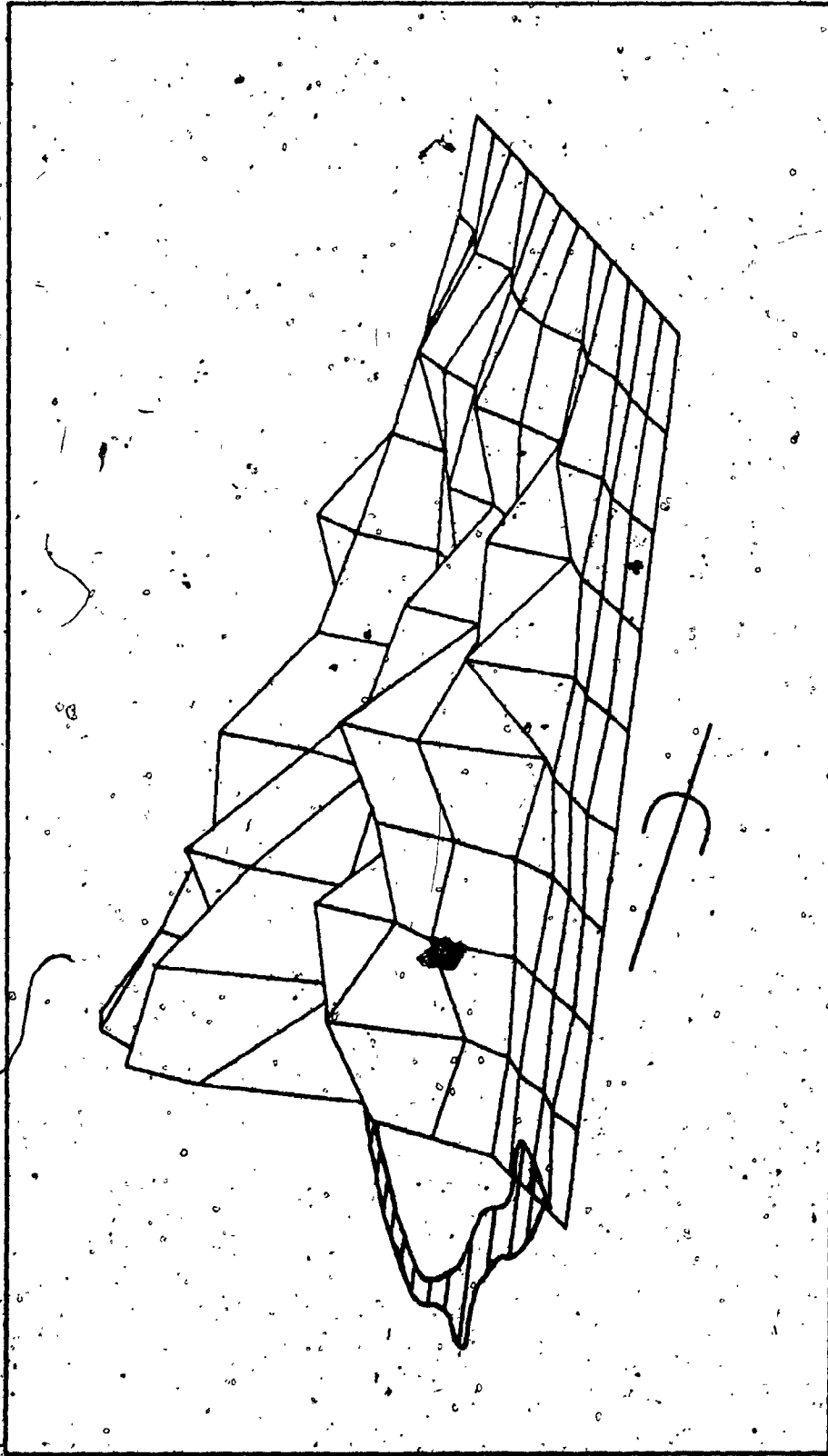


Figure 24. Perspective plot of the abundance of vein rock types in the 4 to 64 mm. fraction of unit C in the Icon Train, viewed from the west. Grid rectangles are 30.5 m. (100 ft.) by 61 m. (200 ft.). The highest peak represents 99 percent. Subcrop of number 1 ore zone has been added.

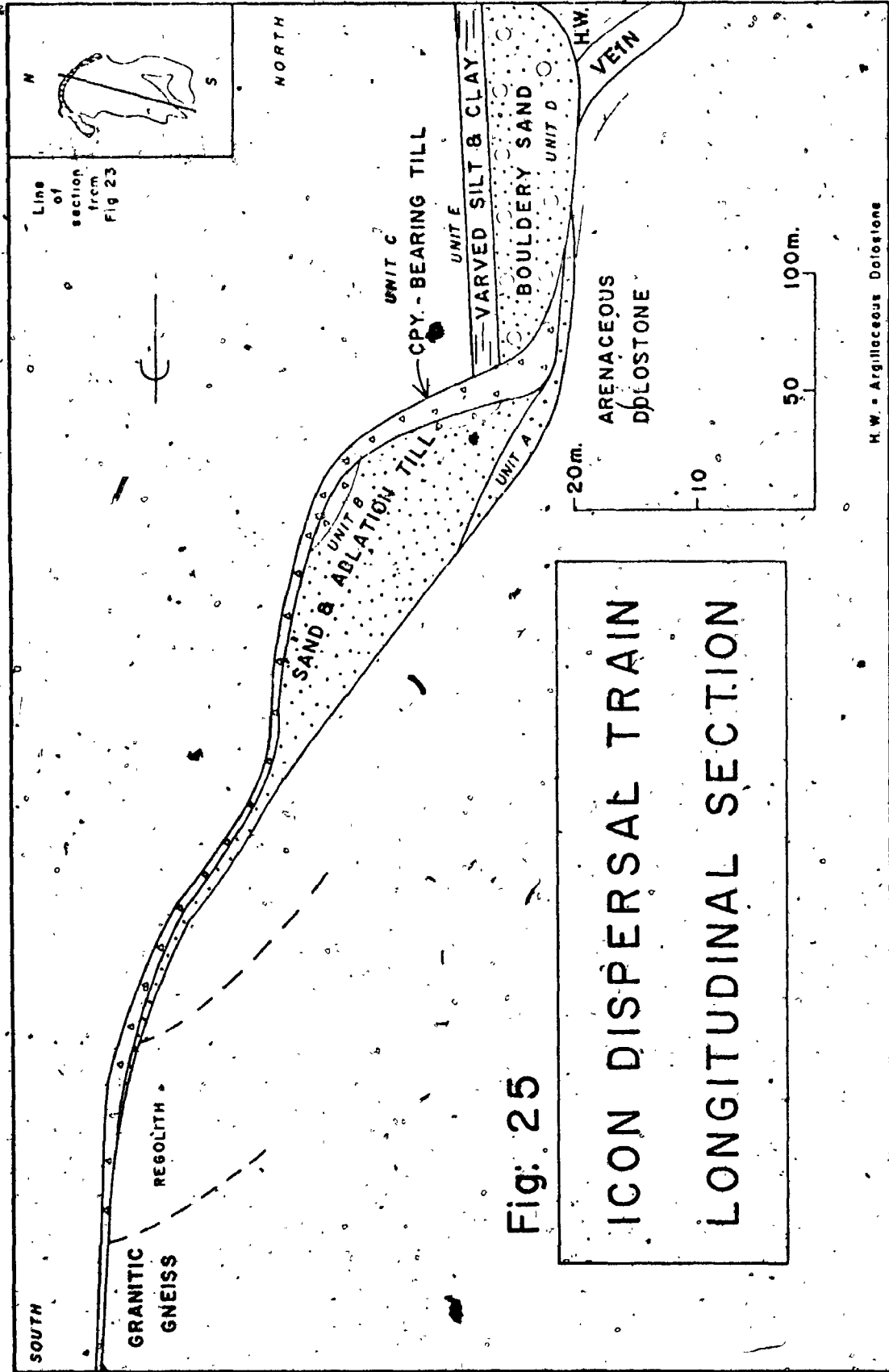
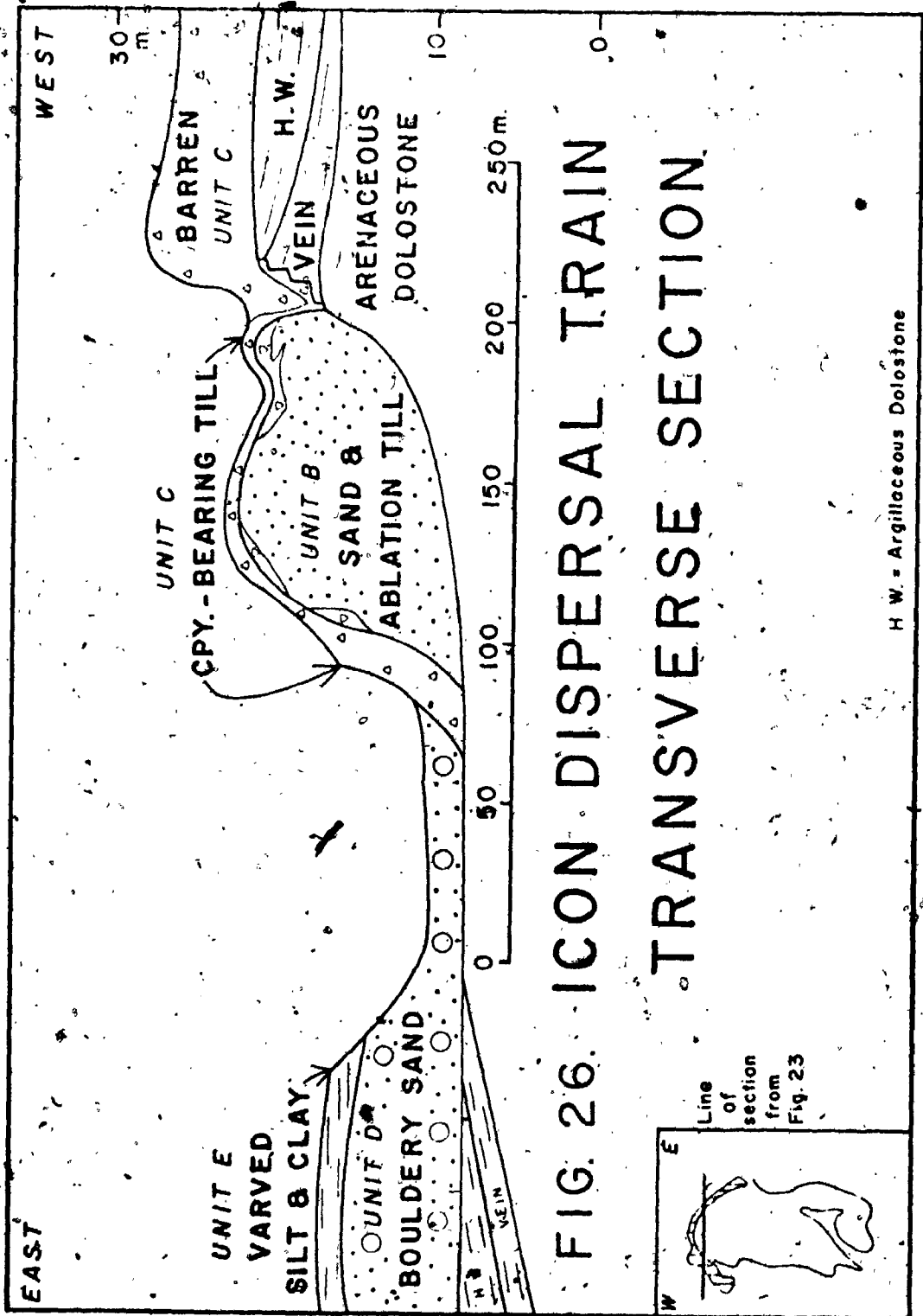


Fig: 25

ICON DISPERSAL TRAIN
LONGITUDINAL SECTION



is thickest, on the west side of the train, only its lowest 1.0 m. contains abundant sediment derived from the vein. It grades upward into physically similar till, the lithology of which is dominated by another local rock type, the argillaceous dolostone of member B of the Lower Albabel Formation, which is the rock overlying and forming the hanging wall of the vein.

In summary, the Icon Train is within unit C, and is a lithologically distinct part of this till because it contains abundant detritus derived from the subcrop of the number 1 ore zone at the mine. The three-dimensional shape of the train is similar to the shape of the inverted bowl of a spoon: convex upward, concave downward, with a thicker steeply north-dipping upglacier end and a thinner, gently north-dipping downglacier end.

Origin

Obviously, the Icon Train was formed by the glacial erosion of the subcrop of the number 1 ore zone followed by deposition of the detritus as basal till a short distance downglacier from its source. Assuming the size and shape of the subcrop are similar to what they were before erosion, the glacier traversed a subcrop width of 20 to 80 m. along a strike length of 370 m. measured at right angles to the direction of glacial flow (Fig. 23). A more specific and detailed explanation of the origin of the Icon Train may be possible. The salient facts which must be con-

sidered in the explanation are outlined below.

The till containing the train (unit C) includes undeformed or folded blocks and slabs of the underlying Quaternary units, and the contact between unit C and the older units is marked by grooves and thrust faults which must be glacial in origin (Plates 11, 12 and 14). The till in the train is everywhere rubbly (Plate 8) and contains several large vein boulders. Rock flour is scarce in the till where it was derived from the vein alone. The till is thickest (vertically) on the lateral and upglacier edges of a mound of older drift (Fig. 26, west side; Fig. 25, north end). Measurements of the orientation of pebbles in unit C in the train (Fig. 27) indicate that the till was acted upon by forces from the north-northeast (sites 21 and 34) and north-northwest (sites 28 and 33). The map of abundance of vein pebbles in the till (Fig. 23) shows a belt of high percentages with a north-northwest trend within the train, which contrasts with the general north-northeast trend of the train. The vein subcrop from which the train was derived lay on the top and on the downglacier side of a slight bedrock structural ridge (Fig. 28). The downglacier and lateral faces of the vein subcrop are ragged and rubbly (Plate 10). All the striae on the bedrock under unit C are oriented north-northeast. If the interpretation of the glacial history of the area is correct, the train was formed by a minor glacial readvance up the Waconichi River valley by a small glacial tongue. The

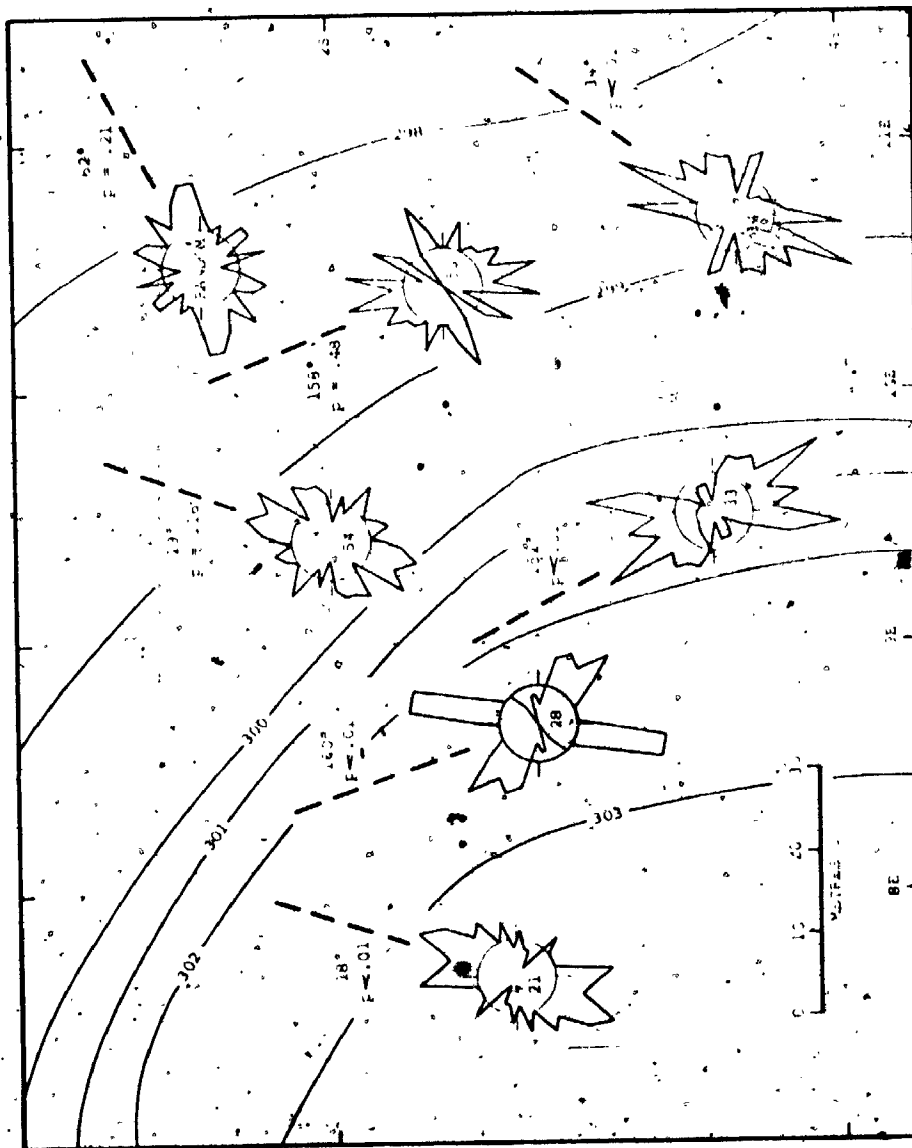


Figure 27. Mirror-image diagrams of till pebble orientations in Unit C in the northeast part of the Icon Train. The sampling grid for Fig. 23 is shown for reference. Each rose diagram has its site number inside an 8 percent scale circle and is accompanied by the calculated resultant trend (also shown by a dashed line), and p , the probability of randomness. The present topography of the pre-writ C surface is shown by contours at 1 m. intervals (same datum as 305 m.).

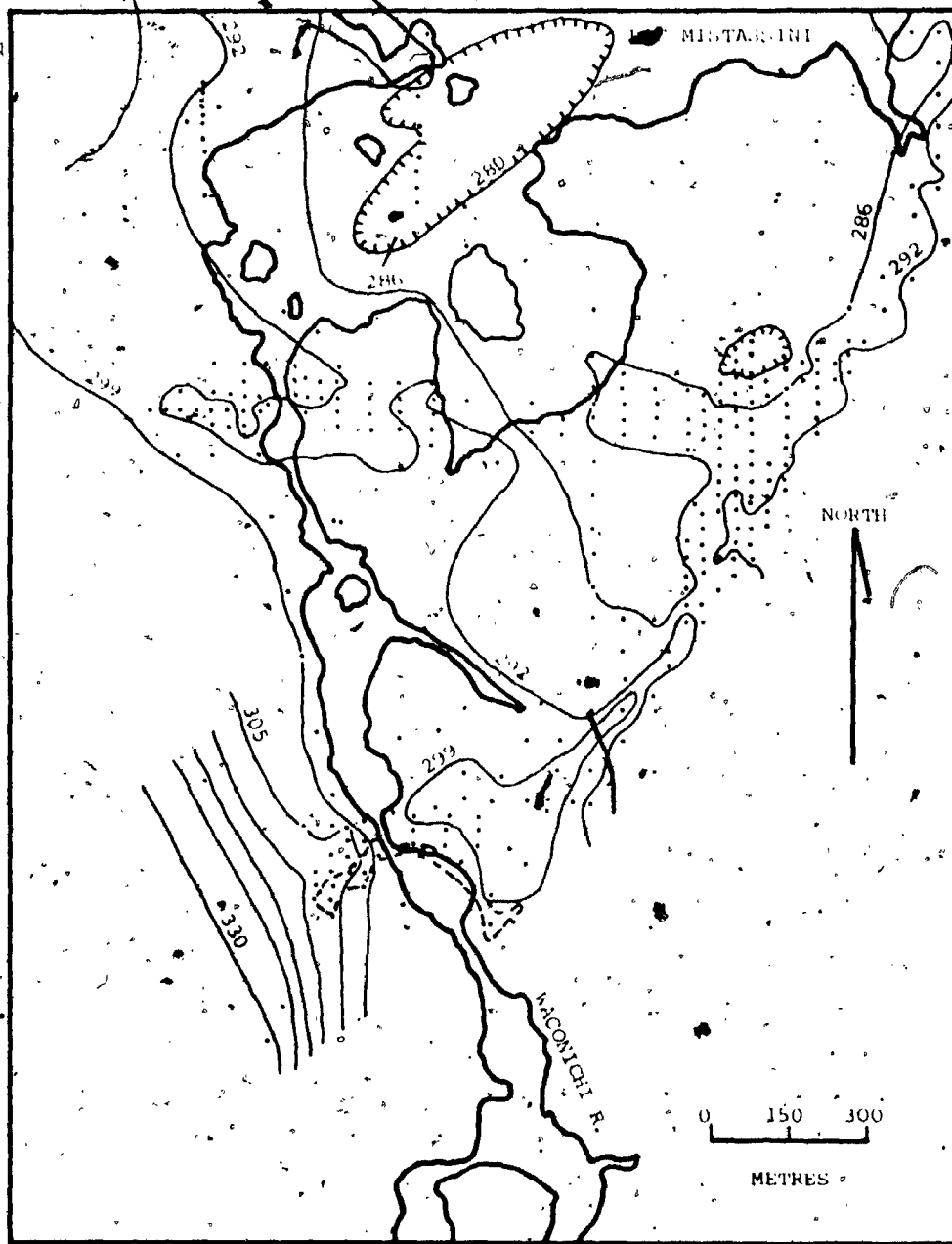


Figure 28. Bedrock topography of the Ikon mine, compiled from drilling records. Each dot is the site of a vertical drill hole. Contour interval is 6 m. (20 ft.) and mine datum is 305 m. (1000 ft.). Subcrop of number 1 ore zone is shown by dashed line.

glacial tongue was probably thin, and the formation of the Icon Train occurred near its margin.

The coarse, rubbly texture of the till is suggestive of quarried (crushed and plucked) sediment. The ragged faces of the vein subcrop are quarried surfaces. The structure and mineralogy of the vein would have made it amenable to quarrying. Thin, incompetent graphitic argillite lenses within the vein and at its contacts with the wallrocks would facilitate the plucking of blocks of vein rock. The quartz masses and crystals in the vein are brittle and highly fractured. The carbonate minerals are easily cleaved. The contacts between quartz, carbonates, and sulphides are often large crystal faces with minor intergrowths, which would act as planes of weakness. The position of the vein subcrop on the downglacier side of a bedrock ridge (Fig. 28) is analogous to the quarried lee side of whaleback bedrock landforms, except for the west end of the subcrop, which is on a surface that rises downglacier. No conclusions can be reached concerning the exact mechanisms of quarrying, but it is believed that plucking dominated over crushing because the mineralogy and structure of the vein rock makes it amenable to plucking without much glacial crushing. The west end of the subcrop apparently was not strongly eroded because unit C contains low amounts of vein rock types downglacier from it (Fig. 23).

Less than 100 m. downglacier from the vein subcrop, the glacier carrying the quarried debris met and overrode

the older mound of units A and B (Fig. 25) which stood at least 7.0 m. higher (Fig. 26) than the substrata immediately upglacier from it. This mound of older drift apparently obstructed glacial flow, and the ice was redirected locally around it. The fact that unit C is thickest on the upglacier end and sides of this mound and is in steep contact with the sediments in the mound supports this view. The debris-rich ice streamed around the obstacle, cutting grooves and depositing till in them. The north-northwest pebble orientations (Fig. 27, sites 28 and 33) on the east side of the train may reflect local deflections of glacial flow, with the ice generally moving from the north-northeast (Fig. 27, sites 21 and 34). However, the results of the pebble orientation measurements may simply reflect between-site variability in unit C. The abundance of vein pebbles in the train (Fig. 23) indicates that the normal transport of debris was from the north-northeast to south-southwest (outline of train), but the belt of high abundances on the east side of the train also shows that a large amount of the debris may have been redirected toward the south-southeast. The bedrock surface, which the downglacier part of the train overlies, dips to the east-northeast (Fig. 28). The combined effects of glacial motion from the north-northeast against this east-northeast-dipping slope may have increased the tendency for the glacial debris to be redirected parallel to the north-northwest strike of the bedrock surface. The downglacier decrease

in abundance of vein pebbles in unit C was caused by comminution during transport and by dilution through incorporation of clasts from the older Quaternary units and other bedrock.

A problem arises concerning the interpretation of the mound of units A and B as an obstacle to glacial flow. Why were the soft sediments in this mound resistant to erosion by the readvancing glacial lobe that deposited unit C? One explanation is that the mound was frozen. Subglacial permafrost is common near glacial margins. The discrete inclusions of units A and B in unit C are compatible with this hypothesis, because they are thin and tabular, the shape that is most amenable to glacial plucking by thrusting out of frozen substrata (Boulton, 1972, p. 9). The thrust faults which extend into unit B from its contact with unit C would be the incipient leading edges of tabular thrust blocks. Subglacial permafrost would theoretically aid quarrying of the ore zone (Boulton, 1972, p. 8). However, if the mound is considered as a frozen mass, it is difficult to account for the till (unit C) overlying its up-glacier end and infilling grooves on its sides. The theories and observations of Boulton (1972, 1974) and others have shown that lodgement of till is greatly suppressed where there is no water and where slip does not take place at the glacier sole.

An alternative explanation is that units A and B under the glacier were not frozen and that net basal melting of the glacier was occurring. According to Boulton (1972,

p. 12; 1974, p. 52) lodgement of till occurs when the effective normal pressure (ice pressure minus pressure of water between ice and substrata) is greater than the ratio of the shear stress at the glacier sole to the coefficient of friction of the bed. The porous sediments in unit B could transmit the subglacial water better than the bedrock, which would increase the effective normal pressure over the mound, perhaps to a point at which lodgement of till rather than erosion would occur. In this way, the mound would act as an obstacle to flow, localizing erosion and till deposition on its sides (zones of relatively lower effective normal pressure) and till deposition on its up-glacier surface (zone of higher effective normal pressure). However, thin ice has low ice pressure, which would limit the power of the glacier to deposit till by lodgement. In addition, the incorporation of discrete slabs of soft substrata into unit C is difficult to visualize for an unfrozen substrate.

All the features observed in the mound cannot be explained by simply stating that it was either frozen or not frozen. It is more probable that the thermal regime changed with time, i.e., the mound was frozen prior to the glacial advance and melting began while it was under the glacier, or the mound was not frozen prior to the advance and freezing began while it was under the glacier. The former explanation is preferred by the author because permafrost is most common beyond the margins of glaciers (Boulton, 1972).

The mound would have acted as an obstacle to flow when net basal melting began.

Depth of erosion

Icon Sullivan Joint Venture mined the till in the train because of the high copper content of the till and because it required very little blasting. The production figures for the till ore were tabulated separately from other ore, so it is possible to estimate the depth of erosion of the subcrop of the number 1 ore zone by the glacier that deposited the Icon Train.

The company mined 60,823 tonnes of till containing an average of 1.276 percent copper from the train (G. Darcy, pers. comm.). This ore contained 685 tonnes of copper. The ore in place in the number 1 ore zone contained 3.28 percent copper (Troop and Darcy, 1973). The difference between the copper content of the ore in place (3.28 percent) and the till ore (1.276 percent) means that the detritus derived from the vein was diluted by about 60 percent between the site of erosion and the site of deposition, about 100 m. from the source. The total weight of the eroded vein rock would be 20,900 tonnes, based on a copper content of 3.28 percent and a weight of 685 tonnes of contained copper. Ore containing 3.28 percent copper would be about 10 percent sulphides and 90 percent gangue minerals by volume. Specific gravity values supplied by Seguin and Laroche (1975) lead to a calculation of the specific

gravity of the ore of about 3.0. A body of ore with mass 20,000 tonnes and specific gravity 3.0 would have a volume of 6967 cubic metres. Assuming the till was abraded from the part of the subcrop that is upglacier from the train (Fig. 23), it was derived from an area of 8,000 square metres, indicating that the depth of erosion was 0.87 m.

The volume of eroded ore is a minimum estimate because only the relatively rich, upglacier end of the train was mined, and because the copper content of the ore in place used in the calculation (3.28 percent) is probably too high. The vein has an average copper content of only 0.29 percent in 9 drill holes near the downglacier edge of the present subcrop, so a better estimate of the copper content of the ore in place would be about 2.0 percent. From these revised numbers, the volume of eroded ore was probably about 20,000 cubic metres, which would indicate a depth of erosion of 2.6 m.

From the foregoing discussion of the origin of the Icon Train, it can be seen that the till was derived from the vein mostly by quarrying and not by abrasion, so it is improper to consider the till as derived from an area the same size as the present subcrop. Using the minimum volume of 6967 cubic metres and a maximum of 20,000 cubic metres, a calculation of the area of vein eroded may be performed for a given thickness of vein. The vein has an average thickness of 2.8 m. in 9 drill holes near the downglacier edge of the present subcrop. The area of the vein that was

eroded is therefore between 2490 and 7140 square metres. The zone of erosion was probably a narrow band on the downglacier edge of the present subcrop. Regardless of the uncertainties involved in the foregoing calculations, the depth of erosion thus indicated due to a minor glacial re-advance is significant.

Comparison of prospecting methods

The map of the copper content of the soil developed on the Icon Train (Fig. 22) is a good guide to the position of the number 1 ore zone. In general, however, soil analyses have limitations and their results can be misleading. A soil which is developed on detrital material, with soil water having transported metal ions, will contain an anomaly which is partly clastic and partly hydromorphic. The field worker may sample soils developed on different sediments (e.g. till, glaciofluvial sands, glaciolacustrine silts, alluvium) while believing they are all the same. The shipping and analysis of the samples takes valuable time and the laboratory is a further source of error. Is there a better way to map a sulphide-bearing dispersal train for prospecting purposes?

Figure 29 shows the abundance of chalcopyrite-bearing pebbles (4 to 64 mm.) in unit C, the till in the Icon Train. Chalcopyrite-bearing pebbles are found up to 540 m. downglacier from the subcrop. The area covered by this map is the same as that shown on Figure 22. In form and in style

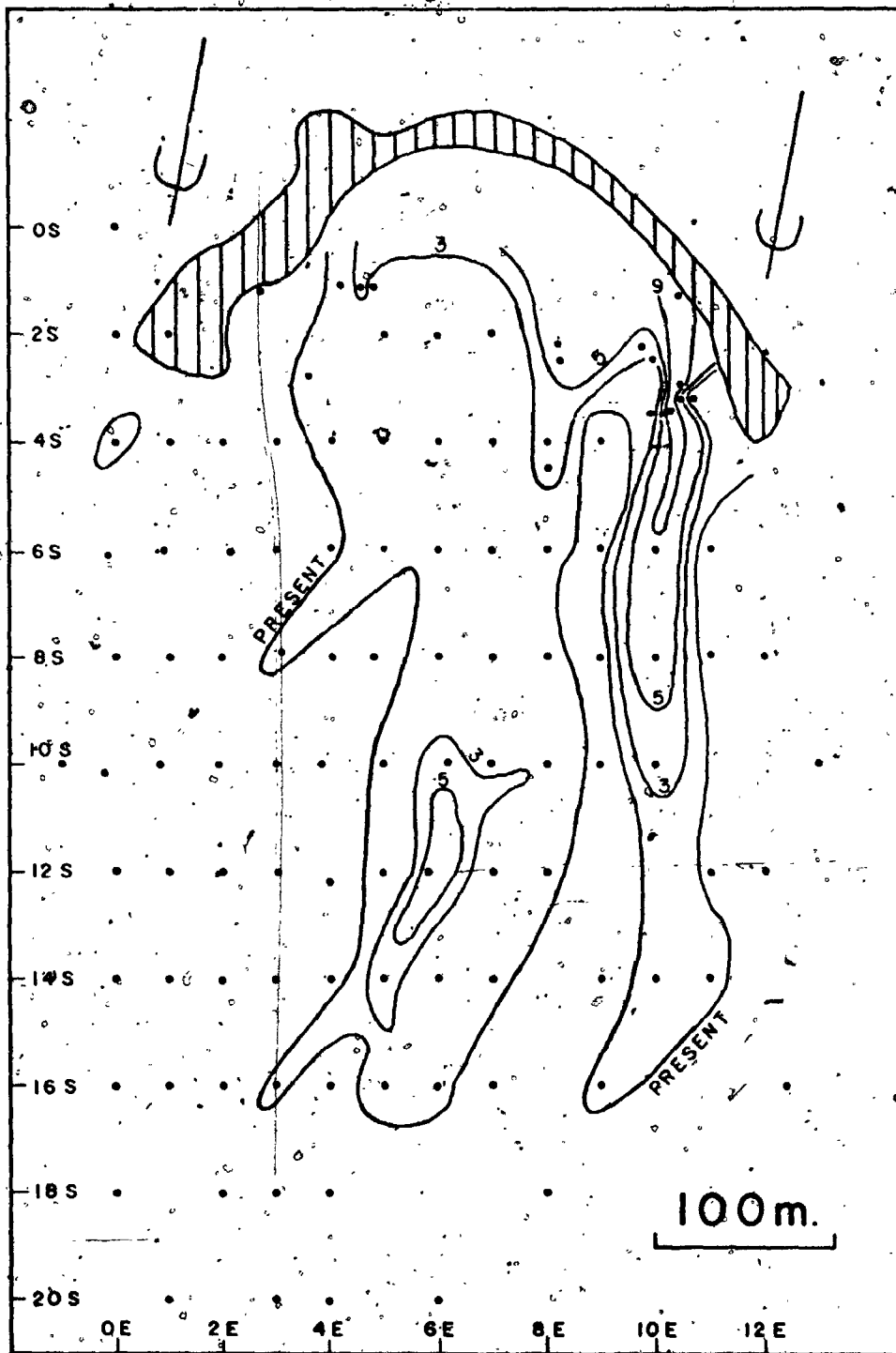


Figure 29. Abundance of chalcopyrite-bearing pebbles (4 to 64 mm.) in unit C, in the Icon Train. Dots are sample sites. Subcrop of number 1 ore zone is shaded. Contour labelled PRESENT encloses sites where unit C contains any chalcopyrite-bearing pebbles. Other contours are at 3, 5 and 9 percent.

the two mapped patterns are similar. Both show two bands of high abundance parallel with the direction of glacial transport. The anomaly of chalcopyrite-bearing pebbles is smaller, because it is solely detrital (not hydromorphic) in origin and because glacial comminution of sulphide-bearing pebbles produced finer detritus which was detected farther downglacier in the soil survey. The two maps yield the same information about the position of the ore in place. Consideration of the procedures used in gathering the data for the maps allows a choice of the most useful map of the two.

The abundance of chalcopyrite-bearing pebbles in the till is free of hydromorphic effects. The pebble anomaly can therefore be more easily interpreted because it is a detrital one. The anomaly can be traced directly upglacier to its source. The collection of pebbles from the till is less prone to sampling error because a pit must be dug to recover the pebbles, giving the sampler an opportunity to inspect the sediment and identify it.

Twenty man-days of field work were required to collect the 111 samples shown on Figure 29. The same number of soil samples could probably be collected in about 5 man-days, unless difficulties are encountered in augering the clast-rich till. The major advantage of collecting pebbles from the till arises out of the time involved in analysis of the samples. Whereas soil samples must be shipped to a laboratory for an expensive form of analysis, the abundance

of chalcopyrite-bearing pebbles can be easily determined in the field by an analyst with elementary geological training. Identification of the pebbles concurrent with sampling provides feedback to the sampler so that sample sites may be chosen efficiently and re-examined while in the field.

The conclusion that is drawn from this comparison is that wherever pebbles or even cobbles and boulders containing economically interesting minerals are found in till, the abundance of ~~those~~ clasts should be mapped. On-site and simultaneous analysis provides rapid return of information at low cost, and the abundance of the clasts in the till is a good guide to their bedrock source.

Drainage of surface water and ground water into Waconichi River from the Icon Train, which is part of the riverbed (Fig. 26) could have supplied copper ions to the river water. In addition, fluvial erosion of the chalcopyrite-bearing till should have added chalcopyrite grains to the sediment load of the river.

Gros' (1975) experimental stream sediment survey included most of the area of the Icon Sullivan Joint Venture property. Of the 137 stream sediment samples collected at a sampling density of about 2 samples per square kilometre, 14 were judged by Gros to be anomalous with respect to copper. None of the anomalous samples gives any indication about the location of the Icon ore zones. They are from streams in different drainage systems 8.4 to 10.8 km. west of Waconichi River. The sample in the most favourable

location, in the Waconichi River 760 m. downstream from the Icon Train, did not detect the copper-bearing till.

Lake sediments have been suggested as sampling media for reconnaissance geochemical exploration in the Canadian Shield (Allan et al., 1973; Nicol et al., 1975). Samples are cored or dredged from the fine sediment in the deepest part of a lake on the assumption that the sediment at a centre-lake site best reflects the chemistry of the surrounding terrain. A core 25 cm. long was collected from Baie du Poste, 17 km. downstream from the Icon Train, (Allan and Timperley, 1975). Five samples taken at equal intervals down the core contained between 14 and 17 parts per million copper, which gives no clue to the location of the Icon Train.

Where chalcopyrite-bearing unit C in the Icon Train forms the bed of Waconichi River, it is overlain by about 2 cm. of fossiliferous oxidized sand of unit F (alluvium). Below the alluvium, the till is fresh and unoxidized, so relatively few copper ions could be moving from the till into the river water. This partly explains why the stream and lake sediments derived from the Icon Train area do not contain anomalous amounts of copper.

Comparison of units A, B, C and D as sampling media

The Quaternary units near the subcrop of the number 1 ore zone at the Icon mine were examined in order to evaluate them as sampling media for prospecting by geochemical

and lithological methods of analysis. The orientation of till pebbles in units A and B and striae under unit B (Fig. 30) indicate that their sediments must have been transported across the vein subcrop along a path similar to that followed by the glacier that deposited unit C.

Figures 31 and 32 show the abundance of vein pebbles and chalcopyrite-bearing pebbles in units A, B, C, and D in sections overlying and downglacier from the subcrop of the number 1 ore zone. It is obvious that unit C is richer in pebbles derived from the vein than are the other Quaternary units. Unit B has been shown to be ice-contact stratified drift and ablation till deposited from a wasting ice sheet. Lithologic analyses of its pebbles (Fig. 15) show that this unit has a high content of sediment derived from distant sources. Its deposition at the Icon mine was from streams running off the ice and by flows of till from the ice. Deposition was the main local process, and local erosion was negligible, so that the lithology of unit B does not reflect the local bedrock. Unit D is a coarse proximal glacio-fluvial gravel containing low percentages of vein pebbles. It is believed to have been deposited over the subcrop of the number 1 ore zone by a glacial stream in which the dominant local process was aggradation. Erosion of the vein subcrop was low because the subcrop was rapidly buried by unit D.

It remains to be explained why unit A, which is stratigraphically closer to the bedrock than unit C, con-

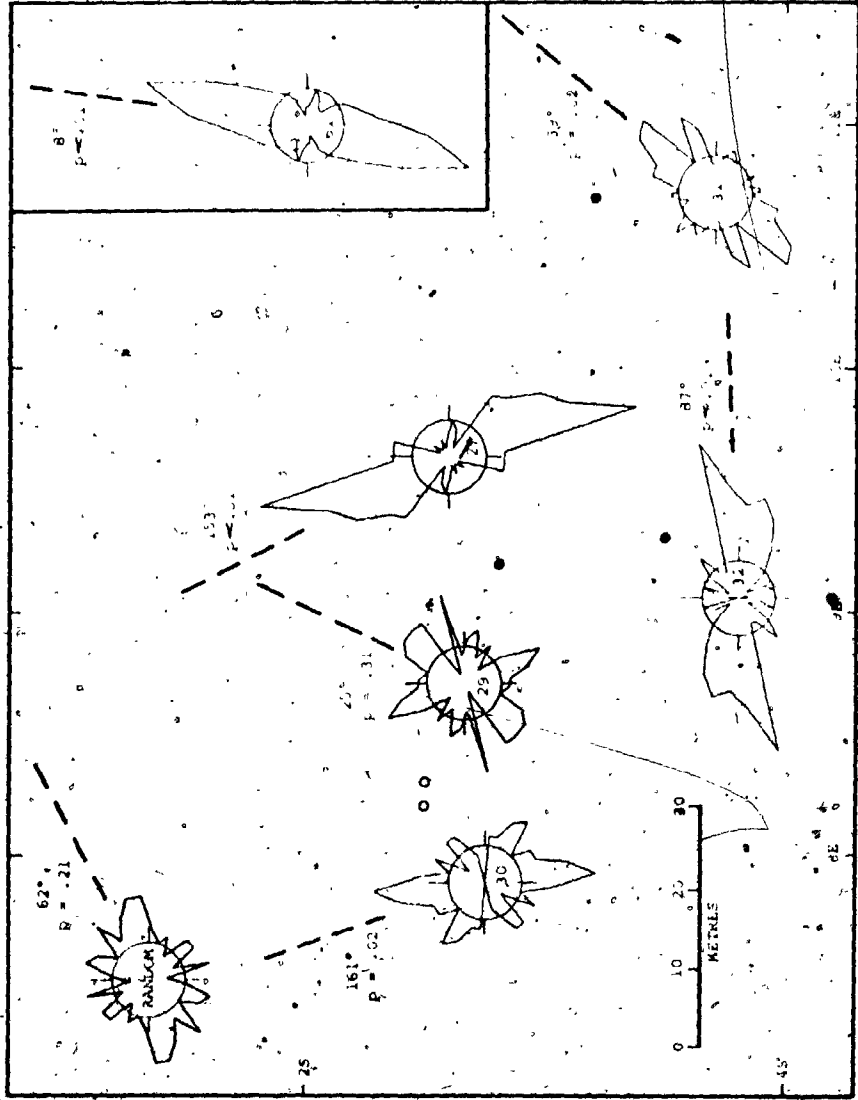
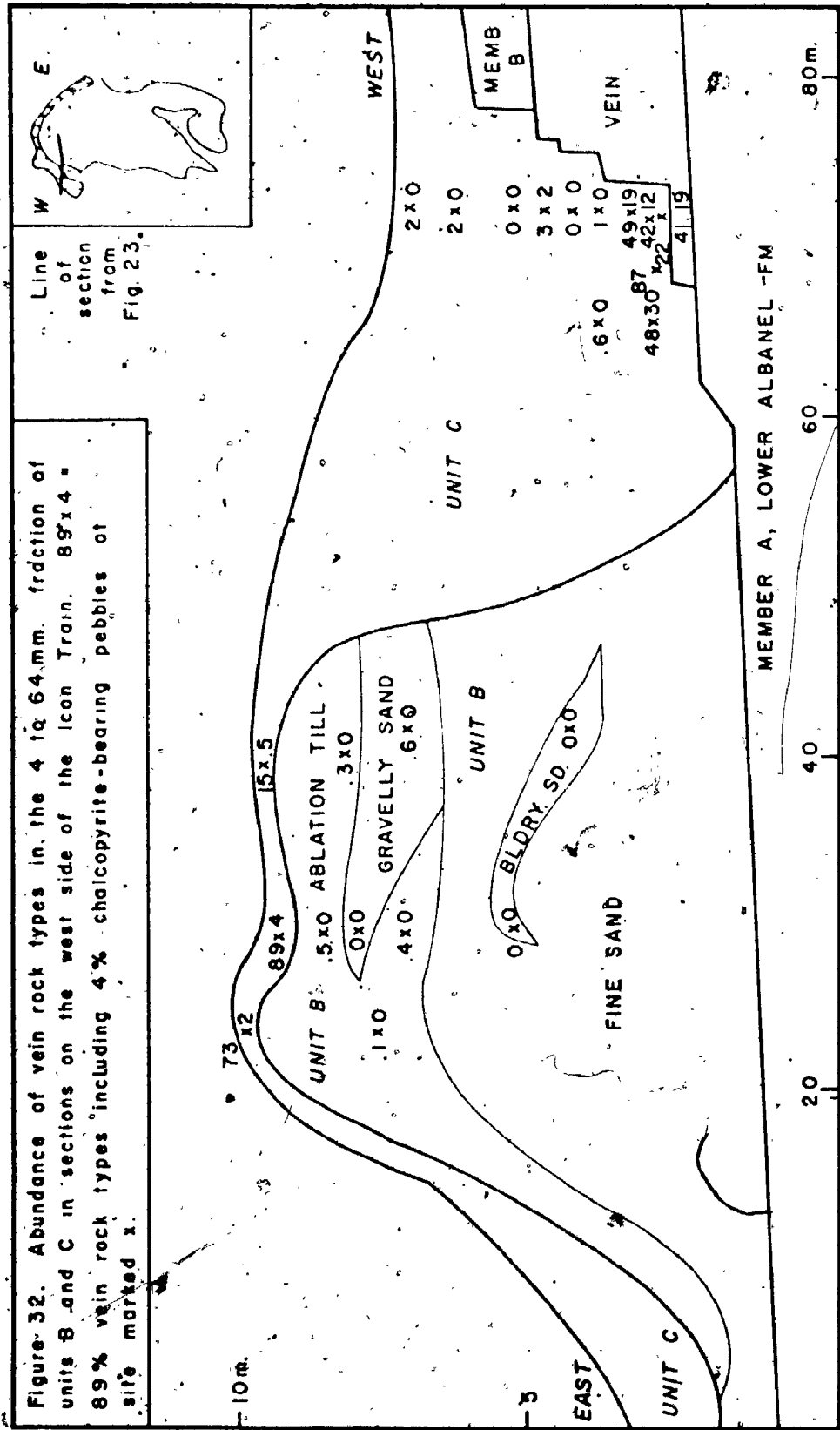


Figure 30. Mirror-image rose diagrams of tuff pebble orientations in unit A 'sides marked by filled circles and unit B (open circles) under the Icoq train, mostly in the same area as Fig. 27. The sampling grid for Fig. 21 is shown for reference. Inset: diagram for site 61, till in unit B at $\approx 10S 4+5E$ on the grid. Each diagram has its site number inside an 8 percent scale circle and is accompanied by the calculated trend (also shown by a dashed line) and P, the probability of randomness.



tains only low percentages of vein pebbles (Fig. 31). Unit A is a basal till of regional extent which was deposited by an ice sheet advancing from the north-northeast. If the orientation of the till pebbles at site 32 (Fig. 30) is assumed to be "transverse" to glacial flow, then all three measurements from this till (sites 27, 31, and 32; Fig. 30) indicate that the glacier that deposited unit A advanced southward across the subcrop of the ore zone. Therefore, unit A should contain large quantities of detritus derived from the vein.

The rare vein pebbles in unit A are weathered, and weathering pits in the pebbles are packed with till matrix. The weathering is probably pre-Wisconsinan; the presence of the pebbles in unit A indicates that the vein was at least partly exposed to erosion at the onset of glaciation. The vein pebbles are distributed in the till in discontinuous bands commonly only one pebble thick. The bands of vein pebbles in unit A are interpreted as reflecting simultaneous glacial transport and comminution of the clasts along discrete planar paths.

One possible explanation for the low content of vein pebbles in unit A is that the vein subcrop was masked during deposition of unit A by an older drift unit that has since been removed from the vein subcrop by erosion during post-unit A time. This explanation is unsatisfactory because there is no physical evidence that an older unit existed. Another possible explanation is that the base of the ice

sheet that deposited unit A was at its pressure-melting point. This would make abrasion and crushing the main erosional processes and lodgement of till the main depositional process at the base of the ice sheet (Boulton, 1972). Local inhomogeneities in subglacial water pressure would govern the distribution of zones of erosion and deposition. The fine-grained texture of, and the lack of rubble in unit A is evidence that plucked sediment is a minor local component of the till. It is believed that lodgement of till was the main process occurring at the Icon Sullivan Joint Venture property during deposition of unit A, but this hypothesis cannot be tested because of a lack of physical evidence.

Comparison of the Icon Train to other sulphide-bearing dispersal trains

The Icon Train is listed in Table 4 with other sulphide-bearing glacial dispersal trains (see Bradshaw, 1975, pp. 104-107 and pp. 190-193 for additional examples). The trains are variable in size and methods of definition, but they are generally finger-shaped or flame-shaped in plan, and all have abrupt lateral edges. The large trains that were defined with low sample densities, Kidd Creek and Mt. Pleasant, are detectable by reconnaissance-scale sampling. Szabo et al. (1975) stated that a sample density of 0.2 samples per square kilometre would be adequate to detect the Mt. Pleasant train. Smaller trains require a

Table 4. Sulphide-bearing glacial dispersal trains.

NAME, METALS, SUBCROP SIZE*	SAMPLE DENSITY (no./sq.km.)	SAMPLING MEDIUM COMPONENT ¹	ANOMALY SIZE (length by width)	ANOMALY SHAPE	REFERENCE
Kidd Creek, Ont., Cu, Zn, Ag, 600 by 30 m.	1.5	Unox. lowest till, Zn and Cu	8 by 1.6 km.	Finger	Skinner, 1972
Mt. Pleasant, N.B. Mo, W, Bi, Cu, Sn, Zn two large sources	1.5	Oxidized till, Cu and Zn Pb Ore host rock	7-16 by 3.5 km. 12-16 by 3.5 km. 8 by 3 km.	Flame	Szabo et al., 1975
Spi Lake, N.W.T., Zn, Pb, Cu, small, linear	8	Soil on till, Cu and Zn	4 by .5-1 km.	Finger	Shilts, 1975
Noranda, Que., Zn, Cu, 800 by 400 m.	9	Soil on till, Cu Zn	2 by 2 km. 1.5 by 1.5 km.	Flame	Dreimanis, 1960
Agricola Lake, N.W.T., Pb, Cu 50 by 400 m.	2320	Soil on till Cu and Pb	500 by 250 m.	Flame	Cameron and Durham, 1975
Icon mine, Que. Cu 30 by 100 m.		Soil on till			
20 to 80 by 370 m.	580	North Train, Cu	1650 by 75 m.	Finger	this study
20 to 80 by 370 m.	580	Icon Train, Cu	630 by 300 m.	Flame	
	580	Icon Tr., vein pbls.	570 by 250 m.	Flame	
Makola, Finland, Ni 80 by 100 m.	09	Soil on till Ni	1 by .25 km.	Finger	Kauranng, 1959
Korsnas, Finland Pb 450 by 100 m.	38	Soil on till Pb	1.8 by .6 km.	Finger	Hyvarinen, 1967

*First number is length of subcrop parallel to direction of glacial flow, second number is length of subcrop at right angles to direction of glacial flow.
¹See references for explanations of methods of analysis.

higher sample density, 8 to 10 samples per square kilometre. Increasing the sample density to 500 or even 2000 samples per square kilometre (Table 4) is required for detailed tracing of trains.

The use of high sample densities, in spite of the high cost, provides information which guides other exploration methods. Detailed sampling more accurately defines the edges and shape of a train, and it facilitates location of the bedrock source of the metal or rock being traced. Once the source is known, study of the till in relation to its source may give detailed information on the processes of glacial erosion and deposition.

CHAPTER 5

GLACIAL COMMINUTION OF CHALCOPYRITE

Unoxidized till

Vagners (1969) and Dreimanis and Vagners (1971) have shown that minerals are glacially comminuted (crushed and abraded) so that the mineral species have peaks of abundance in specific particle size ranges. Near the source of a mineral, a clast-size mode dominates, whereas farther from the source, a matrix mode appears and the clast-size mode diminishes. With continued transport, the matrix mode does not become finer. The process of development of the matrix modes may be analogous to the "equilibrium particle size distribution" observed by Bradshaw (1951), Theimer (1952) and Kelsall (1965) for artificially comminuted minerals.

The selection of the optimum particle size ranges for lithological or geochemical analyses of till for prospecting purposes should take into account the particle size ranges to which ore minerals are glacially comminuted. The selection of these size ranges becomes especially important when samples are collected by overburden drilling techniques, in which small samples are recovered

from subsurface tills that are difficult to identify. An experiment was performed to determine the abundance of chalcopyrite in different particle size fractions of till.

Four samples of 50 to 60 litres of unoxidized till were collected from unit C, the till in the Icon Train. The sample sites were selected to give a wide range in distance of glacial transport, local provenance, and total chalcopyrite content (Table 5). The laboratory procedures and calculations are similar to those of Vagners (1969, pp. 14-41), except that volume or number percentages were used as much as possible instead of weight percentages to avoid biases resulting from the extreme differences between the specific gravities of chalcopyrite and the other minerals. The apparent percentage of chalcopyrite (A_p) was determined for each of 17 size fractions from 128 mm. to less than 0.002 mm. by separation and volumetric measurement of the plus 4 mm. fractions and by point counting of the finer sizes. The abundance of sediment (all mineral species) in each size fraction (G_p) was determined from particle size analyses which were performed volumetrically for fractions coarser than 0.063 mm. and from hydrometer analyses of the finer fractions. The true percentage of chalcopyrite in each fraction (T_p) was determined by multiplying A_p times G_p for each fraction. The sum of the T_p is the total chalcopyrite content of the sample (Table 5). In order to compare the four samples, the true relative percentage of chalcopyrite in

Table 5. Description of samples referred to in text in determinations of abundance of chalcopyrite in till.

Sample Number	73-56	73-57	73-58	73-74	72-12EU46	72-12EU56
Location	1+25S, 3+15E (Fig. 23)	1+20S, 3+20E (Fig. 23)	2+35S, 9+70E (Fig. 27)	3+05S, 10+70E (Fig. 27)	2+50S, 8+20E (Fig. 27)	2+50S, 8+20E (Fig. 27)
Gross Texture	Fine	Fine	Coarse	Coarse	Coarse	Coarse
Transport distance	10 to 50 m.	10 to 50 m.	90 to 125 m.	110 to 150 m.	90 to 125 m.	90 to 125 m.
Provenance of clasts	Vein	Vein	Vein	Vein	Vein	Vein
Provenance of matrix	Unit B (Sand)	Unit B (Sand)	Vein	Vein	Vein	Vein
Chalcopyrite content	14.32%	3.00%	3.48%	23.29%	2.79%	15.99%
Degree of oxidation	Nil	Nil	Nil	Nil	Moderate	High

each fraction (Trp) was calculated by converting the T_0 in each fraction to a percentage of the total T_p . The Trp will be the main variable considered in the following discussion, and all results are tabulated in Appendix C.

The true relative percentages (Trp) of chalcopyrite in the four samples are presented as frequency polygons on Figure 33. All samples have a clast-size mode or modes in the 8 to 1 mm. range, and three samples have matrix modes in the 0.25 to 0.016 mm. range. The two samples with relatively short transport distances (73-56, 73-57) have strong clast modes and weak or irregular matrix modes. The particle size range in the clast modes is believed to reflect the fracture pattern of the chalcopyrite in place, but this cannot be quantified. The samples with relatively long transport distances (73-58, 73-74) have the strongest matrix modes even though these samples are relatively coarse-grained (Table 5).

The effect of incorporation of sand from unit B into the till can be seen in the frequency polygon for sample 73-57. An irregular peak occurs in the size range 0.25 to 0.032 mm. Examination of the data for this sample (Appendix C) shows that this peak is artificial and caused by an abundance of sediment (high Gp) in this size range, not by abundant chalcopyrite (Ap). Hence, the real matrix modes on Figure 33 are between 0.063 and 0.016 mm. (samples 73-58, 73-74).

From the foregoing discussion, it can be seen that

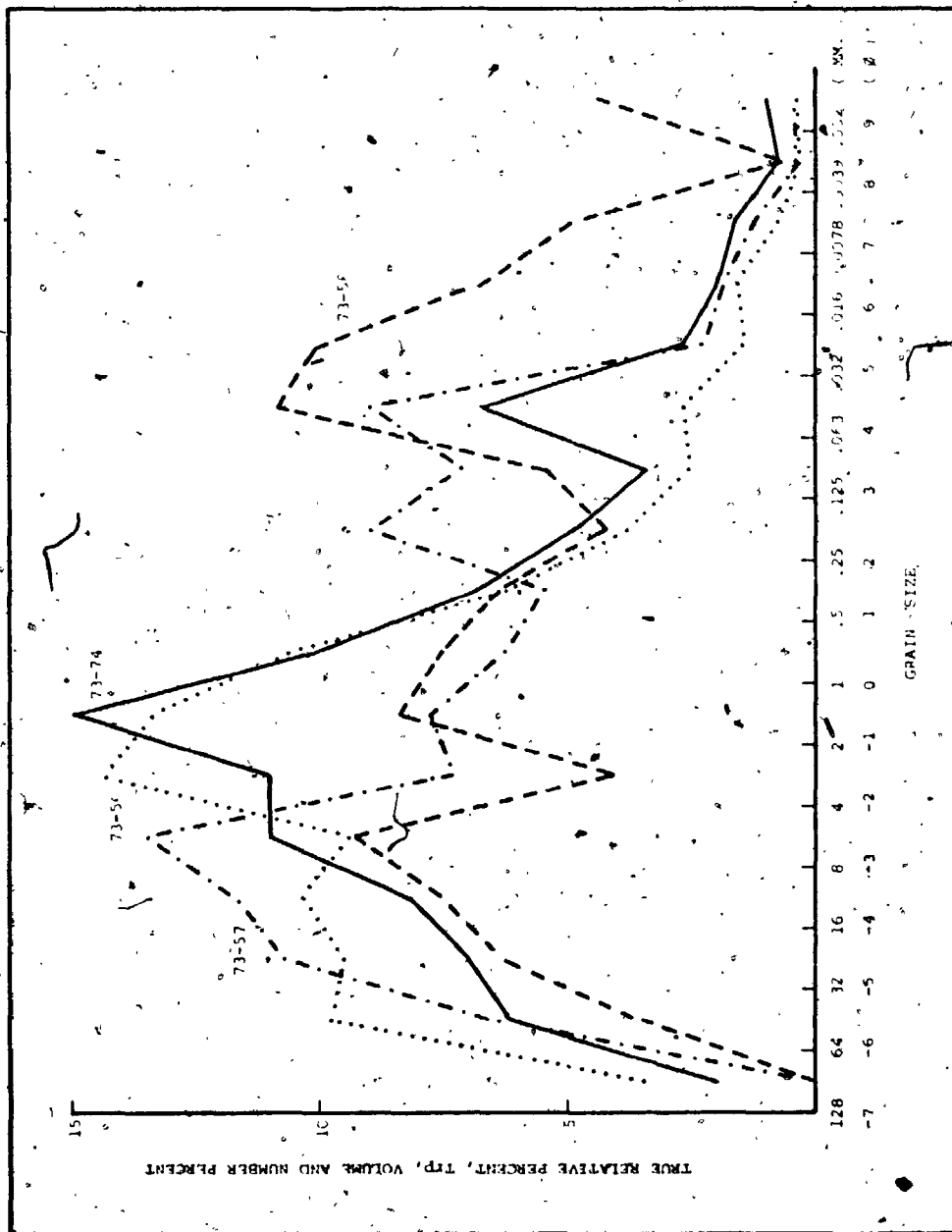


Figure 33. True Chalcopyrite distribution in till samples 73-56, 73-57, 73-58, and 73-74.

within 50 metres of the source, chalcopyrite is glacially comminuted to produce a well-defined clast mode in the 8 to 1 mm. range. A matrix mode is not developed in less than 50 m. of transport. With transport of more than 100 metres, a matrix mode develops in the 0.063 to 0.016 mm. range. Therefore, it is suggested that 0.063 to 0.016 mm. be selected as or included in the analyzed particle size range when unoxidized basal till is sampled for geochemical analysis. Analysis of the heavy mineral fraction of this particle size range will remove unwanted light mineral contaminants and will enhance the geochemical response of the samples. Lithological analysis of the 8 to 1 mm. fraction may provide useful information, especially near the source of the chalcopyrite.

The suggestions given above have limitations. It is obvious that pebbles of solid chalcopyrite will never be found in till derived from fine-grained or disseminated ore in which the maximum size of chalcopyrite grains is less than 1 mm. The chalcopyrite clasts and grains seen in this study were all angular and chalcopyrite powder was rare, which agrees with the interpretation of the detritus in unit C as crushed sediment derived from the vein by quarrying. In other glaciated areas where abrasion has been the main erosional process, the detritus derived from an ore zone should be finer-grained. This type of study must be repeated for tills derived by abrasion of fine-grained ores before positive statements can be made about

the optimum particle size ranges for geochemical analysis of unoxidized till. Other ore minerals should be investigated to broaden the scope of future studies.

Weathering of chalcopyrite-bearing till

The surficial weathering of unit C in the Icon Train has changed the mineralogy of the till. Ferroan dolomite, pyrite, and chalcopyrite from the vein and marcasite from the graphitic argillite host rock have all been weathered. Quartz is unaltered. Pyrite and marcasite are rare in the oxidized till. Ferroan dolomite is present as powdery limonitic pseudomorphs where the till is strongly oxidized and as soft, oxidized grains where the till is less weathered. The relative weathering resistances of chalcopyrite and ferroan dolomite were estimated by examining clasts containing these minerals and by comparing their relief relative to quartz crystals in the same clasts. Quartz crystals protrude 1 to 3 mm. from massive chalcopyrite whereas ferroan dolomite is weathered 1 to 2 mm. into the chalcopyrite. Therefore, ferroan dolomite has weathered more rapidly than chalcopyrite. Weathered chalcopyrite clasts are brown to dark brown (7.5YR 4/2), coated with 0.5 to 2.0 mm. of limonite. Limonite also occurs in fractures that are 0.5 to 1.0 mm. wide in the chalcopyrite. Under the limonite, the chalcopyrite is fresh. The author believes that a coating of limonite impedes further oxidation of the chalcopyrite.

Malachite and limonite are the main secondary minerals in the till. Limonite is present as cement, sand-sized grains, and coatings on chalcopyrite grains. Limonitic surfaces are usually coated with malachite. Malachite occurs as cement, sand-sized grains, and banded botryoidal masses in weathering pits in the till. Azurite is found with the malachite, but it is much less common. It usually forms a finely crystalline coating on botryoidal malachite, and it is a cement below malachite in cemented sediments. Where oxidized unit C overlies unit B, malachite and azurite are cement in unit B up to 5 cm. below the contact. Bornite and chalcocite form a tarnish on a few chalcopyrite grains only in the slightly oxidized parts of the till. Rare dolostone pebbles plated with native copper were found near the surface of the till.

An experiment was performed to estimate the amount of chalcopyrite destroyed during the weathering of unit C and to find the optimum grain size ranges for geochemical and lithological analyses of oxidized chalcopyrite-bearing till. Samples of 1 to 2 kg. of oxidized till were collected from the B and C horizons of the soil profile developed on unit C. Each sample was split into 11 size fractions between 64 mm. and 0.037 mm. and the weight percentage of heavy minerals (chalcopyrite, malachite, and limonite) was determined for each fraction after separation in tetrabromoethane ($S.G. = 2.96$). Malachite and limonite were removed from the splits with a weak hydro-

chloric acid wash. The abundance of chalcopryrite in the remaining heavy minerals was converted to true relative percentage (Trp) for each split in the same way as for the unoxidized till samples already described, except that the data were weight percentages. The results of these analyses are tabulated in Appendix D.

The abundances of heavy minerals (Hp) and chalcopryrite (Ap) in sample 72-12EU56 are shown on Figure 34. This sample is from the B horizon 0.3 m. below the surface of the soil profile developed on unit C. The gap between the curves is the percentage of malachite plus limonite present in the sample. Malachite and limonite are most common in the particle size range 0.5 to 0.037 mm. The true distribution of chalcopryrite (Trp) in the same sample is shown on Figure 35. A strong clast mode appears in the range 32 to 8 mm., and no matrix mode is present. The sample is from till that was transported at least 100 m. from its source (Table 5), so that modes were expected in the same particle size ranges that were found for unoxidized till samples 73-58 and 73-74 (Fig. 33). Either the till at site 72-12EU56 never had a matrix mode or the matrix mode was altered to malachite plus limonite and the clast mode shifted into coarser sizes in response to the removal of the finer chalcopryrite.

A sample of oxidized till (sample 72-12EU46) was collected 0.3 m. below sample 72-12EU56 from the less strongly oxidized C horizon of the soil profile. The true distri-

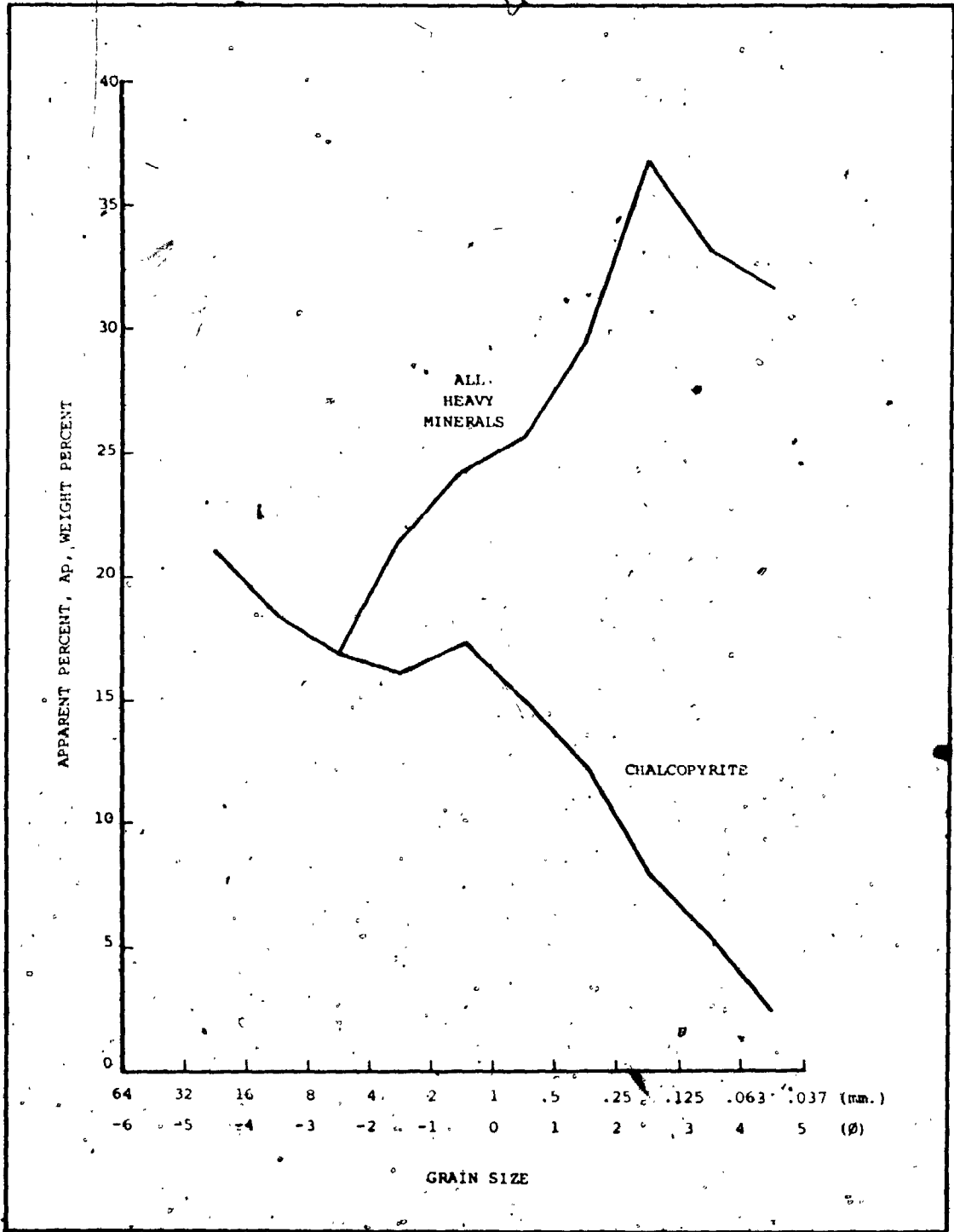


Figure 34. Apparent heavy mineral and chalcopyrite distributions in till sample 72-12EU56.

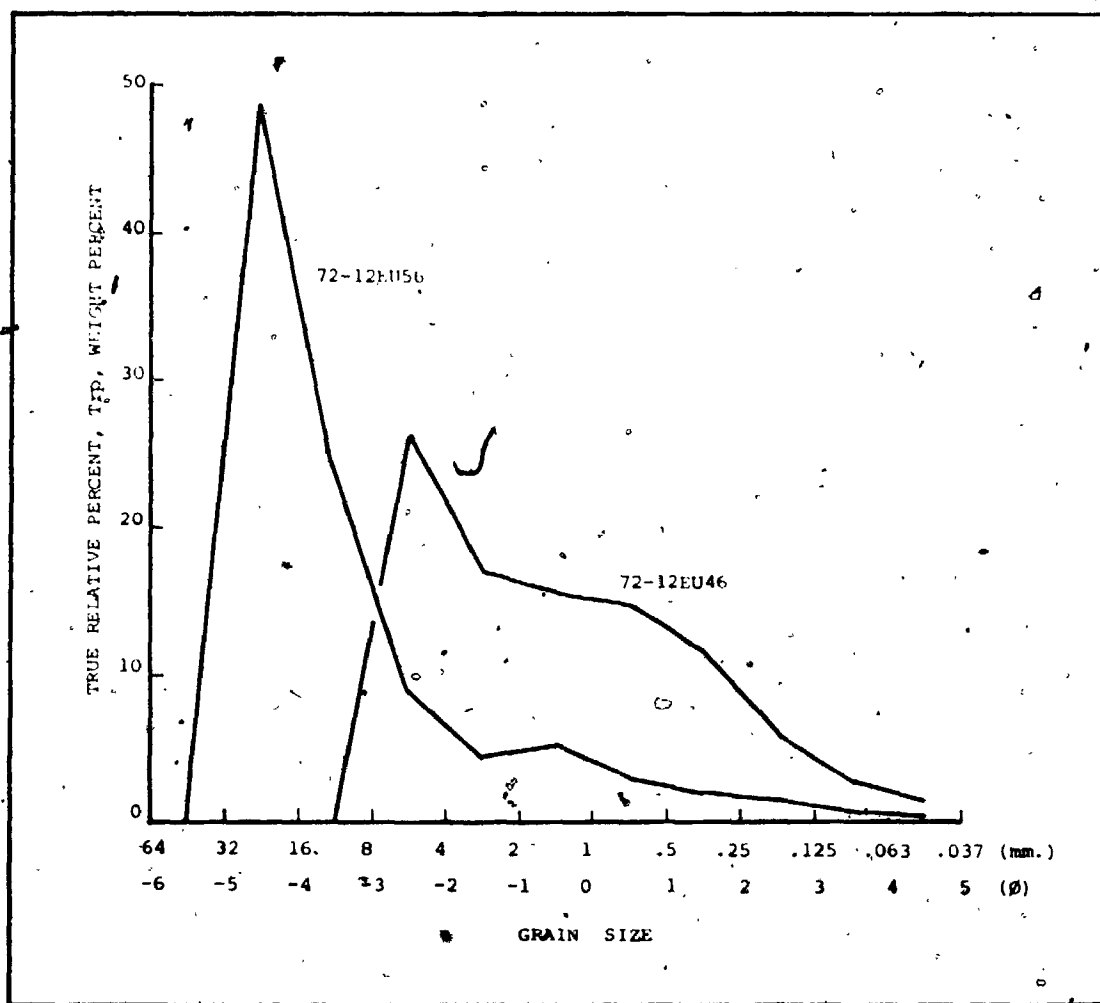


Figure 35. True chalcopyrite distribution in till samples 72-12EU56 and 72-12EU46.

bution of chalcopyrite (Trp) in this sample (Fig. 35) has a clast mode in the range of 4 to 2 mm. and a broad shoulder in the sand sizes. This indicates that the till did contain a matrix mode of chalcopyrite which has been partly or entirely removed depending on the degree of weathering. The finer chalcopyrite grains disappear earliest, and coarser grains are altered as weathering proceeds.

It should be noted that these samples are small and many do not contain the full range of particle sizes (e.g. no chalcopyrite greater than 16 mm. in sample 72-12EU46, Fig. 35), but the following consistent relationships are present from sample to sample (Appendix D):

a) The abundance of chalcopyrite has an inverse relationship to the abundance of malachite plus limonite with respect to particle size

b) The finer sizes contain the highest amounts of malachite plus limonite and the lowest amounts of chalcopyrite.

This means that when samples of oxidized chalcopyrite-bearing till are collected for geochemical analysis, 0.5 to 0.037 mm. is the optimum particle size range because it is in this range that most of the malachite is found.

This conclusion can only be made for tills that contain detrital carbonate minerals and have a low content of such sulphides as pyrite, pyrrhotite, and marcasite.

Weathering of detrital carbonate minerals and rocks pro-

duces carbonate ions which fix copper ions as malachite. Without a source of carbonate ions, the copper ions from weathering chalcopyrite could be mobilized and would remain in the soil only as adsorbed ions. A high content of pyrite-like minerals might produce enough acid to mobilize both copper and carbonate ions. The importance of carbonate ions from other sources (e.g. rain, air) in malachite formation is unknown for this till.

About 7,700 years have elapsed since unit C was initially exposed to significant weathering (Prest, 1970, pp. 724-725). In this period, most chalcopyrite grains in the till finer than 0.5 mm. and within 0.6 m. of the surface have been altered to malachite plus limonite. Limonite is believed to have formed largely in place, as the insoluble residue of chalcopyrite. The occurrence of malachite as cement in unit B up to 5 cm. below its contact with weathered unit C is evidence of the mobility of copper released during weathering of chalcopyrite, but most of the malachite is in unit C, fixed locally by carbonate ions released during weathering of ferroan dolomite and dolostone.

CHAPTER 6

CONCLUSIONS AND RECOMMENDATIONS

Conclusions

(1) The Quaternary units in the Lac Mistassini - Lac Waconichi area are the products of a simple glacial cycle of: major advance - recession - minor readvance - completed recession - glaciofluvial sedimentation - glaciolacustrine sedimentation - organic sedimentation. These events occurred during the Wisconsinan and Holocene. The units are time-transgressive and many of the events were partly synchronous within the area.

(2) The pebble lithology of the most widespread till in the area (unit A) closely reflects the lithology of the underlying bedrock. This hampers the use of pebble lithology for the mapping of till, but conversely, it means that the pebble lithology can be used to map bedrock, indirectly determine glacial flow direction, and trace distinctive rock types to their sources. The texture and carbonate content of the till matrix respond slowly to changes in the texture and carbonate content of the bedrock, which also allows their use as mapping tools for basal tills. The texture and carbonate content of the

till matrix appear to have been influenced by addition of fine sediment to the debris load of the glacier through comminution during transport of the coarser part of the debris load.

(3) The copper-bearing dispersal trains at the Icon mine were formed by glacial erosion, transport, and deposition during the minor readvance that deposited unit C. The processes of formation of the trains were orderly, not chaotic.

(4) The dispersal trains are three-dimensional bodies, the shape and lithology of which were strongly influenced by the substrata. They are ribbon- or flame-shaped in plan view. The Icon Train has a longitudinal shape like an elongated and attenuated tear-drop. The trains have sharp edges and high geochemical and lithological contrast to the surrounding till. It is possible to map dispersal trains at a detailed scale.

(5) It is estimated that between 7,000 and 20,000 cubic metres of rock were eroded from the subcrop of the number 1 ore zone at the Icon mine by the small glacial tongue that deposited unit C. These volume estimates are equivalent to a slab of rock 2.8 m. thick with an area between 2440 and 7140 square metres. The erosion is believed to have taken place mainly by quarrying of the downglacier edge of the vein subcrop.

(6) Mapping the abundance of chalcopyrite-bearing pebbles in the Icon Train is a more efficient guide to

the location of the ore in place than geochemical analyses for copper in the soil on the train. Chalcopyrite is most abundant in the range 32 to 8 mm. in strongly oxidized till. When clasts containing economically interesting minerals are discovered in a till, the abundance of those clasts should be mapped.

(7) In unoxidized till, chalcopyrite has a clast mode between 8 and 1 mm. and a matrix mode from 0.063 to 0.016 mm. The clast mode develops after short transport distances and the matrix mode requires at least 100 m. of transport to develop. The size range to be analyzed for copper should include the matrix mode when samples are collected from unoxidized till by subsurface sampling techniques during mineral exploration programmes.

(8) Oxidized till containing chalcopyrite plus carbonates has abundant malachite in the range 0.5 to 0.037 mm. Sampling of oxidized till for prospecting purposes should include this size range. This conclusion applies only for tills that have not been completely leached of carbonates.

(9) Basal tills (units A and C) reflect the local bedrock lithology better than ablation till (in unit B), ice-contact stratified drift (in unit B), outwash gravel (unit D), and postglacial stream or lake sediments (unit F). Basal tills are the preferred media for geochemical or lithological sampling of glacial drift in mineral exploration. Unit C contains more detritus derived from the

Icon ore zones than does unit A because the deposition of unit C was accompanied by strong local glacial quarrying, whereas the dominant process during deposition of unit A was lodgement with minor erosion of the ore zones.

Recommendations for future research

(1) The lithology and texture of unit A should be mapped in a larger part of the Mistassini basin to determine regional trends in the properties of this till.

(2) Other glacial dispersal trains should be mapped at a detailed scale to provide additional examples of the size, shape, and structure of dispersal trains. Such studies are useful for interpreting glacial processes and they provide guidelines for mineral exploration in glaciated terrain.

(3) The abundance of chalcopyrite with respect to grain size should be determined for unoxidized and oxidized tills derived from texturally and structurally different ore deposits in other areas.

(4) The abundance of other ore minerals (e.g. sphalerite) with respect to grain size should be determined for unoxidized and oxidized tills in other areas.

REFERENCES

- Allan, R. J., Cameron, E. M., and Durham, C. C., 1973, Reconnaissance geochemistry using lake sediments of a 36,000-square-mile area of the northwestern Canadian Shield (Bear-Slave operation, 1972): Geol. Surv. Can., Paper 72-50, 70p.
- _____, and Timperley, M. H., 1975, Prospecting by use of lake sediments in areas of industrial heavy metal contamination: in Jones, M. J., Ed., Prospecting in areas of Glaciated Terrain 1975: Institution of Mining and Metallurgy, London, pp. 87-111.
- Allard, G. O., and Cimon, J., 1974, Minimal Pleistocene Glaciation in the Chibougamau area, Quebec: Geol. Assoc. Can. - Mineralog. Assoc. Can., Abstracts of papers presented at Annual Meeting, St. John's, Newfoundland, p. 1.
- American Commission on Stratigraphic Nomenclature, 1970, Code of Stratigraphic Nomenclature: Am. Assoc. Pet. Geol., 22p.
- American Society for Testing and Materials, 1964, Procedure D422-63: in Procedures for testing soils, 4th edition: A.S.T.M., Philadelphia, pp. 95-106.
- Andrews, J. T., and Shimizu, K., 1966, Three-dimensional vector technique for analyzing till fabrics: discussion and FORTRAN program: Geograph. Bull., v. 8, pp. 151-165.
- Bell, R., 1897, Report on Exploration on Nottaway River Basin: Geol. Surv. Can., Sum. Rept. for 1896, pp. 64-74.
- Bergeron, R., 1957, Lake Precambrian rocks of the North shore of the St. Lawrence River and of the Mistassini and Otish Mountains areas, Quebec: in The Proterozoic of Canada: Roy. Soc. Can., Spec. Publ. No. 2, pp. 124-131.
- Bostock, H. S., 1970, Physiographic Subdivisions of Canada: in Douglas, R.J.W., Ed., Geology and Economic Minerals of Canada: Geol. Surv. Can., Econ. Geol. Rept. No. 1, pp. 9-30.
- Boulton, G. S., 1972, The role of thermal regime in glacial sedimentation: in Price, R. J., and Sugden, D. E., Eds., Polar Geomorphology: Inst. of British Geographers, Spec. Publ. No. 4, pp. 1-19.

- _____, 1974, Processes and patterns of glacial erosion: in Coates, D. R., Ed., *Glacial Geomorphology*, Proc. 5th Annual Geomorphology Symposium, Binghamton, N.Y.: State Univ. New York, Binghamton, pp. 11-40.
- Bradshaw, B. C., 1951, Effect of grinding on particles: *J. Chem. Phys.*, v. 19, pp. 1057-1059.
- Bradshaw, P.M.D., Ed., 1975, Conceptual models in exploration geochemistry: *J. Geochem. Explor.*, v. 4, pp. 1-223.
- Cameron, E. M., and Durham, C. C. (1975). Soil geochemistry of the Agricola Lake massive sulphide prospect: *Geol. Surv. Can.*, Paper 75-1, Pt. A, pp. 199-202.
- Caty, J.-L., and Chown, E. H., 1973, Etude Geologique, Region de la Baie Abatagush, Territoire de Mistassini: *Que. Ministeres des Richesses Naturelles*, D. P. 189, 18p.
- Chown, E. H., and Caty, J.-L., 1973, The clastic members of the Mistassini-Otish Basin: in Young, G. M., Ed., *Huronian Stratigraphy and Sedimentation*: *Geol. Assoc. Can.*, Spec. Paper No. 12, pp. 49-71.
- Collins, J. A., Brown, A. C., and Smith, L., 1974, The Precambrian Mistassini Group, Grenville overthrusting and the Icon copper deposit: *Geol. Assoc. Can. - Mineralog. Assoc. Can.*, Abstracts of papers presented at Annual Meeting, St. John's, Newfoundland, p. 19.
- Curray, J. R., 1956, The analysis of two-dimensional orientation data: *J. Geol.*, v. 64, pp. 117-131.
- Dallmeyer, R. D., 1974, $^{40}\text{Ar}/^{39}\text{Ar}$ incremental release ages of biotite and hornblende from pre-Kenoran gneisses between the Matagami-Chibougamau and Frotet-Troilus greenstone belts, Quebec: *Can. J. Earth Sci.*, v. 11, pp. 1586-1593.
- Deland, A.-N., and Sater, G. S., 1967, Duquet-McQuat area, Mistassini Territory: *Que. Dept. Nat. Resources*, *Geol. Rept.* 126, 29p.
- Dixon, W. J., and Massey, Jr., F. J., 1969, *Introduction to Statistical Analysis*: McGraw-Hill, New York, 638p.
- Dreimanis, A., 1956, Steep Rock iron ore boulder train: *Proc. Geol. Assoc. Can.*, v. 8, Pt. I, pp. 27-70.

_____, 1960, Geochemical prospecting for Cu, Pb, and Zn in glaciated areas, eastern Canada: 21st Int. Geol. Cong., Norden, Pt. II, pp. 7-19.

_____, 1962, Quantitative gasometric determination of calcite and dolomite by using Chittick apparatus: J. Sed. Pet., v. 32, pp. 520-529.

_____, 1976, Tills; their origin and properties: in Legget, R. F., Ed., Glacial Till, an Interdisciplinary Study: Univ. of Toronto Press, Toronto, pp. 11-49.

_____, and Karrow, P. F., 1972, Glacial history of the Great Lakes-St. Lawrence region, the classification of the Wisconsin(an) Stage, and its correlatives: 24th Int. Geol. Cong., Section 12, pp. 5-15.

_____, and Vagners, U. J., 1971, Bimodal distribution of rock and mineral fragments in basal tills: in Goldthwait, R. P., Till/A Symposium, Ohio State University Press, Columbus, pp. 237-250.

Duquette, G., 1970, Archean Stratigraphy and ore relations in the Chibougamau district: Que. Dept. Nat. Resources, Spec. Paper 8, 16p.

_____, 1972, The Chibougamau-Chapais greenstone belt: in Allard, G. O., Ed., Precambrian Geology and mineral deposits of the Noranda-Val d'Or and Matagami-Chibougamau greenstone belts, Quebec: 24th Int. Geol. Cong. Guidebook to Excursion A41 and C41, pp. 51-70.

Elson, J. A., 1961, The Geology of tills: in Penner, E., and Butler, J., Eds., Proc. 14th Can. Soil Mechanics Conf.: N.R.C. Canada, Assoc. Comm. Soil and Snow Mechanics, Tech. Mem. 69.

Faribault, E. R., Gwillim, J. C., and Barlow, A. E., 1911, Geology and mineral resources of the Chibougamau region, Quebec, by the Chibougamau Mining Commission: Que. Dept. Colonization, Mines and Fisheries, 224p.

Fielder, F. M., 1975, Canadian Mines Handbook, 1975-1976: Northern Miner Press, Toronto, 420p.

Flint, R. F., 1971, Glacial and Quaternary Geology: John Wiley and Sons, Inc., New York, 892p.

- Forgeron, F. D., 1971, Soil Geochemistry in the Canadian Shield: C.I.M.M. Bull., v. 64, no. 715, pp. 37-42.
- Fryer, B. J., 1972, Age determinations in the Circum-Ungava Geosyncline and the evolution of Precambrian banded iron-formations: Can. J. Earth Sci., v. 9, pp. 652-663.
- Gadd, N. R., 1971, Pleistocene Geology of the central St. Lawrence Lowland: Geol. Surv. Can., Mem. 359, 153p.
- Gilbert, J. E., 1958, Bignell area, Mistassini and Abitibi Territories: Que. Dept. Mines, Geol. Rept. 79, 37p.
- Gillett, L. B., 1962, Bedrock and Pleistocene Geology of the Vienne-Blaklock area, Quebec, with observations on Magnetic Diabase Dikes in Northeast Ontario and Northwest Quebec: Unpublished Ph.D. Thesis, Princeton Univ., 222p.
- Goldthwait, R. P., 1971, Introduction to Till, Today: in Goldthwait, R. P., Ed., Till/A Symposium: Ohio State Univ. Press, Columbus, pp. 3-26.
- Grant, D. R., 1975, Glacial style and the Quaternary stratigraphic record in the Atlantic Provinces, Canada: Geol. Surv. Can., Paper 75-1, Pt. B, pp. 109-110.
- Gros, J.-J., 1975, Geology of south part of Poste Bay, O'Sullivan and Gauvin Townships: Que. Ministry of Nat. Resources, Prelim. Rept. 610, 33p.
- Guilloux, L., 1969, Sud-est du Canton d'O'Sullivan, Territoire de Mistassini: Que. Ministère des Richesses Nat. D. P. 166, 46p.
- _____, 1972, Geology of the Icon mine: in Allard, G. O., Ed., Precambrian Geology and mineral deposits of the Noranda-Val d'Or and Matagami-Chibougamau greenstone belts, Quebec: 24th Int. Geol. Cong. Guidebook to Excursions A41 and C41, pp. 83-91.
- Hageman, B. P. (1971). Report of the Commission on the Holocene (1957): in Ters, M., Ed., Etudes sur le Quaternaire dans le Monde, v. 2: VIII Congress INQUA, Paris, p. 679.
- Hawkes, H. E., and Webb, J. S., 1962, Geochemistry in Mineral Exploration: Harper and Row, New York, 415p.
- Holmes, C. D., 1941, Till fabric: Geol. Soc. Amer. Bull., v. 52, pp. 1299-1354.

Hyvarinen, L., 1967, Geochemical prospecting for lead ore at Korsnas: in Kvalheim, A., Ed., Geochemical Prospecting in Fennoscandia: Interscience, New York, pp. 171-179.

Ignatius, H., 1958, On the late-Wisconsin deglaciation in eastern Canada: Acta Geographica, v. 16, no. 3, pp. 1-34.

Jones, L. M., Walker, R. L., and Allard, G. O., 1974, The Rubidium-Strontium whole-rock age of major units of the Chibougamau greenstone belt, Quebec: Can. J. Earth Sci., v. 11, pp. 1550-1561.

Jones, M. J., (Ed.), 1973, Prospecting in Areas of Glacial Terrain: Institution of Mining and Metallurgy, London, 138p.

_____, 1975, Prospecting in Areas of Glaciated Terrain 1975: Institution of Mining and Metallurgy, London, 154p.

Karup-Moller, S., and Brummer, J. J., 1970, The George Lake zinc deposit, Wollaston Lake area, northeastern Saskatchewan: Econ. Geol., v. 65, pp. 862-874.

Kauranne, L. K., 1959, Pedogeochemical prospecting in glaciated terrain: Comm. Geol. Finl., Bull. 184, pp. 1-10.

Kelsall, D. F., 1965, A study of breakage in a small continuous open circuit wet ball mill: in Arbiter, N., Ed., VII International Mineral Processing Congress, v. 1: Gordon and Breach, New York, pp. 33-42.

Kokkola, M., 1975, Stratigraphy of till at Hitura open-pit, Nivala, western Finland, and its bearing on geochemical prospecting: in Jones, M. J., Ed., Prospecting in areas of Glaciated Terrain 1975: Institution of Mining and Metallurgy, London, pp. 149-154.

Kvalheim, A., Ed., 1967, Geochemical Prospecting in Fennoscandia: Interscience, New York, 350p.

Laurin, A. F., Coordinator, 1969, Geological Map of Quebec: Que. Dept. Nat. Resources, Map.

Levinson, A. A., 1974, Introduction to Exploration Geochemistry: Applied Publishing, Calgary, 612p.

Long, D.G.F., 1973, The Stratigraphy and Sedimentology of the Chibougamau Formation: Unpublished M.Sc. Thesis, Univ. Western Ontario, London, Ontario, 305p.

_____, 1974, Glacial and paraglacial genesis of conglomeratic rocks of the Chibougamau Formation (Aphebian); Chibougamau, Quebec: Can. J. Earth Sci., v. 11, pp. 1236-1252.

Low, A. P., 1885, Report of the Mistassini Expedition, 1884-5: Geol. and Nat. Hist. Surv. Can., Ann. Rept. New Ser., v. I, pp. 1D-55D.

_____, 1896, Report on explorations in the Labrador Peninsula along the East Main, Koksoak, Hamilton, Manicouagan and portions of other rivers in 1892-93-94-95: Geol. Surv. Can., Ann. Rept., New Ser., v. VIII, p. 1L-387L.

_____, 1906, Geological Report on the Chibougamau Mining Region: Geol. Surv. Can., Publ. No. 923, 61p.

Mark, D. M., 1971, Rotational vector procedure for the analysis of till fabrics: Geol. Soc. Amer. Bull., v. 82, pp. 2661-2666.

_____, 1973, Analysis of axial orientation data, including till fabrics: Geol. Soc. Amer. Bull., v. 84, pp. 1369-1375.

McDonald, B. C., 1971, Late Quaternary stratigraphy and deglaciation in eastern Canada: in Turekian, K. K., Ed., Late Cenozoic Glacial Ages: Yale Univ. Press, New Haven, pp. 331-353.

_____, and Shilts, W. W., 1971, Quaternary stratigraphy and events in southeastern Quebec: Geol. Soc. Amer. Bull., v. 82, pp. 683-698.

McGlynn, J. C., 1970, Superior Province: in Douglas, R.J.W., Ed., Geology and Economic Minerals of Canada: Geol. Surv. Can., Econ. Geol. Rept. No. 1, pp. 54-71.

Munsell Color Co., 1971, Munsell Soil Color Charts: Munsell Color Company Inc., Baltimore.

Neilson, J. M., 1953, Albanel Area, Mistassini Territory: Que. Dept. Mines, Geol. Rept. 53, 35p.

_____, 1963, Lake Albanel iron range, northern Quebec: C.I.M.M. Bull., v. 56, no. 609, pp. 35-41.

_____, 1966, Takwa River Area: Que. Dept. Nat. Res., Geol. Rept. 124, 53p.

- Nicol, I., Coker, W. B., Jackson, R. G., and Klassen, R. A., 1975, Relation of lake sediment composition to mineralization in different limnological environments in Canada: in Jones, M. J., Ed., *Prospecting in areas of Glaciated Terrain 1975*: Institution of Mining and Metallurgy, London, pp. 112-125.
- Norman, G.W.H., 1938, The last Pleistocene ice-front in the Chibougamau district, Quebec: *Roy. Soc. Can., Trans., Sect. 4*, v. 32, pp. 69-86.
- _____, 1939, The south-eastern limit of glacial lake Barlow-Ojibway in the Mistassini Lake region Quebec: *Roy. Soc. Can., Trans., Sect. 4*, v. 33, pp. 59-65.
- _____, 1940, Thrust faulting of Grenville gneisses northwestward against the Mistassini Series of Mistassini Lake, Quebec: *J. Geol.*, v. 48, pp. 512-525.
- O'Donnell, N. D., 1973, Glacial Indicator Trains near Gullbridge, Newfoundland: Unpublished M.Sc. Thesis, Univ. Western Ontario, London, Ontario, 259p.
- Prest, V. K., 1968, Nomenclature of moraines and ice-flow features as applied to the glacial map of Canada: *Geol. Surv. Can., Paper 67-57*, 32p.
- _____, 1970, Quaternary Geology of Canada: in Douglas, R.J.W., Ed., *Geology and Economic Minerals of Canada: Geol. Surv. Can., Econ. Geol. Rept. No. 1*, pp. 675-764.
- Quirke, Jr., T. T., Goldich, S. S., and Krueger, H. W., 1960, Composition and age of the Temiscamie iron-formation, Mistassini Territory, Quebec, Canada: *Econ. Geol.*, v. 55, pp. 311-326.
- Richardson, J., 1872, Report on the Country North of Lake St. John: *Geol. Surv. Can., Rept. of Progress for 1870-71*, pp. 283-308.
- Seguin, M. K., and Laroche, P., 1975, Physical properties of specimens from sulphide deposits in Quebec: *C.I.M.M. Bull.*, v. 68, no. 757, pp. 57-66.
- Shaw, G., 1944, Moraines of late Pleistocene ice fronts near James Bay, Quebec: *Roy. Soc. Can., Trans., Sect. 4*, v. 38, pp. 79-85.

Shaw, J., and Freschauf, R. C., 1973, A kinematic discussion of the formation of glacial flutings: *Can. Geog.*, v. 17, pp. 19-35.

Shilts, W. W., 1971, Till studies and their application to regional drift prospecting: *Can. Mining J.*, v. 92, no. 4, pp. 45-50.

_____, 1973, Glacial dispersal of rocks, minerals, and trace elements in Wisconsinan till, southeastern Quebec, Canada: in Black, R. F., Goldthwait, R. P., and Willman, H. B., Eds.; *The Wisconsinan Stage: Geol. Soc. Amer., Mem.* 136, pp. 189-219.

_____, 1975, Principles of geochemical exploration for sulphide deposits using shallow samples of glacial drift: *C.I.M.M. Bull.*, v. 68, no. 757, pp. 73-80.

_____, 1976, Glacial till and mineral exploration: in Legget, R. F., Ed., *Glacial Till, an Interdisciplinary Study: Univ. of Toronto Press, Toronto*, pp. 205-224.

Skinner, R. G., 1972, Overburden study aids search for ore in Abitibi clay belt: *Northern Miner*, v. 58, no. 37, p. 62.

_____, 1973, Quaternary Stratigraphy of the Moose River Basin, Ontario: *Geol. Surv. Can., Bull.* 225, 77p.

Starkey, J., 1970, A computer programme to prepare orientation diagrams: in Paulitsch, P., Ed., *Experimental and Natural Rock Deformation: Springer-Verlag, Berlin*, pp. 51-74.

Stockwell, C. H., 1970, Introduction to Geology of the Canadian Shield: in Douglas, R.J.W., Ed., *Geology and Economic Minerals of Canada: Geol. Surv. Can., Econ. Geol. Rept. No. 1*, pp. 44-54.

Szabo, N. L., Govett, G.J.S., and Lajtai, E. Z., 1975, Dispersion trends of elements and indicator pebbles in glacial till around Mt. Pleasant, New Brunswick, Canada: *Can. J. Earth Sci.*, v. 12, pp. 1534-1556.

Theimer, O., 1952, The statistical mechanics of crushing processes: *Kolloidschr.*, v. 128, pp. 1-6.

Troop, A. J., and Darcy, G., 1973, Geology of the Icon Sullivan Joint Venture copper deposit, Quebec: *C.I.M.M. Bull.*, v. 66, no. 729, pp. 89-95.

- Vagners, U. J., 1969, Mineral Distribution in Tills of southcentral Ontario: Unpublished Ph.D. Thesis, Univ. Western Ontario, London, Ontario, 277p.
- Wahl, W. G., 1953, Temiscamie River area, Mistassini Territory: Qué. Dept. Mines, Geol. Rept. 54, 37p.
- Warren, B., 1974, Rapport Preliminaire sur les depots des surface de la region de Baie du Poste; Que: Ministère des Richesses Nat., D. P. 267, 8p.
- Watson, G. S., 1956, A test for randomness of directions: Roy. Astron. Soc. Monthly Notices (Geophys. Supp.), v. 7, pp. 160-161.

APPENDIX A

Analysis of till pebble orientations

The field methods used by the author were: (1) excavation of a horizontal bench in the till to a depth at which visually massive fresh till was met, (2) scraping of the bench surface to expose the till pebbles, (3) measurement of the trend and plunge of the long axis of any pebble with a long:intermediate axial ratio greater than 3:2.

Tables A-1 and A-2 contain the statistics calculated from the field data. The vectorial techniques of Andrews and Shimizu (1966) produce a trend and plunge for each resultant, and three other statistics (Table A-1). Vector magnitude, R , is tested against a null hypothesis of randomness using Watson's (1956) formula:

$$R_{95} = \frac{N \chi^2_{95}}{3}$$

where χ^2_{95} is the value for chi-square with 3 degrees of freedom and N is the number of pebbles in the sample. If N is equal to 100, R (for acceptance) should be above 16.13 at the 95 percent level, and if N is equal to 50, R should be above 11.39. Confidence limits, C , on the resultant are produced. The estimate of precision parameter, k , (Watson, 1956) is calculated from

$$k = \frac{(N-1)}{(N-R)}$$

If k is equal to or greater than 3, the sample approximates a spherical-normal distribution.

The technique of Andrews and Shimizu (1966) was designed to calculate a three-dimensional vector sum of the individual measurements at a site, the long axis of each pebble being considered as a lineation having a trend and a plunge. Unfortunately, most pebbles have a plunge relative to the horizontal of less than twenty degrees and the distribution of pebble orientations may be such that many pairs of pebbles have trends that are diametrically opposed. These properties produce a cancellation of vectors during a three-dimensional summation, resulting in the calculation of resultants having low magnitudes and erroneous directions. Andrews and Shimizu (1966) suggested the use of a rotation of the reference plane through ninety degrees about an axis whose direction must be chosen on an a priori basis. This approach has been tested and criticized by Mark (1971, 1973) on the grounds that such rotations always result in the rejection of the null hypothesis of Watson's (1956) test that the data are drawn from a spherically random population. In addition, many distributions of till pebble orientations are bimodal or multimodal, implying the presence of more than a single population. A vector solution per-

formed on such data often produces a resultant that lies between the modes and which may only be an artifact of the method of calculation.

The vector magnitude, R (Table A-1), is always above the limit of acceptance, although many of the diagrams produced from the same data are indecipherable (Figs. 8, 9, 10). The estimate of precision parameter, k , is always less than the lower limit of acceptance of the hypothesis that the samples are drawn from a spherical-normal distribution.

For the above reasons, the statistics calculated by VECTOR for three-dimensional vectorial analysis of the till pebble orientation data have not been considered. The statistics are tabulated in Table A-1 simply for comparison with those calculated by VECTOR for the two-dimensional treatment, which are found in Table A-2.

Curray's (1956) formulae produce a resultant trend, a vector magnitude, L , and a probability of randomness, p , which are listed in Table A-2. These statistics accompany each rose diagram (Figs. 8, 9, 10, etc.) and they are explained in Chapter 3.

Table A-1. Statistics calculated by VECTOR for three-dimensional analysis of till pebble orientations, based on the techniques of Andrews and Shimizu (1966).

SITE NUMBER	RESULTANT TREND (DEGREES)	RESULTANT PLUNGE (DEGREES)	R (%)	C (DEG.)	k	UNIT	NUMBER OF PEBBLES
73-1	49	59	36.14	19.0	1.55	A	100
2	112	39	37.89	18.3	1.59	A	100
3	357	62	33.70	20.0	1.49	A	100
5	57	44	41.67	16.9	1.69	A	100
6	213	55	32.85	20.4	1.47	A	100
7	325	78	31.75	20.9	1.45	A	100
8	26	71	23.47	25.9	1.29	A	100
9	280	80	20.50	28.3	1.25	A	100
10	237	59	29.52	22.1	1.41	A	100
11	70	41	39.54	17.7	1.63	A	100
12	2	72	24.99	24.8	1.32	A	100
14	124	58	32.53	20.6	1.47	A	100
15	115	59	27.91	23.0	1.37	A	100
16	332	56	32.81	20.4	1.47	A	100
17	145	58	30.99	21.4	1.43	A	100
18	114	70	28.94	22.4	1.39	A	100
19	40	54	25.61	24.4	1.33	A	100
20	37	58	24.41	25.2	1.31	A	100
21	9	65	30.25	21.7	1.41	C	100
22	230	76	24.42	25.2	1.31	A	100
23	47	72	20.89	27.9	1.25	A	100
24	239	73	24.51	24.1	1.31	A	100
25	74	39	43.42	16.3	1.75	A	100
26	49	61	30.46	21.6	1.42	A	100
27	22	68	24.34	25.3	1.31	A	100
28	10	41	38.00	18.2	1.60	C	100
29	360	65	31.90	20.9	1.45	B	100
30	25	49	42.12	16.7	1.71	B	100
31	125	44	32.85	20.4	1.47	A	100
32	271	54	36.30	18.9	1.55	A	100
33	234	83	30.97	21.3	1.43	C	100
34	290	55	35.20	20.3	1.48	C	100
35	326	53	19.15	26.0	1.59	C	50
39	283	87	13.05	34.8	1.33	C	50
40	159	79	17.70	27.9	1.50	C	50
54	6	28	44.38	16.0	1.78	C	100
55	33	41	43.36	16.3	1.75	C	100
61	344	38	49.09	14.5	1.95	B	100
RANDOM	129	80	35.15	19.4	1.53		100

Table A-2. Statistics calculated by VECTOR for two-dimensional analysis of till pebble orientations, based on techniques of Curray (1956).

SITE NUMBER	RESULTANT TREND (DEGREES)	L (%)	PROBABILITY OF RANDOMNESS, p
73-1	79	19	.0285 *
2	9	11	.3238 B
3	116	33	.0000 *
5	78	34	.0000 *
6	100	8	.5243
7	67	10	.3789
8	129	18	.0444 *
9	170	21	.0123 *
10	18	36	.0000 *
11	148	11	.2994
12	148	10	.3497 B
14	148	21	.0138 *
15	16	13	.2048 B
16	156	13	.1921 B
17	129	24	.0027 *
18	78	9	.4072
19	28	26	.0014 *
20	117	22	.0096 *
21	18	27	.0006 *
22	9	17	.0542 B
23	24	34	.0000 *
24	10	33	.0000 *
25	113	24	.0033 * C
26	28	39	.0000 *
27	153	55	.0000 *
28	160	25	.0017 *
29	25	11	.3122
30	161	20	.0193 *
31	39	20	.0198 *
32	87	45	.0000 *
33	152	33	.0000 *
34	34	23	.0064 *
35	118	33	.0045 * D
39	157	13	.4252 D
40	42	41	.0002 * D
54	19	14	.1585
55	158	9	.4797
61	8	45	.0000 *
RANDOM	62	12	.2125

* Significant at the 95 percent level.

B Bimodal distribution.

D Pebbles disturbed by roots, rejected.

C Colluvium, rejected.

APPENDIX B

Methods and results of textural, carbonate, and lithologic analyses of Quaternary unitsField methods

At each site, a bulk sample of approximately 1 kg. of sediment was taken by channelling the sediment. At least 300 pebbles (4 to 64 mm.) were collected at random from the sediment.

Laboratory analysesTextural analysis

After air drying, each bulk sample was dry-sieved on a 4 mm. sieve and the oversize added to the pebble sample and the undersize retained for analysis. A subsample of 100 grams of the minus 4 mm. sediment was wet-sieved on a 0.037 mm. sieve and the oversize was dried and retained and the undersize funnelled into a sedimentation cylinder for hydrometer analysis. The plus 0.037 mm. fraction was dry-sieved to determine the weight percentage in size ranges between 4.0 mm. and 0.037 mm. The hydrometer analysis procedure was similar to the ASTM procedure D422-64 (ASTM, 1964), except that a water bath was not used and the plus 0.037 mm. fraction was not present in the sedimentation cylinder. The textural classes used were sand (4.0 to 0.063 mm.), silt (0.063 to 0.002 mm.) and clay (minus 0.002 mm.).

Carbonate analysis

The weight percentage of calcite and dolomite in the minus 0.063 mm. fraction of each sample was found using a modified version of the method of Dreimanis (1962). In this method, hydrochloric acid (20%) is added to a weighed sample and the volume of CO₂ evolved is recorded after 30 seconds and about 30 minutes (or complete dissolution). The first reading is used to calculate weight percent calcite, and both readings are used to calculate weight percent dolomite. The modification of the method is the use of a stopwatch instead of a time-calibrated acid burette to time the first 30 seconds.

Because the samples contained mostly dolomite and only traces of calcite, samples of 1.70 grams were used. Two analyses of each sample were performed. Malachite and azurite react like dolomite (slowly) in this procedure, and samples of oxidized unit C containing abundant carbonates (Table B-3) are those containing abundant malachite and azurite.

Pebble lithology

Each sample of pebbles (4 to 64 mm.) was soaked in a dispersant solution (0.5% sodium hexametaphosphate) for about 24 hours to remove adhering matrix. The dispersant was decanted and replaced with hot hydrochloric acid (5%) for 30 seconds to complete the matrix removal. The pebbles were wet-sieved with cold water on a 4 mm. sieve

to complete the washing. The plus 4 mm. fraction was dried and classified lithologically.

Tabulation of analytical results

The results of the foregoing analyses are listed in Tables B-1 to B-4. In these tables, texture is recorded as percent sand (4 to 0.063 mm.), silt (0.063 to 0.002 mm.) and clay (minus 0.002 mm.). Carbonate abundance (CARB) is recorded as percent in the minus 0.063 mm. fraction. Pebble lithology is recorded as the percentage of various rock types in the 4 to 64 mm. fraction. The column headings for pebble lithology are V (total vein), CP (chalcopyrite-bearing part of V, vein), PCH (Papasquasati plus Cheno Fm.), TM (Temisgamie Fm.), LA (Lower Albanel Fm.), UA (Upper Albanel Fm.), CHB (Chibougamau Fm.), IGMT (igneous and metamorphic crystallines), and NUM (number of pebbles in the sample).

Table B-1. Texture and lithology of Unit A.

SAMPLE NUMBER	TEXTURE (%)			CARB (%)	PEBBLE LITHOLOGY								
	SND	SLT	CLY		V	CP	PCH	TM	LA	UA	CHB	IGMT	NUM
72-1-1	43	50	7	18.9	0	0	1.4	.3	62.0	9.2	.6	26.5	347
72-1-2	44	50	6	18.6	.9	0	1.7	.3	73.2	6.8	0	17.3	347
72-1-3	39	54	7	20.8	.9	0	1.5	.3	65.1	11.1	.3	20.8	332
72-2-1	50	44	6	16.5	.6	0	1.4	0	50.4	6.1	0	41.5	359
72-2-2	47	47	6	17.8	.7	0	1.3	0	42.1	10.0	0	45.3	309
72-2-3	49	43	8	17.8	.6	0	1.5	0	55.8	10.4	0	31.8	346
72-5-2	45	49	6	18.5	.8	0	1.1	.3	56.6	13.5	1.1	27.2	364
72-6-1	62	36	2	1.4	0	0	2.1	.6	15.1	0	1.5	80.7	387
72-7-1	61	34	5	1.3	0	0	1.0	0	19.1	.2	11.2	68.4	418
72-7-2	62	30	8	16.1	0	0	.8	0	35.7	3.6	4.0	55.9	476
72-10-1	70	27	3	1.5	0	0	1.2	0	5.2	0	10.4	83.1	249
72-11-1	65	30	5	1.3	.3	0	1.0	0	25.5	0	4.6	68.6	389
72-13-1	71	27	2	14.5	.3	0	1.6	0	53.9	5.9	3.1	35.3	388
72-14-1	50	45	5	16.7	0	0	0	0	71.3	3.6	0	25.1	362
72-14-2	52	42	6	18.5	.3	0	.8	0	68.3	2.5	0	28.1	398
72-14-3	56	39	9	16.3	0	0	.3	0	72.0	3.2	0	24.5	372
73-1-1	45	46	9	21.1	.4	0	0	0	54.3	2.0	3.2	40.1	465
73-1-2	42	49	9	22.9	0	0	.4	0	66.0	3.8	1.9	27.8	468
73-2-2	42	53	5	18.5	.3	0	3.0	0	59.7	12.8	0	24.2	335
73-4-1	52	43	5	28.0	0	0	1.8	0	74.8	22.1	0	1.3	163
73-10-1	47	49	4	19.7	.6	0	2.7	.2	61.6	4.9	0	30.0	531
73-11-1	43	50	7	16.0	0	0	.8	.3	56.3	8.8	0	34.0	400
73-12-1	48	48	4	15.1	.3	0	.8	0	59.8	9.8	0	29.3	388
73-13-1	47	45	8	20.0	.2	0	2.4	.2	49.9	11.8	.2	35.3	425
73-13-2	46	47	7	40.4	.6	0	.2	.2	61.7	6.9	0	30.4	493
73-14-2	45	49	6	17.3	.8	0	2.0	.3	66.8	12.8	0	17.3	397
73-15-1	46	50	4	15.5	.6	0	1.5	0	51.2	11.8	0	25.0	340
73-16-1	49	46	5	17.4	1.1	0	.7	0	61.0	7.1	0	30.1	451
73-17-1	50	44	6	16.7	.6	0	1.5	0	59.3	11.2	0	27.4	332
73-18-1	49	46	5	13.0	.6	0	4.1	0	59.7	9.7	0	25.9	340
73-19-1	45	47	8	14.9	.6	0	2.3	0	60.2	16.1	0	20.8	347
73-20-1	37	57	6	17.3	0	0	.9	0	70.8	7.1	0	21.2	435
73-22-1	46	47	7	17.2	.5	0	1.6	0	68.8	8.8	0	20.3	365
73-23-1	46	49	5	13.7	.3	0	1.3	.3	79.2	9.2	0	9.7	303
73-24-1	48	47	5	16.0	.8	0	1.0	0	66.4	18.1	0	13.7	387
73-25-1*	20	52	28	3.6	.3	0	1.8	0	88.4	8.9	0	.6	395
73-26-1	38	50	12	19.4	.6	0	1.1	0	75.5	13.2	0	9.6	355
73-27-1	30	58	12	19.3	.5	0	.9	.2	80.3	9.5	0	8.6	431
73-31-1	29	61	10	25.1	3.7	.3	2.0	.3	75.3	13.2	0	5.4	295
73-32-1	41	51	8	13.7	5.3	.3	2.6	.6	64.5	11.4	0	15.5	341
73-36-1	50	42	8	17.0	2.0	0	2.3	.3	50.5	11.6	0	33.3	345
73-37-1	54	37	9	17.1	1.3	0	2.8	0	56.0	12.6	0	27.3	396
73-67-1	49	44	7	20.2	.7	0	.7	0	69.0	9.2	0	20.4	284
73-67-2	47	46	7	21.0	.2	0	.6	.4	58.5	9.1	0	31.2	497
73-67-3	42	50	8	20.5	0	0	.8	0	56.0	6.1	0	37.2	661
73-67-4	43	50	7	20.5	.2	0	1.6	.2	57.1	7.4	0	33.7	645
73-67-5	45	47	8	19.6	0	0	1.7	.5	55.3	7.5	0	33.4	637
73-69-2-4	-	-	-	-	1.7	0	1.7	1.7	69.0	15.5	0	10.4	58
73-69-6	-	-	-	-	6.5	0	3.2	0	74.2	9.7	0	6.5	31
73-73-1	53	42	5	19.0	0	0	.8	0	44.4	4.9	17.7	32.2	388
74-13-1	25	61	14	20.0	-	-	-	-	-	-	-	-	-

*Colluvium

Table B-2. Texture and lithology of unit B.

SAMPLE NUMBER	TEXTURE (%)			CARB (%)	PEBBLE LITHOLOGY							NUM	
	SND	SLT	CLY		V.	CP	PCH	TM	LA	UA	CHB		IGMT
Till in unit B at the Icon mine:													
72-12AL06	60	34	6	23.2	0	0	5.5	0	65.6	10.2	0	18.7	343
72-12BL06	64	28	8	22.0	0	0	4.5	0	67.2	12.3	0	16.0	399
72-12BL2	61	32	7	22.5	1.0	3	4.3	0	63.0	11.2	0	20.4	392
72-12BL4	67	28	5	37.7	5	0	3.8	7	70.9	7.8	0	16.4	426
72-12CL06	60	33	7	19.2	2.3	2	8.3	2	59.3	12.2	0	17.7	435
72-12CL2	64	26	10	21.6	0	0	11.8	3	59.8	7.4	0	20.8	366
72-12CL4	63	30	7	26.6	4.4	0	4.1	5	62.5	12.1	0	16.5	413
72-12DLO6	64	30	6	19.9	0	0	14.6	3	59.2	7.4	3	18.2	390
72-12DL2	63	32	5	18.9	3	0	11.3	0	62.0	8.4	0	18.1	382
72-12DL4	63	33	4	20.6	1.6	0	9.9	3	61.8	7.6	0	19.0	406
72-12EL1	52	40	8	18.0	0	0	7.8	0	63.7	8.8	0	19.7	295
72-12EL3	60	34	6	20.4	0	0	10.9	0	59.3	9.9	5	19.4	396
72-12GLO6	67	27	6	19.7	0	0	18.7	0	39.6	6.1	0	35.7	311
26-5E-F	-	-	-	-	1.3	0	7.0	0	58.9	12.0	0	20.9	158
6S-8E-F	61	36	3	23.9	8	0	3.8	4	79.3	5.9	0	9.7	237
71-3	66	30	4	21.0	0	0	14.6	0	55.1	8.4	-	21.9	356
71-15	-	-	-	-	8	0	4.6	0	76.4	0	0	18.2	259
71-18	-	-	-	-	7	0	19.9	0	50.3	8.0	0	21.1	302
73-61-1	41	54	5	20.3	3	0	1.2	0	83.6	5.1	0	9.8	604
74-9-1	65	30	5	21.6	5	0	7.7	5	58.3	6.0	0	27.0	182
71-4	62	35	3	17.3	9	0	16.4	9	48.3	6.9	0	26.7	116
73-64-15-17	-	-	-	-	5	0	2.7	0	70.7	11.2	0	14.9	402
73-65-23	-	-	-	-	1	0	6.4	3	70.3	11.3	0	11.7	1140
71-30	60	37	2	25.4	3	0	4.8	6	71.5	9.8	0	13.1	337
71-31	41	56	3	19.6	9	9	0	0	80.5	8.9	0	9.7	143
74-5-2	57	39	4	39.0	-	-	-	-	-	-	-	-	-
6S-11E-E	-	-	-	-	0	0	0	0	92.6	3.3	0	4.1	122
10S-12E-D	-	-	-	-	0	0	2.0	2.0	78.2	11.6	0	6.2	147
10S-12E-E	8	84	8	4.5	0	0	0	0	89.8	3.4	0	6.8	59
Ice-contact stratified drift in unit B at the Icon mine:													
2S-3D-E	-	-	-	-	1.1	4	1.6	0	81.5	4.9	0	10.9	184
73-62-9-11	-	-	-	-	6	0	2.2	0	85.1	6.5	0	5.6	321
73-62-18	-	-	-	-	0	0	1.9	0	87.4	5.1	0	5.6	214
73-64-13,14	-	-	-	-	0	0	2.5	2	81.8	5.3	0	10.3	610
73-64-19	-	-	-	-	4	0	5.6	0	68.9	10.1	0	15.0	1351
73-64-20	-	-	-	-	0	0	6	1	84.2	6.7	0	8.4	1163
74-5-1'	89	9	2	35.9	0	0	18.0	0	54.5	5.6	0	21.9	517
72-12F2	85	13	2	30.8	-	-	-	-	-	-	-	-	-
72-12FO6	45	51	4	15.7	-	-	-	-	-	-	-	-	-
72-12G2	57	39	4	14.7	-	-	-	-	-	-	-	-	-
73-66-2	61	37	2	20.3	-	-	-	-	-	-	-	-	-
73-62-19	-	-	-	-	5	0	1.8	0	86.7	4.6	0	6.4	218
Till in unit B elsewhere in the study area:													
72-5-1	80	18	2	16.4	2	0	9	2	46.4	6.5	11.3	34.7	681
72-8-1	-	-	-	-	0	0	1.2	0	38.7	8.8	14.7	36.7	251
72-8-2	-	-	-	-	4	0	2.7	0	44.1	3.5	16.4	32.8	256
73-63-1	-	-	-	-	0	0	1.1	0	18.3	0	4.4	76.2	1041
73-72-1	-	-	-	-	0	0	1.3	0	44.6	2.8	2.8	48.5	634
Ice-contact stratified drift in unit B elsewhere in the study area:													
72-3-1	81	17	2	23.6	4	0	1.2	3	45.0	8.6	1	44.3	733
72-4-1	85	14	1	28.3	5	0	2.9	0	44.0	9.9	0	42.8	587
72-9-1	-	-	-	-	4	0	8	0	46.2	8.8	12.5	31.3	249
73-53-1	-	-	-	-	0	0	1.2	1	43.5	6.0	4	48.8	1147
73-43-1	-	-	-	-	1.0	0	2.4	1	52.2	13.6	0	30.7	1436
73-44-1	-	-	-	-	1.1	0	3.4	6	51.5	15.2	0	28.3	1493
73-45-1	-	-	-	-	2	0	2.7	0	76.6	15.2	0	5.3	1332
73-46-1	-	-	-	-	2	0	3.8	2	76.9	12.0	0	6.9	1289
73-41-1*	-	-	-	-	1.7	0	7.9	0	28.5	10.3	0	51.6	808
73-42-1	-	-	-	-	9	0	3.6	1	43.0	14.6	0	37.8	1435

Table B-3. Texture and lithology of unit C.

SAMPLE NUMBER	TEXTURE (%)			CARB (%)	PEBBLE LITHOLOGY								IGMT NUM
	SND	SLT	CLY		V	CP	PCH	TM	LA	UA	CHB		
Unoxidized:													
71-2	63	30	7	35.4	100.0	36.6	0	0	0	0	0	0	172
71-42	50	45	5	24.0	86.8	22.4	0	0	12.3	.6	0	.3	357
71-43	59	37	4	22.3	48.2	30.2	1.4	0	43.7	2.7	0	4.1	222
71-44	45	51	4	26.6	.6	0	0	0	97.9	.9	0	.6	337
73-54-1	59	36	5	27.0	56.9	4.2	.1	0	38.7	.2	0	4.1	1799
73-55-1	72	21	7	26.0	96.4	3.1	0	0	3.0	0	0	0	2421
73-56	56	40	4	24.6	-	-	-	-	-	-	-	-	-
73-57	53	44	3	23.3	-	-	-	-	-	-	-	-	-
73-58	61	34	5	25.1	-	-	-	-	-	-	-	-	-
73-74	70	26	4	25.4	-	-	-	-	-	-	-	-	-
74-4-1	51	41	8	16.4	5.7	.5	0	0	48.0	0	0	.3	367
74-12-2	65	26	9	17.2	77.6	4.7	.1	0	22.2	0	0	.1	817
74-14-1	67	27	6	14.5	88.6	11.0	0	0	11.2	0	0	0	975
73-69-1	-	-	-	-	67.5	2.5	.8	0	30.8	0	0	.8	120
73-69-5	-	-	-	-	52.6	17.1	0	0	43.4	1.3	0	2.6	76
73-69-7	-	-	-	-	97.5	35.3	0	0	2.5	0	0	0	122
73-69-8	-	-	-	-	74.5	36.4	0	0	25.1	0	0	.4	247
73-69-9	-	-	-	-	13.8	.7	0	0	86.2	0	0	0	290
73-69-10	-	-	-	-	55.8	27.9	0	0	43.0	1.2	0	0	86
73-68-3	-	-	-	-	41.4	19.0	3.4	0	53.5	0	0	1.7	58
73-68-4	-	-	-	-	42.0	12.4	1.2	0	53.1	1.2	0	2.5	81
73-68-5	-	-	-	-	49.3	18.7	0	0	50.7	0	0	0	75
71-8	36	49	15	13.0	0	0	.4	0	93.5	3.0	0	3.0	263
71-9	64	29	7	23.4	.5	0	2.1	0	88.0	3.2	0	6.1	376
71-10	70	23	7	23.8	.5	0	1.1	.3	89.5	3.0	0	5.7	371
74-12-1	-	-	-	-	100.0	39.0	0	0	0	0	0	0	308
Oxidized:													
71-1	64	33	3	9.3	77.4	4.8	0	0	22.1	0	0	.5	208
71-14	-	-	-	-	6.7	0	.5	0	87.1	0	0	5.8	224
71-17	-	-	-	-	52.3	0	.9	0	39.5	0	0	7.3	109
71-19	-	-	-	-	30.1	.8	1.6	0	61.0	0	0	7.3	123
71-20	-	-	-	-	0	0	4.3	0	77.4	0	0	18.3	115
71-21	-	-	-	-	2.6	0	2.0	0	77.3	0	0	18.1	343
71-22	-	-	-	-	2.0	0	0	.7	92.7	0	0	4.6	151
71-23	-	-	-	-	.5	0	0	0	98.4	0	0	1.1	184
72-12AU2	74	23	3	28.9	62.8	7.0	.4	0	31.2	3.0	0	2.7	529
72-12AU4	80	17	3	8.7	94.1	3.6	0	0	5.6	0	0	.3	609
72-12AU6	63	33	4	8.6	74.0	9.7	0	0	26.0	0	0	0	381
72-12BU6	64	32	4	5.4	69.3	7.4	0	0	30.7	0	0	0	501
72-12CU6	67	29	4	11.3	69.9	5.2	0	0	29.6	0	0	.5	601
72-12DU5	69	28	3	4.2	74.5	5.7	0	0	25.3	0	0	.2	597
72-12EU46	68	27	5	11.4	84.7	8.2	.3	0	13.8	.5	0	.7	588
72-12EU56	70	27	3	4.3	71.0	15.8	0	0	29.0	0	0	0	590
72-12FU3	71	25	4	14.4	86.2	5.1	.4	0	11.8	.4	0	1.2	507
72-12FU4	58	38	4	2.8	76.4	9.5	0	0	23.6	0	0	0	454
72-12GU36	74	22	4	5.4	93.2	5.4	0	0	6.8	0	0	0	636

Table B-3, continued

SAMPLE NUMBER	TEXTURE (%)			CARB (%)	V	PEBBLE LITHOLOGY							IGMT NUM
	SND	SLT	CLY			CP	PCH	TM	LA	UA	CHB		
73-33-1	16	69	15	6.5	82.8	2.0	0	0	16.3	0	0	.9	449
73-34-1	34	59	7	14.6	73.2	10.9	3	0	22.9	2.1	0	1.5	671
73-62-17	51	46	3	6.9	14.8	.5	.4	0	83.9	0	0	.9	569
73-64-18	54	43	3	5.0	89.3	3.8	0	0	9.8	0	0	.9	346
73-66-1	56	41	3	28.1	-	-	-	-	-	-	-	-	-
74-10-1	67	27	6	14.1	97.7	3.8	0	0	2.3	0	0	0	686
73-65-22	-	-	-	-	73.5	2.4	.7	0	24.3	0	0	1.4	805
73-70-3	-	-	-	-	98.5	7.9	0	0	1.5	0	0	0	192
73-68-6	-	-	-	-	1.0	0	0	0	98.0	0	0	1.0	100
73-68-7	-	-	-	-	0	0	0	0	98.6	1.4	0	0	69
73-68-8	-	-	-	-	3.0	1.5	0	0	97.0	0	0	0	66
73-68-9	-	-	-	-	0	0	0	0	97.7	0	0	2.3	86
73-68-10	-	-	-	-	1.9	0	0	0	96.2	0	0	1.9	52
73-68-11	-	-	-	-	1.5	0	0	0	97.0	0	0	1.5	68
Oxidized samples from the grid shown on Figs. 23 and 29. The site in the northwest corner of the grid is OS-OE and the most southwesterly site is 20S-1E:													
6S-5E-E	33	65	2	2.0	23.7	0	1.8	.9	67.6	2.6	0	3.5	114
6S-8E-E	49	46	5	0.0	47.3	2.0	2.7	0	41.9	.7	0	7.4	148
8S-8E-E	15	71	14	0.0	66.7	6.7	0	0	33.3	0	0	0	30
12S-8E-E*	22	73	5	4.2	10.5	1.2	2.3	.0	80.2	0	0	7.0	86
14S-10E-E	38	58	4	10.2	16.7	.2	.7	0	74.8	.2	0	7.6	564
14S-11E-E	57	41	2	24.9	3.8	.2	1.4	.2	82.0	6.4	0	6.2	629
16S-9E-E	51	46	3	24.7	12.6	0	.5	0	75.6	5.3	0	6.0	398
Oxidized samples from the grid, pebble lithology only:													
OS-OE-D	-	-	-	-	0	0	1.6	0	93.3	0	0	6.1	163
2S-OE-D	-	-	-	-	0	0	1.5	0	89.5	0	0	9.0	134
2S-1E-D	-	-	-	-	.8	0	.8	0	95.9	0	0	2.5	121
2S-3E-D	-	-	-	-	18.8	.9	.9	0	79.5	0	0	.9	117
2S-5E-E	2	-	-	-	31.7	1.7	0	0	65.8	0	0	2.5	120
2S-6E-D	-	-	-	-	24.6	.9	0	0	75.4	0	0	0	110
2S-7E-D	-	-	-	-	79.8	0	0	0	20.2	0	0	0	114
4S-OE-D	-	-	-	-	3.5	.7	1.4	0	91.6	0	0	3.5	144
4S-1E-D	-	-	-	-	0	0	0	0	98.4	0	0	1.6	127
4S-2E-D	-	-	-	-	3.3	0	1.6	0	87.7	0	0	7.4	122
4S-3E-D	-	-	-	-	1.4	0	3.6	.7	85.7	0	0	8.6	139
4S-4E-D	-	-	-	-	10.2	.9	3.7	0	83.3	0	0	2.9	108
4S-5E-D	-	-	-	-	51.6	.8	1.6	0	44.3	0	0	2.5	122
4S-6E-D	-	-	-	-	46.0	.7	0	0	48.9	0	0	5.1	137
4S-7E-D*	-	-	-	-	33.9	0	14.2	0	32.3	0	0	19.7	127
4S-7E-E	-	-	-	-	29.8	2.1	2.8	0	61.7	0	0	5.7	141
4S-8E-D	-	-	-	-	93.1	2.6	0	0	6.0	0	0	.9	116
4S-9E-D	-	-	-	-	63.7	0	0	0	36.3	0	0	0	102
6S-OE-D	-	-	-	-	0	0	4.4	.7	87.1	.7	0	7.1	140
6S-1E-D	-	-	-	-	.6	0	4.3	0	86.5	0	0	8.6	163
6S-2E-D	-	-	-	-	2.1	0	.7	0	95.1	0	0	2.1	142
6S-3E-D	-	-	-	-	2.9	0	.7	0	87.8	0	0	8.6	139
6S-4E-D	-	-	-	-	24.0	0	.8	0	72.1	0	0	3.1	129

*Incorporation of unit B in unit C.

Table B-3, continued

SAMPLE NUMBER	V	CP	PCH	PEBBLE LITHOLOGY				IGMT	NUM
				TM	LA	UA	CHB		
6S-4E-E	26.3	0	1.9	0	66.2	0	0	5.6	160
6S-5E-D	31.9	1.3	3.1	0	57.5	0	0	7.5	160
6S-6E-D	54.4	.7	2.0	0	42.3	0	0	1.3	149
6S-7E-D	37.3	1.8	3.0	0	56.1	0	0	3.6	169
6S-8E-D	65.5	1.8	0	0	27.5	3.5	0	3.5	113
6S-9E-D	80.5	7.1	0	0	9.5	0	0	0	113
6S-10E-D	66.3	8.9	1.2	0	32.5	0	0	0	169
6S-11E-D	2.5	0	1.7	0	93.3	1.7	0	.8	120
8S-0E-D	.8	0	1.6	0	92.8	0	0	4.8	125
8S-1E-D	0	0	0	0	97.9	.7	0	1.4	147
8S-2E-D	0	0	.9	0	95.6	2.6	0	.9	117
8S-3E-D	7.1	.7	.7	0	87.2	0	0	5.0	140
8S-4E-D	21.9	0	.6	0	76.6	0	0	1.9	155
8S-5E-D	43.0	0	4.4	0	46.2	0	0	5.8	158
8S-6E-D*	12.2	.6	3.0	0	70.8	6.7	0	7.3	165
8S-7E-D*	31.1	.7	.7	0	55.4	5.4	0	7.4	148
8S-8E-D	26.6	0	.8	0	66.1	0	0	6.5	124
8S-9E-D	42.9	0	0	0	50.7	1.6	0	4.8	126
8S-10E-D	68.3	8.1	.8	0	27.6	0	0	3.3	123
8S-11E-D	4.9	0	.6	0	87.3	0	0	7.2	166
8S-12E-D	.8	0	1.5	0	90.0	.8	0	6.9	132
10S-1W-D	.8	0	0	0	95.4	0	0	3.8	130
10S-0E-D	4.1	0	0	0	87.6	0	1.4	6.9	145
10S-1E-D	3.9	0	3.9	0	89.4	0	0	2.8	180
10S-2E-D	3.8	0	1.5	.8	89.4	0	0	4.5	132
10S-3E-D	1.5	0	2.5	0	90.1	.5	0	5.4	203
10S-4E-D	39.3	0	.9	0	56.4	0	0	3.4	117
10S-5E-D	60.3	.8	0	0	34.8	0	0	4.1	121
10S-6E-D	45.4	4.3	5.7	0	41.1	0	0	7.8	141
10S-7E-D	23.3	1.5	5.3	0	61.6	0	0	9.8	133
10S-8E-D	22.7	2.5	3.4	0	57.0	3.4	0	13.5	118
10S-9E-D	5.8	0	1.3	0	88.4	0	0	4.5	155
10S-10E-D	39.3	3.3	0	0	60.0	0	0	5.7	150
10S-13E-D	.0	0	.6	0	95.0	0	0	4.4	159
12S-0E-D	1.1	0	3.4	0	91.0	0	0	4.5	179
12S-1E-D	2.7	0	.7	0	93.2	0	0	3.4	148
12S-2E-D	.7	0	0	.7	90.0	4.3	0	4.3	138
12S-3E-D	33.1	0	1.4	0	60.0	0	0	5.5	145
12S-4E-D*	23.1	0	5.4	0	64.6	0	0	6.9	130
12S-5E-D	15.8	.8	2.4	0	77.8	.8	0	3.2	127
12S-6E-D	36.5	6.1	6.1	0	46.1	0	0	11.3	115
12S-7E-D	11.9	.6	3.4	.6	65.9	2.3	0	15.9	176
12S-8E-D*	4.8	0	9.7	0	75.0	4.0	0	6.5	124
12S-11E-D	37.7	0	0	0	56.1	.9	0	5.3	114
12S-12E-D	.7	0	2.9	0	85.0	2.1	0	9.3	140

* Incorporation of unit B in unit C.

Table B-3, continued

SAMPLE NUMBER	V	CP	PCH	TM	PEBBLE LITHOLOGY (%)			IGMT	NUM
					LA	UA	CHB		
14S-OE-D	1.3	0	.7	0	96.0	0	0	2.0	153
14S-1E-D	2.1	0	.7	0	92.9	0	0	4.3	140
14S-2E-D	0	0	0	0	67.2	0	0	32.8	116
14S-3E-D	1.4	0	.7	0	90.0	1.4	0	5.6	143
14S-4E-D	23.9	0	2.9	0	65.4	0	0	7.8	138
14S-5E-D	8.2	4.1	3.4	0	79.6	0	0	8.8	147
14S-6E-D	9.5	.8	4.1	.8	65.4	3.3	0	16.5	121
14S-7E-D	19.7	.8	5.5	0	54.3	.8	0	19.7	127
14S-9E-D	10.4	0	2.6	0	81.8	0	0	5.2	116
14S-10E-D	22.5	.7	.7	0	70.7	.7	0	5.4	147
14S-11E-D	11.0	2.2	0	0	83.2	2.2	0	3.5	137
16S-OE-D	1.5	0	2.3	0	90.3	0	0	5.3	132
16S-1E-D	3.2	0	0	0	90.3	0	0	6.5	124
16S-2E-D	0	0	2.7	0	93.8	0	0	3.5	113
16S-3E-D	10.2	.8	.8	0	74.2	0	0	14.8	128
16S-4E-D	3.2	0	1.6	0	55.2	0	0	40.0	125
16S-5E-D	11.5	1.5	1.5	0	65.6	.8	0	20.6	131
16S-6E-D	21.3	1.6	2.4	0	55.9	0	0	22.8	127
16S-7E-D	14.9	0	4.1	0	71.9	0	0	9.1	121
16S-9E-D	22.8	1.0	1.0	0	75.2	0	0	1.0	101
16S-12E-D	0	0	1.2	0	79.2	4.3	.6	14.7	163
18S-OE-D	.7	0	.7	0	97.2	0	0	1.4	147
18S-2E-D	0	0	0	9	69.3	0	0	29.8	114
18S-3E-D	3.7	0	0	0	91.3	0	0	5.0	161
18S-4E-D	0	0	.7	0	42.6	0	0	56.7	141
18S-8E-D	.7	0	.7	0	81.5	0	0	17.1	140
20S-1E-D	3.2	0	6.4	0	81.5	0	0	8.9	124
20S-3E-D	0	0	0	0	95.6	.7	0	3.7	136
20S-4E-D	.8	0	0	0	38.5	0	0	60.7	122
20S-6E-D	8.9	0	2.0	0	64.3	0	0	24.8	101

154

APPENDIX C

True distribution of chalcopyrite in unoxidized till

Vaagners (1969, pp. 4-7) described the concept of true and apparent distribution of a mineral in till in the following way:

"In most ... till studies, the percentages of each mineral have been determined for each grain size fraction separately, and then presented in a table or as a histogram ... This is an apparent distribution because it is valid only for each particle size fraction, but does not give the true distribution of the mineral throughout the entire till sample.

The true distribution of each mineral in the entire till sample depends upon two factors:

- (1) the abundance of the mineral in each particle size fraction
- (2) the relative percentage of all mineral matter in each particle size fraction in relation to the total till sample, i.e. - the granulometric composition of the till ...

If these two factors are considered, then the true distribution of a mineral ... may be determined as follows. First the true percentage of each mineral, in relationship to the total till sample, has to be determined. The true percentage (T_p) of a mineral in each grain size fraction is calculated using the basic formula:

$$T_p = A_p \times \frac{G_p}{100}$$

where A_p is the percentage of the mineral in the grain size considered (from the apparent distribution), and G_p is the percentage of all mineral matter present in the same grain size fraction in relation to the total till sample (from the granulometric composition of the till).

Because the sums of the true percentages of each mineral for all grain size fractions are not constant in all the till samples, it is difficult to compare the distributions of the minerals and impossible to calculate percentages for their average distributions. Therefore relative percentages have to be determined for each grain size, considering the sum of these percentages for all the grain size fractions of each mineral as one hundred percent. The following formula is used for this calculation:

$$\text{Relative true percentage (Trp)} = \frac{T_p \times 100}{S_{T_p}}$$

where T_p is the true percentage of a mineral in a grain size fraction and S_{T_p} is the sum of the true percentages of the mineral in all the grain sizes of the sample investigated. The distribution of these relative percentages in all the grain sizes is termed true distribution of each mineral investigated."

Table C-1 lists the A_p , G_p , T_p , and Trp for the four bulk samples of unoxidized chalcopyrite-bearing till (unit C).

Table C-1. Abundance of chalcopyrite with respect to grain size in unoxidized till samples.

Sample number: 73-56

Fraction (mm.)	Ap	Gp	Trp	Trp
128-64	28.3	2.04	.49	3.42
64-32	31.2	4.44	1.39	9.71
32-16	27.1	5.02	1.36	9.50
16-8	30.8	4.79	1.48	10.34
8-4	36.8	3.63	1.34	9.36
4-2	38.6	5.30	2.05	14.32
2-1	33.2	5.75	1.91	13.34
1-.5	31.2	4.85	1.51	10.55
.5-.25	13.2	6.77	.89	6.22
.25-.125	6.3	8.46	.54	3.77
.125-.063	4.8	7.44	.36	2.52
.063-.032	3.7	10.33	.38	2.65
.032-.016	2.5	8.25	.20	1.40
.016-.0078	3.0	7.21	.22	1.54
.0078-.0039	2.6	3.84	.10	.70
.0039-.002	2.1	2.08	.04	.30
<.002	1.5	3.52	.05	.36
Totals		93.72	14.32	100.00

Sample number: 73-57

Fraction (mm.)	Ap	Gp	Trp	Trp
128-64	.0	1.39	.0	.0
64-32	4.9	3.89	.19	6.39
32-16	5.3	6.09	.32	10.65
16-8	7.4	4.72	.35	11.65
8-4	9.1	4.46	.41	13.43
4-2	8.5	2.58	.22	7.29
2-1	7.3	3.22	.23	7.79
1-.5	5.0	3.76	.19	6.29
.5-.25	2.4	6.98	.17	5.49
.25-.125	2.0	13.21	.27	8.96
.125-.063	1.8	11.81	.21	7.12
.063-.032	1.3	20.30	.27	8.92
.032-.016	1.0	7.01	.07	2.26
.016-.0078	1.3	4.27	.06	1.83
.0078-.0039	1.2	2.98	.04	1.23
.0039-.002	1.1	.89	.01	.30
<.002	.5	2.17	.01	.33
Totals		99.73	8.00	99.98

Table C-1, continued.

Sample number: 73-58

Fraction (mm.)	Ap	Gp	Tp	Trp
128-64	.0	3.04	.0	.0
64-32	1.56	7.70	.120	3.45
32-16	2.18	10.12	.220	6.32
16-8	2.95	8.94	.264	7.58
8-4	4.06	7.94	.323	9.27
4-2	1.57	8.80	.138	3.96
2-1	2.60	11.21	.291	8.36
1-.5	3.54	7.47	.264	7.58
.5-.25	3.38	6.56	.222	6.37
.25-.125	2.63	5.56	.146	4.19
.125-.063	6.20	3.07	.190	5.46
.063-.032	6.81	5.54	.377	10.82
.032-.016	6.45	5.42	.350	10.05
.016-.0078	5.66	4.17	.236	6.78
.0078-.0039	5.24	3.24	.170	4.88
.0039-.002	5.35	2.43	.021	.60
< .002	4.41	3.42	.151	4.34
Totals		104.63	3.483	100.02

Sample number: 73-74

Fraction (mm.)	Ap	Gp	Tp	Trp
128-64	24.8	1.84	.456	1.96
64-32	40.9	3.50	1.43	6.14
32-16	21.7	7.47	1.62	6.96
16-8	27.2	7.00	1.90	8.16
8-4	35.3	7.21	2.55	10.95
4-2	23.7	10.79	2.56	10.99
2-1	24.1	14.49	3.49	14.98
1-.5	25.9	9.10	2.36	10.13
.5-.25	22.3	7.19	1.60	6.87
.25-.125	16.6	6.77	1.12	4.81
.125-.063	20.4	3.81	.78	3.35
.063-.032	18.7	8.32	1.56	6.70
.032-.016	18.2	3.43	.624	2.68
.016-.0078	17.2	2.70	.464	1.99
.0078-.0039	14.4	2.70	.389	1.67
.0039-.002	10.2	1.61	.164	.70
< .002	7.86	2.99	.225	.97
Totals		100.92	23.292	100.01

APPENDIX D

Distribution of heavy minerals and chalcopyrite in oxidized till

The results of the analyses of the oxidized chalcopyrite-bearing till are listed in Table D-1. The calculations performed are the same as for the unoxidized samples (Appendix C), and for explanations of Ap, Gp, Tp and Tro see Appendix C. Hp is the weight percentage of heavy minerals (chalcopyrite, malachite, and limonite).

Table D-1. Abundance of heavy minerals and chalcocryrite in oxidized till samples.

Sample number: 72-12BU6

Fraction (mm.)	Hp	Ap	Gp	To	Trp
64-32	.0	.0	.0	.0	.0
32-16	13.7	13.7	35.0	4.80	49.4
16-8	6.2	6.2	17.6	1.09	11.2
8-4	8.6	8.6	9.1	0.78	8.0
4-2	12.7	10.0	5.5	0.55	5.7
2-1	17.5	14.1	5.9	0.83	8.6
1-.5	22.7	15.8	4.2	0.66	6.8
.5-.25	25.3	13.9	3.3	0.46	4.7
.25-.125	33.0	9.6	3.4	0.33	3.4
.125-.063	32.8	6.4	2.3	0.15	1.5
.063-.037	31.0	2.1	2.6	0.06	0.6
<.037	ND	ND	11.2	ND	ND
Totals			100.1	9.71	99.9

Sample number: 72-12EU46

Fraction (mm.)	Hp	Ap	Gp	To	Trp
64-32	.0	.0	5.0	.0	.0
32-16	.0	.0	18.8	.0	.0
16-8	.0	.0	19.5	.0	.0
8-4	6.4	6.4	11.9	0.76	27.2
4-2	9.5	7.4	6.7	0.50	17.9
2-1	8.8	7.2	6.4	0.46	16.5
1-.5	10.9	8.2	5.2	0.43	15.4
.5-.25	10.6	7.2	4.7	0.34	12.2
.24-.125	12.3	4.1	4.4	0.18	6.5
.125-.063	14.5	2.7	2.9	0.08	2.9
.063-.037	15.7	1.3	3.1	0.04	1.4
<.037	ND	ND	11.4	ND	ND
Totals			100.0	2.79	100.0

Table D-1, continued

Sample number: 72-12EU56

Fraction (mm.)	Hp	Ap	Gp	Tp	Trp
64-32	.0	.0	4.0	.0	.0
32-16	21.1	21.1	37.2	7.85	49.1
16-8	18.5	18.5	21.2	3.92	24.5
8-4	16.8	16.8	8.7	1.46	9.1
4-2	21.4	16.2	4.4	0.71	4.4
2-1	24.2	17.3	4.8	0.83	5.2
1-.5	25.6	14.9	3.3	0.49	3.1
.5-.25	29.4	12.1	2.8	0.34	2.1
.25-.125	36.6	7.9	3.0	0.24	1.5
.125-.063	33.0	5.3	1.9	0.10	0.6
.063-.037	31.5	2.4	2.0	0.05	0.3
< .037	ND	ND	6.8	ND	ND
Totals			100.1	15.99	99.9

Sample number: 72-12GU36

Fraction (mm.)	Hp	Ap	Gp	Tp	Trp
64-32	.0	.0	.0	.0	.0
32-16	.0	.0	32.3	.0	.0
16-8	0.9	0.9	20.6	.19	16.4
8-4	2.2	2.2	10.1	.22	19.0
4-2	2.3	1.9	7.5	.14	12.1
2-1	3.4	2.7	6.9	.19	16.4
1-.5	5.4	3.7	4.5	.17	14.7
.5-.25	6.6	3.1	3.3	.10	8.6
.25-.125	12.7	2.8	3.0	.08	6.9
.125-.063	14.1	2.1	1.9	.04	3.5
.063-.037	13.8	1.5	2.1	.03	2.6
< .037	ND	ND	7.8	ND	ND
Totals			100.0	1.16	100.2

Table D-1, continued

Sample number: 72-12FU3

Fraction (mm.)	Hp	Ap	Gp	Tp	Trp
64-32	.0	.0	.0	.0	.0
32-16	.0	.0	30.8	.0	.0
16-8	1.2	1.2	24.7	.30	14.3
8-4	4.7	4.7	8.2	.39	18.6
4-2	6.1	5.4	4.8	.26	12.4
2-1	7.9	6.5	5.3	.35	16.7
1-.5	11.0	7.5	4.7	.35	16.7
.5-.25	10.1	5.0	4.3	.22	10.5
.25-.125	14.8	3.8	3.9	.15	7.1
.125-.063	13.3	2.2	2.7	.06	2.9
.063-.037	13.0	.5	3.1	.02	1.0
< .037	ND	ND	7.5	ND	ND
Totals			100.0	2.10	100.2

Sample number: 72-12FU4

Fraction (mm.)	Hp	Ap	Gp	Tp	Trp
64-32	.0	.0	.0	.0	.0
32-16	1.6	1.6	35.6	.57	14.5
16-8	3.5	3.5	27.8	.97	24.7
8-4	8.5	8.5	7.1	.60	15.3
4-2	19.0	13.3	3.4	.45	11.5
2-1	17.3	13.5	3.6	.49	12.5
1-.5	14.6	12.6	3.0	.38	9.7
.5-.25	17.7	8.4	2.6	.22	5.6
.25-.125	20.6	5.4	2.4	.14	3.6
.125-.063	16.6	3.9	1.9	.074	1.9
.063-.037	15.3	1.4	2.5	.035	.9
< .037	ND	ND	9.9	ND	ND
Totals			100.0	3.929	100.2

Table D-I, continued

Sample number: 72-12CU6

Fraction (mm.)					
64-32	.0	.0	.0	.0	.0
32-16	.0	.0	33.8	.0	.0
16-8	10.8	10.8	19.6	2.12	45.0
8-4	6.2	6.2	10.1	.63	13.4
4-2	9.7	8.3	6.2	.51	10.8
2-1	11.6	9.3	5.3	.49	10.4
1-.5	14.4	10.4	3.7	.38	8.1
.5-.25	16.5	8.9	3.2	.28	5.9
.25-.125	17.6	5.6	3.4	.19	4.0
.125-.063	18.9	2.7	2.3	.06	1.3
.063-.037	20.0	1.8	2.6	.05	1.1
< .037	ND	ND	9.8	ND	ND
Totals			100.0	4.71	100.0